Noble Gas Isotope Geochemistry of Mid-Ocean Ridge and Ocean Island Basalts: Characterization of Mantle Source Reservoirs

David W. Graham

College of Oceanic & Atmospheric Sciences
Oregon State University
Corvallis, Oregon 97331

In: *Noble Gases in Geochemistry and Cosmochemistry*
D. Porcelli, C. J. Ballentine and R. Wieler (editors)
Reviews in Mineralogy and Geochemistry, Vol. 47
Mineralogical Society of America
Washington, DC
pp. 247-319 (2002)

INTRODUCTION

The study of noble gases in oceanic basalts is central to understanding chemical heterogeneity of the Earth's mantle and origin of the atmosphere. In the terrestrial environment the abundances of noble gases are quite low because they were excluded from solid materials during planetary formation in the inner solar system. This low background inventory helps to make the noble gases excellent tracers of mantle reservoirs. In this context, mid-ocean ridge and ocean island basalts provide valuable windows into the Earth's mantle. These oceanic basalts are not prone to the degree of contamination often observed in continental lavas that results from their passage through thick continental lithosphere and crust. Mid-ocean ridge basalts (MORBs) form by partial melting as the ascending mantle beneath spreading ridges reaches its solidus temperature, and MORBs are generally accepted to represent a broad sampling of the convecting upper mantle. Ocean island basalts (OIBs) represent melting 'anomalies' that are generally related to mantle upwelling. The extent to which ocean islands are derived from a thermal boundary layer in the deep mantle (e.g., as a mantle plume) or from chemical heterogeneities embedded within the mantle convective flow (e.g., as a mantle 'blob') has been debated for decades, and is not currently resolved. The isotope compositions of noble gases in oceanic basalts bear significantly on such debates over the chemical structure of the mantle. When oceanic basalts erupt as submarine lavas, their quenched rims of glass may contain high volatile abundances (especially when they are deeply erupted under elevated hydrostatic pressure), providing the best available opportunity for precisely characterizing the noble gas composition of the Earth's mantle. In favorable cases, inclusions of melt or fluids trapped within magmatic phenocrysts and mantle xenoliths can also be precisely analyzed for noble gas composition.

Measurable changes in the isotope compositions of noble gases are closely related to the geochemical processes controlling the distribution of K, U and Th, the major heat producing nuclides in the Earth. The isotopic makeup of every noble gas is modified by the radioactive decay of one or more of these heat-producing nuclides (Table 1). (Radon is an unusual case because it has no stable isotopes, and its geochemical distribution is completely controlled by radioactive decay of U and Th). The geochemical distribution of He is directly related to α-particle-production by U and Th. The Ne isotope composition in terrestrial systems is modified by nucleogenic processes in which ^{21}Ne is dominantly produced when neutrons or α-particles collide with Mg and O atoms. The radioactive decay of ^{40}K generally controls the Ar isotope composition. Small amounts of ^{84}Kr and ^{86}Kr have been produced over geological time by the spontaneous fission of ^{238}U. Production of ^{131,132,134,136}Xe has occurred over geological time by the spontaneous fission of ^{238}U and extinct ^{244}Pu (half-life $t_{1/2}$ = 82 Ma), while ^{129}Xe production occurred by radioactive decay of extinct ^{129}I ($t_{1/2}$ = 17 Ma).

One of the most significant observations is the ubiquitous presence of 'excess' ^{3}He in mantle-derived rocks from ocean ridges and islands, indicating that primordial volatiles are still escaping from the Earth's interior. The highest ^{3}He/^{4}He ratios, along with ^{20}Ne/^{22}Ne and ^{21}Ne/^{22}Ne ratios that approach solar values, are found at ocean islands, most notably Iceland and Hawaii. The He-Ne isotope systematics of these ocean island basalts are currently the strongest geochemical evidence that some portions of the mantle have remained relatively undegassed over geologic time. These are striking findings, because they directly conflict with some geophysical and geochemical models that argue that the mantle convects as a single system and that no primordial or undegassed material remains in the Earth's interior.

The high ^{40}Ar/^{36}Ar and non-atmospheric ^{129}Xe/^{130}Xe in MORBs also provide funda-mental clues to ancient planetary outgassing. Volatile loss from the Earth's interior over time, during ancient formation of the ocean and atmosphere and/or by continuing depletion through partial melting and magma generation, produces a range of parent/daughter ratios and is the primary cause for variable ratios of radiogenic to non-radiogenic noble gas species. Plate tectonic recycling also plays a significant role for the budget of the lithophile parental nuclides U, Th and K. In contrast, the importance of subduction in the mantle budgets of heavier noble gases such as Ar and Xe is still debatable (Staudacher and Allègre 1988; Porcelli and Wasserburg 1995a,b; Sarda et al. 1999a; Burnard 1999b).

Several books (Alexander and Ozima 1978; Ozima and Podosek 2002; Mamyrin and Tolstikhin 1984; Matsuda 1994) and review articles (Craig and Lupton 1981; Lupton 1983; Farley and Neroda 1998; Ozima 1994; McDougall and Honda 1998) currently provide a comprehensive background to terrestrial noble gas geochemistry. The aim of this chapter is to provide an up-to-date overview of key observations on noble gas isotopes in ocean ridge and island basalts that bear on models for the composition and evolution of the Earth's mantle (e.g., see the chapter by Porcelli and Ballentine 2002).

1529-6466/00/0047-0008$10.00

BACKGROUND

Noble gas chemical behavior

As a group, the noble gases are chemically inert, exhibiting only weak van der Waals type interactions. This serves to produce systematic and predictable variations within the group as a whole, often resulting in a coherent light-to-heavy noble gas trend that reflects the physical processes at hand, such as vapor/liquid/solid partitioning, molecular diffusion, and adsorption. Igneous processes such as partial melting, crystal fractionation, and magmatic degassing of major volatile species (CO_2 and H_2O) should lead to systematic elemental fractionations of the noble gases that are related to their variation in atomic size and the extent to which their electron cloud may be polarized (Keevil 1940). The elemental abundances of noble gases in oceanic basalts may therefore provide clues about petrogenetic processes (e.g., Dymond and Hogan 1978; Batiza et al. 1979).

Our ability to characterize noble gas reservoirs in the mantle depends to some extent on understanding vapor/liquid and solid/liquid partitioning. For example, if the amount of gas loss from a magma is known to be small (or zero), then measured noble gas concentrations in a basalt could be used in combination with vapor/melt and mineral/melt partition coefficients to estimate mantle source abundances. A meaningful determination of the relative elemental abundances in the mantle source requires a 'correction' of the measured concentrations in igneous samples for any fractionation or contamination that occurred during petrogenesis. This is a formidable task, and it can only be effectively carried out by using isotopic relationships among noble gas species. Argon provides a clear example. $^{40}Ar/^{36}Ar$ ratios >30,000 have been measured in some MORBs. In the case of a MORB sample with $^{40}Ar/^{36}Ar$ = 5,000 (a seemingly high value because it is more than an order of magnitude above the air ratio of 296) it is still possible that >80% of the measured Ar is derived from atmospheric contamination, and it would be erroneous to draw conclusions about noble gas abundance ratios in the mantle source region based on the concentration data alone. Fortunately, much of this problem can be circumvented through the ratios of certain radiogenic species (e.g., $^{4}He/^{40}Ar^{*}$). This approach is discussed in the section on *Coupled Radiogenic/Nucleogenic Production*.

Much less uncertainty and fewer assumptions are involved when isotopic ratios (e.g., $^{3}He/^{4}He$ vs. $^{40}Ar/^{36}Ar$) are compared directly. Therefore, wherever possible, this review focuses on isotopic relationships rather than on elemental abundances alone. The isotopic approach allows one to best discern the effects of atmospheric contamination, which can be quite large, and it circumvents some of the ambiguities that result from using the concentrations measured in rocks to interpret the inter-elemental fractionations that occur during igneous processes. The observational data upon which the review is based are presented in diagrams that form an integral part of the chapter. The key points provided by the figures are described in the review, but a detailed description of what they readily show for all the individual localities is not always given, in order to maintain a focus on the general characterization of mantle source reservoirs.

Vapor-melt partitioning. Noble gas solubility in basaltic melt decreases with increasing atomic mass, and is directly related to the atomic radius of the gas (Jambon et al. 1986; Lux 1987; Broadhurst et al. 1992; Shibata et al. 1998). At 1400°C the experimentally determined values for mid-ocean ridge basalt are 56, 25, 5.9, 3.0 and $1.7\square10^{-3}$ std cm^3/g-bar for He, Ne, Ar, Kr and Xe, respectively (Jambon et al. 1986). Degassing of basaltic melts will therefore lead to significant fractionation in the relative abundance of the noble gases, with the exsolved (volatile) phase enriched in the heavier noble gases, such as Ar and Xe, compared to the lighter species, such as He and Ne. The residual melt will show the opposite effect, with a preferential depletion in the heavier species compared to the lighter ones. The low solubilities lead to elevated concentrations in the vesicle phase of basalts. Mid-ocean ridge basalt glasses generally exhibit equilibrium vesicle/melt partitioning for helium (Kurz and Jenkins 1981) and for argon (Marty and Ozima 1986).

Noble gas solubility is only weakly dependent on temperature (Lux 1987) but it depends on melt composition. The compositional control is well described by the 'ionic porosity' (Carroll and Stolper 1993; Carroll and Draper 1994) or by the ratio of non-bridging oxygens to silicon (Shibata et al. 1998). The ionic porosity is the difference between the unit cell volume of a material and the calculated volume of the anions and cations, and provides an integrated measure of the interstitial sites available within the melt structure. The logarithm of noble gas solubility is linearly correlated with ionic porosity. The solubility also shows an increasing sensitivity to small changes in ionic porosity as the size of the gas atom increases. This observation led Carroll and Stolper (1993) to suggest that, as melt structure becomes more tightly packed, the availability of interstitial sites capable of accommodating the larger atoms decreases dramatically.

Noble gas solubility also depends on H_2O and CO_2 content of silicate melts (Paonita et al. 2000; Nuccio and Paonita 2000). Paonita et al. (2000) applied a novel method to study these effects, by adding a known amount of He-bearing glass to their experimental runs. The solubility of He was determined over a range of mixing proportions of H_2O and CO_2 in a rhyolite and in a trachybasalt. The He solubility is strongly influenced by H_2O content, showing about a factor of 3 increase with the addition of 3 wt % H_2O, apparently because the addition of water increases the availability of sites in the melt that accommodate noble gases. Solubility also increases exponentially with atomic size due to the addition of H_2O (Nuccio and Paonita 2000), so while Xe is less soluble than He in anhydrous melts, Xe and He solubilities are nearly the same when several percent H_2O is dissolved. The effect of CO_2 is more uncertain but it appears to be the opposite of H_2O, showing a decrease in the solubility of He by a factor of ~1.5 with addition of 0.05 wt % CO_2 (Nuccio and Paonita 2000). The major volatile composition of the melt therefore affects the relative degassing behavior of the noble gases. During extended degassing, a CO_2–rich anhydrous magma will retain its dissolved He more efficiently than a H_2O–rich magma (Paonita et al. 2000). Variations in the amount of H_2O and CO_2 that were initially present in variably degassed melts may be partly responsible for the observed range of $CO_2/^{3}He$ in oceanic basalts (see the Helium subsection *Relation to Major Volatiles*).

The effect of pressure on noble gas solubility in silicate melts is currently an active area of investigation. Chamorro-Perez et al. (1998) reported an order of magnitude decrease for Ar solubility in an olivine melt near 5 GPa, corresponding to mantle depths near 150 km. They inferred that melt densification makes it impossible to accommodate Ar in interstitial sites near this pressure. This is a surprising result, because it would imply that Ar is moderately compatible at depth, and partial melting would not be an effective means of mantle degassing. However, more recent data indicate that the Ar clinopyroxene/silicate melt partition coefficient is relatively constant at ~4×10^{-4} for pressures up to at least 8 GPa (Chamorro et al. 2002), so there is no structural change in the melt over that pressure range. Recent work on Ar and Xe solubility in synthetic melts also does not show a decrease in solubility even at pressures of 11 GPa. Instead, it appears that Ar solubility increases to about 6 GPa, above which it reaches a threshold concentration of 0.8 wt % (Schmidt and Keppler 2002). An important consideration in applying the experimental results for solubility and partitioning should be the very low abundance of noble gases in the mantle.

Crystal-melt partitioning. Compared to noble gas solubility in melts, much less is known about their solubility in minerals. Several different approaches can be used to determine a crystal/melt partition coefficient D (where D = weight concentration in crystal/weight concentration in melt) but each one has its limitations. The presently available data are contradictory and the D values range by orders of magnitude, from $<10^{-4}$ to >1. A thoughtful summary of the issues involved in these estimates is presented by Carroll and Draper (1994).

A few experimental studies of noble gas mineral/melt partitioning have been carried out (Hiyagon and Ozima 1982, 1986; Broadhurst et al. 1990, 1992). These studies show a very wide range in partition coefficients for some minerals, and their applicability to mantle melting is difficult to evaluate. Hiyagon and Ozima (1982, 1986) powdered their run products to physically separate the glass from the crystals, so there are questions of atmospheric adsorption, the extent to which all adhering glass could be removed from crystals, and the possible presence of fluid inclusions. They obtained olivine/melt values of $D_{He} \leq 0.07$, $D_{Ar} = 0.05\text{-}0.15$ and $D_{Xe} \leq 0.3$. Broadhurst et al. (1990, 1992) used separate containers for minerals and melts and were extremely careful to use inclusion-free starting materials, but they also obtained a wide range of D values. They observed a weak increase in D from He through Xe for each of the minerals studied (forsterite, diopside, anorthite and spinel) and suggested that this was related to the increasing polarizability with atomic number. They also suggested that the wide range in partition coefficients is related to the number of lattice defects, because variation in the density of interstitial sites in the minerals on the scale needed to explain the range seemed unreasonable. All of these experimental studies obtained D values indicating that the noble gases, especially the heavier species, are more compatible than is usually assumed. Given the experimental difficulties, these D values should be considered as upper limits.

A second approach for obtaining crystal/melt partition coefficients is to use naturally occurring glass-mineral pairs. This approach has been used to study partitioning between olivine and basalt melt (Marty and Lussiez 1993; Kurz 1993; Valbracht et al. 1994). In two studies that used similar approaches to analyze olivine-rich basalts from the Mid-Atlantic Ridge, Marty and Lussiez obtained a value of $D_{He} \leq 0.008$ and $D_{Ar} \leq 0.003$, while Kurz (1993) obtained $D_{He} \leq 0.0058$. These investigators analyzed olivine and glass from the samples both by crushing in vacuum, to release He trapped in inclusions and bubbles, and by fusion, to release the trapped plus the dissolved components. Marty and Lussiez (1993) showed that the olivine and glass have the same $^3He/^4He$ ratio, and appear to be in chemical equilibrium based on their Fe/Mg ratio, although this was questioned by Hiyagon (1994a). The He and Ar released from this glass is dominated by the vesicle gas fraction (Marty and Lussiez 1993), and the He and Ar released from the olivine by crushing appears to be dominated by gas in shrinkage bubbles associated with trapped melt inclusions (Marty and Lussiez 1994). The latter observation would support the notion that the olivine crystals grew before the magma was vapor-saturated. If this was not true then the investigated partitioning involves three phases and is much more complicated. The presence of melt and fluid inclusions in crystals and the possibility of vesicle loss from a magma following crystallization are limitations to using natural samples, and led Marty and Lussiez (1993) and Kurz (1993) to present their D values as minima.

In situ laser analysis is becoming increasingly important in addressing crystal/melt partitioning of noble gases. In a preliminary study using a UV laser ablation microprobe, Brooker et al. (1998) obtained a range of Ar partition coefficients from 0.013-0.14 for olivine and 0.0016-0.589 for clinopyroxene. The low values are probably more realistic and less affected by possible adsorption effects, early partial melting of the crystals and the presence of fluid inclusions.

Although the partitioning behavior of the noble gases between minerals and melts is currently poorly understood and further work is needed, the least ambiguous results indicate that the noble gases have D values below 1. Given the low abundances of the noble gases in the mantle, the experimental data give some indication that mineral defects may play an important role. Both the experiments and the naturally occurring mineral/melt pair studies indicate that He behaves as a highly incompatible element. U and Th are also known to be highly incompatible, having bulk D values on the order of 10^{-3} or less, so the behavior of He relative to U and Th still needs to be established. Given that the lowest D value determined for He is likely to be a maximum, the large differences in $^3He/^4He$ between the mantle sources for MORBs and OIBs can be taken to reflect differences in their degassing history.

Mantle structure and noble gases

The chemical structure of the Earth's mantle is directly related to the style of mantle convection, and the debate over whole mantle vs. layered mantle convection has gone on for decades. There are several scales of mantle convection indicated by seismic tomography, gravity and geochemistry (Anderson 1998b). The largest scale is controlled by the pattern of cooling associated with subducting plates, while the smaller scales (400-1000 km) are probably controlled by the depth of phase transitions and the thickness of the upper mantle low viscosity region. Seismic evidence now clearly

shows that some subducting slabs penetrate below the 660 km seismic discontinuity (van der Hilst et al. 1997), so this depth can no longer be viewed as a strong barrier to mass transport between the upper and lower mantle. Some investigators take this as sufficient evidence for whole mantle convection. In this case, the isotopic differences between depleted MORBs and enriched OIBs might be explained by a mantle that contains large scale blobs of chemically enriched or primitive material (e.g., Manga 1996; Becker et al. 1999). The origin of such blobs is unclear, and detecting them (if they exist) is currently beyond the resolution capabilities of seismology. Alternatively, the mantle may have some form of layered structure. If so, then buoyant upwellings produced at thermal or chemical boundary layers (mantle plumes) will be an important mechanism by which deep material is brought close to the Earth's surface, where it partially melts to form ocean island basalt magmas. Mantle plumes have been implicated in the origin of many ocean islands since the discovery of plate tectonics (Morgan 1971). Bathymetric tracks of volcanoes such as the Hawaiian-Emperor chain indicate that these plume sources move laterally much more slowly than the plates, so the depth of origin must lie below the convecting upper mantle, although the exact depth is currently not well constrained. Such plumes most likely originate from boundary layers, perhaps as deep as the core-mantle boundary, and they are expected to entrain small amounts of material from the underlying reservoir. In actuality there is a slow relative motion between the hotspots on the Earth's surface that is explained by advection of the plumes by large-scale mid-mantle flow. This mid-mantle flow is generally toward ridges and opposite in direction to the flow field in the upper mantle as indicated by plate motion directions (Steinberger and O'Connell 1998). In some cases, most notably East Africa, the upwelling also appears to be much broader than expected for a narrow plume conduit (Ritsema et al. 1999).

Obviously much less is known about the deep mantle than the upper mantle. The style and vigor of mantle convection are described by the Rayleigh number (Ra). Ra is estimated to be 10^7 for the uppermost mantle; the estimate for the deep mantle is more uncertain but it may be several orders of magnitude smaller, mostly due to its higher viscosity (Tackley 1998). Consequently, the mixing time for the upper mantle is relatively rapid compared to the deep mantle, and compositional heterogeneities have a greater likelihood of surviving deeper in the Earth's interior (Gurnis and Davies 1986). Nevertheless, state-of-the-art coupled convection-degassing models that incorporate a high viscosity lower mantle, a phase transition at the base of the upper mantle, and temperature- and pressure–dependent rheology, currently fail to produce an isolated, high $^3He/^4He$ region in the Earth (van Keken and Ballentine 1998, 1999).

Recent seismic tomography seems to indicate that some type of boundary may be present at a depth near 1700 km in the lower mantle (van der Hilst and Kárason 1999; Kellogg et al. 1999). Below this depth the mantle may be denser than the overlying mantle due to differences in bulk composition. However, the deeper material could contain more of its original inventory of heat producing elements, so it is hot and only slightly more dense than mantle at the same depth lying on the adiabat (the pressure-temperature path for material that expands or contracts without gaining or losing heat). This configuration is dynamically stable but it may lead to the development of significant topography on the surface of this layer. The resulting small density differences (~0.5%) would be sufficient to inhibit mixing, but the layer's surface could respond dramatically to down-going slabs and rising thermal plumes (Kellogg et al. 1999). This model is consistent with laboratory studies of thermochemical convection in a chemically heterogeneous fluid that has a stratified density and viscosity structure (Davaille 1999). These lab experiments show that hot domes oscillate vertically through the fluid while thin plumes rise from their upper surface. There are other 'layered' models. For example, the 'perisphere' model places all OIB sources in a thin, shallow enriched layer beneath the lithosphere (Anderson 1995). It accounts for the presence of enriched basalts in continental rifts, but it is difficult to reconcile with the voluminous volcanism at some ocean islands. Many of the proposed models do not readily satisfy the noble gas observations that support the preservation of relict primitive mantle. Some contrasting ideas on mantle convection and its structure and evolution that consider the noble gas constraints are given in papers by Kellogg (1992), Davies and Richards (1992), Albarède (1998), Coltice and Ricard (1999) and Tackley (2000). Two books on mantle dynamics are also now available (Davies 1999; Schubert et al. 2001).

Intriguingly, there is no compelling evidence for the survival of primitive mantle based on refractory element ratios or the isotopes of Sr, Nd and Pb in ocean island basalts (Hofmann 1997). Hofmann et al. (1986) showed that certain elemental ratios, such as Ce/Pb and Nb/U, had uniform and similar values in both MORBs and OIBs. These Ce/Pb and Nb/U ratios are distinct from values for either the primitive mantle or the continental crust, indicating that the chemical signature of crust extraction over geologic time has mostly been homogenized throughout the mantle. Therefore, the observed Sr, Nd and Pb isotopic differences between MORBs and OIBs must be the result of more recent processes. Hofmann and White (1980) convincingly established that the extreme isotopic compositions of OIBs are probably controlled by plate-tectonic recycling, in which OIBs are produced by the heating and melting of subducted slabs. Zindler and Hart (1986b) and Weaver (1991) also demonstrated that the OIBs with the most radiogenic Pb isotopes were probably dominated by recycled oceanic crust, while other enriched OIB end-members probably contain a small percentage of recycled sediments (terrigenous vs. pelagic) mixed into their mantle source region.

In the layered mantle model, OIB magmas from intraplate hotspots with high $^3He/^4He$ come from deep mantle source regions that are convectively isolated from the upper mantle source of MORBs. These deep mantle regions contain some proportion of relatively undifferentiated, primitive mantle. OIBs that do not have elevated $^3He/^4He$ may originate from shallower source regions. The upwelling, deep OIB mantle source also supplies material to the MORB mantle. The steady-state model for the upper mantle is a current paradigm in noble gas geochemistry (e.g., Allègre et al. 1986/1987; O'Nions 1987; Kellogg and Wasserburg 1990; O'Nions and Tolstikhin 1994, 1996; Porcelli and Wasserburg 1995a,b). This steady-state is reached through a balance of deep mantle input from below, slab subduction from above, and radiogenic production. Further discussion of the steady-state model is provided by Porcelli and Ballentine (2002, this volume).

HELIUM

Significance

Helium isotope measurements in ocean ridge and island basalts provide some of the most basic geochemical information on mantle source reservoirs. More helium isotope analyses have been performed for oceanic volcanic rocks than for other noble gas species, and helium isotopes have played a leading role in the study of mantle heterogeneity. Helium isotope analyses are readily performed by modern mass spectrometers because there is a general absence of atmospheric contamination in samples due to the low concentration of helium in air (5.24 parts per million by volume at standard temperature and pressure). There are 2 naturally occurring isotopes of helium. ^{3}He is much less abundant than ^{4}He; for example, the atmospheric ^{3}He/^{4}He ratio (R_A) is 1.39×10^{-6} (Mamyrin et al. 1970; Clarke et al. 1976). Nearly all of the terrestrial ^{4}He has been produced as α-particles from the radioactive decay of ^{238}U, ^{235}U and ^{232}Th over geological time, while nearly all of the ^{3}He is primordial. Because helium undergoes gravitational escape from the thermosphere and has an atmospheric residence time of 1 to 10 million years, it is not recycled by plate tectonics to the Earth's interior, and this makes the ^{3}He/^{4}He ratio unique among isotopic tracers of mantle sources involved in volcanism (Lupton 1983). By far the most important terrestrial source of ^{3}He is degassing from the Earth's interior. Excess ^{3}He in volcanic rocks was first reported by Krylov et al. (1974) and Lupton and Craig (1975). The presence of this ^{3}He in mantle-derived materials has profound implications; it means that the Earth is still outgassing volatiles that were trapped at the time of its accretion more than 4500 Ma ago.

Other sources of ^{3}He to the atmosphere include the auroral precipitation of solar wind, direct accretion from cosmic rays, and the flux of cosmic dust and meteorites (Lupton 1983). Small, but measurable amounts of ^{3}He are produced in rocks at the Earth's surface by high energy cosmic rays, predominantly from spallation of O, Si, Mg and Fe atoms, providing a means for determining surface exposure ages and erosion rates (Kurz 1986). Very small amounts of ^{3}He are also produced during radioactive decay of U and Th as a result of neutron interactions with Li, by the reaction ^{6}Li(n,α)^{3}H β^- ^{3}He (Morrison and Pine 1955). The neutrons are produced by α-particle interactions on target elements such as Mg, Si and O in the host rock. This results in a low ^{3}He/^{4}He production ratio (typically <0.02 R_A), even in crustal rocks that are relatively enriched in Li. Consequently, the terrestrial ^{3}He/^{4}He ratio varies by several orders of magnitude, from high values (>10^{-5}) in mantle-derived lavas and fluids, to low values (~10^{-8}) in continental regions due to increased amounts of radiogenic ^{4}He. The general pattern in oceanic basalts is one in which MORBs show a relatively small range in ^{3}He/^{4}He (8.75±2.14 R_A; Table 2), while OIBs are much more variable, and extend to values that are higher than the MORB mean by more than a factor of 4.

Radiogenic production

The amount of ^{4}He produced in a closed system, at secular equilibrium and over time t is given by

$$^4\text{He}^* = {}^{238}\text{U}\{8\,(e^{\lambda_{238}t} - 1) + (7/137.88)\,(e^{\lambda_{235}t}-1) + 6\,\kappa\,(e^{\lambda_{232}t}-1)\} \quad (1)$$

where ^{238}U is the amount present, λ_{238}, λ_{235} and λ_{232} are the decay constants for ^{238}U, ^{235}U and ^{232}Th (0.155125, 0.98485 and 0.049475 Gy^{-1}, respectively), 1/137.88 is the present ratio of ^{235}U/^{238}U and κ is ^{232}Th/^{238}U. The range of κ values in the Earth's mantle is about a factor of 2, from κ of ~2 to ~4 (Allègre et al. 1986; O'Nions and McKenzie 1993). By convention, the helium isotope ratio is often expressed as ^{3}He/^{4}He, i.e., as the non-radiogenic to radiogenic isotope, which causes some inconvenience when formulating changes due to radioactive ingrowth. The ^{3}He/^{4}He ratio in igneous samples, R, is usually expressed relative to the atmospheric ratio, i.e., as R/R_A. Marine air provides a convenient and useful standard given its isotopic homogeneity for ^{3}He/^{4}He.

Mid-ocean ridge basalts

Global variability. Helium isotope variations along mid-ocean ridges have been extensively studied, and the variability along ridges is important to understand in the context of convective mixing and melt generation in the upper mantle. The difference in ^{3}He/^{4}He ratio commonly observed between MORBs and OIBs is accepted by most investigators as evidence for two distinct mantle source regions. This viewpoint has been challenged by Anderson (2000a,b; 2001) on the basis of a statistical comparison of MORB and OIB data sets. The choice of basalt samples included in these data sets directly impacts the accuracy of any conclusions about the mantle, so it is important to discuss this choice in some detail and to make it wisely. Anderson (2001) chose to include lavas from Iceland as mid-ocean ridge basalts, on the grounds that the Mid-Atlantic Ridge passes through its center. He also included near-axis seamounts and back-arc basin basalts. The inclusion of Iceland certainly affects the mean and variance in any such comparison, because the ^{3}He/^{4}He ratios near its center are higher than those observed anywhere along the global ocean ridge system. The inclusion of seamounts and back-arc basin basalts affects the variance much more than the mean, due to the presence of lavas that experienced shallow-level degassing and significant lowering of their ^{3}He/^{4}He ratio by interaction with seawater or altered wallrock (e.g., Graham et al. 1988; Staudacher and Allègre 1989; Hilton et al. 1993). Anderson did not carry out a similar data compilation of the OIB data set, but used a mean value for 23 ocean islands summarized by Allègre et al. (1995) based on 276 individual OIB analyses. The OIB data included lavas from very different stages of evolution in the volcanic history of the islands, and the sources of the original data were not given in detail. Anderson (2001) compared the mean value for these 23 islands with the mean for ~500 individual MORB glasses, so the two data sets were also not treated in the same way. In this section I have made a first-order attempt to objectively estimate the mean ^{3}He/^{4}He, its variance and skewness, for mid-ocean ridges from the Atlantic, Pacific and Indian Oceans, and for all ridges collectively. I arrive at different values for the mean and standard deviation compared to Anderson's work (Table 2).

Mid-ocean ridge basalts display a relatively narrow range of ^{3}He/^{4}He, while ocean-island basalts are more variable and often extend to higher values. The full range in

MORBs is between 1 and 18 R_A. This range excludes subaerial lavas from Iceland, but not submarine lavas from the ridges to its south or north (Reykjanes or Kolbeinsey). In making this comparison, I also have not included seamounts or back-arc basin basalts, because their clear tectonic association with ridge mantle is questionable. I have included only one analysis from any individual sampling locality (i.e., one sample per dredge or rock core), as a very coarse attempt to avoid sampling bias from the few areas that have been studied in considerably more detail. I have also excluded a handful of glass samples with $^3He/^4He < 2.5$ R_A, which, given their differentiated and highly degassed nature ([He] $<3\square10^{-8}$ std cm^3/g) and their elevated chlorine contents, have clearly been influenced by contamination with seawater or altered crust (Michael and Cornell 1998). These sample types occur along propagating rifts or overlapping spreading centers, often areas having a low magma budget. This may lead to a prolonged residence in the crust, during which the magma can undergo significant gas loss and interaction with altered wallrock. Including these degassed, low $^3He/^4He$ samples does not lead to a very different estimate of population means, but it does lead to higher estimates of variance. No other filtering has been done, and it should be emphasized that the data used represent more than 95% of the original collection of $^3He/^4He$ analyses for submarine glasses sampled along mid-ocean ridges. The spatial distribution of the ~660 MORB localities that have been studied is shown in Figure 1.

The mean and standard deviation for the respective populations from each ocean basin, and for all MORBs, are presented in Table 2 and displayed in Figure 2. For all MORB samples considered in the manner just described (n = 658), the mean is 8.75 R_A and the standard deviation is 2.14 R_A. MORB samples with the highest $^3He/^4He$ are from ridge sections that display other anomalous geochemical features, quite often where the sub-ridge mantle is influenced by nearby ocean islands. The range in MORBs is usually stated to be about 7 to 9 R_A, and this qualitatively describes most of the data when spreading ridges adjacent to ocean island hotspots are excluded. In only a handful of cases do ridge localities away from ocean islands show values outside of the 7 to 9 R_A range for a significant distance along-axis (≥50 km). These areas also show isotopic anomalies in other systems such as Sr, Nd and Pb. The cases are the super fast spreading section of the southern East Pacific Rise ($^3He/^4He$ up to 10.9 R_A; Mahoney et al. 1994), the Australian-Antarctic Discordance ($^3He/^4He$ down to 6.2 R_A; Graham et al. 2001), the 33°S isotope anomaly on the Mid-Atlantic Ridge (down to 6.2 R_A; Graham et al. 1996a), the ultraslow-spreading Southwest Indian Ridge from 9°-24°E (down to 6.3 R_A; Georgen et al. 2001) and the southern Chile Rise (down to 3.5 R_A; Sturm et al. 1999). In this last case, low Ce/Pb ratios indicate that crustal recycling has occurred into the MORB mantle source from a nearby subduction zone (Klein and Karsten 1995). Intriguingly, all of the other localities having low $^3He/^4He$ appear to show a limiting value near 6 R_A.

High $^3He/^4He$ localities other than Iceland seem to show an upper limiting value of ~15 R_A. These localities include the east and west rifts of the Easter Microplate (11.7 R_A; Poreda et al. 1993), the Southeast Indian Ridge near Amsterdam and St. Paul islands (14.1 R_A; Graham et al. 1999), the Gulf of Tadjoura near Afar (14.7 R_A; Marty et al. 1993b), the Shona and Discovery sections of the southern Mid-Atlantic Ridge (12.3 and 15.2 R_A, respectively; Moreira et al. 1995; Sarda et al. 2000), the Southwest Indian Ridge near Bouvet Island (14.9 R_A; Kurz et al. 1998) and the Manus Basin back-arc spreading center (15.1 R_A; Shaw et al. 2001). In each of these areas, the high $^3He/^4He$ signal can be attributed to introduction of high $^3He/^4He$ material from a nearby mantle hotspot. The apparent upper limit to the measured $^3He/^4He$ in these cases is usually presumed to stem from dilution with ambient upper mantle having $^3He/^4He$ between ~7 and 9 R_A.

No relationship between He isotope composition and ridge spreading rate is evident. However, the *variance* of $^3He/^4He$ along ridges may be inversely related to spreading rate (Graham 1994, Allègre et al. 1995). There are several caveats that go with such an inferred simple relationship, however. First, an inverse relationship only applies when the high $^3He/^4He$ localities discussed above are excluded, because these localities naturally display the highest variance and they occur across most of the range in seafloor spreading rates. An inverse relationship also only holds when the length of ridges used in the comparison are relatively long, generally more than a few hundred kilometers. Finally, the proposed relationship has recently been called into question by Georgen et al. (2001), because a relatively narrow $^3He/^4He$ range is observed for basalts along the ultra-slow spreading Southwest Indian Ridge. Despite all these qualifications, there does appear to be some systematic behavior for most other sections of the ocean ridge system. An inverse relationship between variance and spreading rate may reflect either variations in the efficiency of upper mantle mixing, or differences in the degree of magma homogenization during MORB petrogenesis. By the first explanation, faster spreading ridges are ultimately a consequence of faster turnover rates in the upper mantle. The implicit assumption here is that $^3He/^4He$ in the upper mantle represents a balance between input of relatively high $^3He/^4He$ material from the lower mantle and *in situ* radiogenic addition of ^4He. Blobs of OIB material injected from the deeper mantle would be stirred into the upper mantle, and presumably this stirring is more thorough in the mantle beneath faster spreading ridges (Allègre et al. 1984). By the second explanation, "averaging" of small-scale heterogeneities occurs more effectively at faster spreading ridges, either during partial melting or during magma storage in the crust (Holness and Richter 1984, Batiza et al. 1984).

Despite the relatively narrow range of MORB $^3He/^4He$ in a global context (i.e., considering that OIBs extend to values above 30 R_A), it is important to realize that our ability to measure variations in $^3He/^4He$ signal along mid-ocean ridges is comparable to that for other isotopic systems. For example, in the case of Sr isotopes the range of $^{87}Sr/^{86}Sr$ in typical MORB away from hotspots is 0.7022-0.7030 compared to an analytical uncertainty of ~0.00001, a ratio of ~80:1. For $^3He/^4He$ the comparable range is 6.2-9.5 R_A relative to an analytical uncertainty of ~0.05 R_A, a ratio of ~65:1.

Regional variability—Mid-Atlantic Ridge. The two best examples of detailed regional variations in $^3He/^4He$ are the Mid-Atlantic Ridge (MAR) (Fig. 3) and the Southeast Indian Ridge (Fig. 4). The Mid-Atlantic Ridge has been a major focus of ocean ridge geochemical studies, largely through the efforts of J.-G. Schilling and co-workers. It has been especially targeted for numerous studies of mantle plume-

spreading ridge interactions, particularly near Iceland (e.g., Schilling 1973; Hart et al. 1973; Sun et al. 1975; Schilling et al. 1998; Poreda et al. 1986; Hilton et al. 2000b), the Azores (White et al. 1976; Kurz et al. 1982b; Moreira et al. 1999) and in the South Atlantic (Schilling et al. 1985; Hanan et al. 1986; Graham et al. 1992b; Moreira et al. 1995; Kurz et al. 1998; Douglass et al. 1999; Sarda et al. 2000). The variation of $^3He/^4He$ along the Mid-Atlantic Ridge from north of Iceland to south of the Bouvet triple junction is shown in Figure 3. Very high $^3He/^4He$ ratios, near 30 R_A, are present in subaerial lavas centered on the Iceland hotspot. Northward and southward, along submarine portions of the oceanic ridge, $^3He/^4He$ ratios up to 18 R_A are present. The spatial extent of high $^3He/^4He$ ratios, when measured from the center of Iceland to the south along the Reykjanes Ridge, is about twice as long as it is to the north along the Kolbeinsey Ridge (Fig. 3). This has been interpreted as reflecting a more prominent southerly flow of plume material in the upper mantle (Schilling et al. 1998). It has also been noted that where plumes or blobs affect spreading ridges, the wavelength of He isotope variation is sometimes less than that of other tracers such as Sr and Pb isotopes (e.g., Poreda et al. 1993; Mahoney et al. 1994; Taylor et al. 1997; Schilling et al. 1998). This has been attributed to a relatively deep degassing process within the rising mantle plume, causing a strong $^3He/^4He$ peak near the plume center, while relatively degassed plume material that is still effectively traced by Sr, Nd or Pb isotopes becomes laterally dispersed at shallower depths (e.g., Schilling et al. 1998; Breddam et al. 2000).

Other island hotspots, such as the Azores in the North Atlantic, and St. Helena, Tristan da Cunha and Gough Island in the South Atlantic, also show a strong effect on the Sr and Pb isotope compositions of nearby ridge basalts. Their effect on $^3He/^4He$ along the ridge is much less compared to Iceland (Fig. 3), probably due to the smaller He isotopic difference between the hotspot and MORB mantle sources, as well as the more distal nature of those hotspots. The ridge basalts in these regions generally display $^3He/^4He$ ratios <7 R_A, consistent with the hypothesized plume-ridge interaction and the lower $^3He/^4He$ ratios that have been measured at these respective hotspots. For example, in the Azores, $^3He/^4He$ ranges down to 3.5 R_A at the island of Sao Miguel (Kurz et al. 1990), while values as high as 11.3 R_A have been measured at the island of Terceira (Moreira et al. 1999). The lower $^3He/^4He$ ratios are associated with more radiogenic $^{206}Pb/^{204}Pb$ in the Azores, indicating significant He isotope heterogeneity within this plume (Moreira et al. 1999). At St. Helena, Tristan da Cunha and Gough, $^3He/^4He$ is below 6 R_A (Kurz et al. 1982a; Graham et al. 1992a). The low $^3He/^4He$ signatures at these hotspots may indicate the presence of some recycled material in their mantle source, but the origin is still debated (see *He-Sr-Nd-Pb isotopic relations*). The observation that ridge basalts have low $^3He/^4He$ where other isotope tracers suggest plume input to the sub-ridge mantle supports the idea that low $^3He/^4He$ is an intrinsic feature of the hotspot mantle source in these areas, rather than a result of shallow level contamination with crust or lithosphere as suggested for some ocean islands (e.g., Hilton et al. 1995).

In the equatorial Atlantic, the range of $^3He/^4He$ is 8.6-8.9 R_A (Graham et al. 1992), where the combined Sr, Nd and Pb isotope systematics reveal a MORB mantle source that is one of the most highly depleted areas along the global ridge system ($^{87}Sr/^{86}Sr$ = 0.7021, ε_{Nd} = +13, $^{206}Pb/^{204}Pb$ = 17.7; Hanan et al. 1986, Schilling et al. 1994). The He isotope composition of the most depleted MORB mantle therefore appears to lie close to the upper limit of the MORB range away from high $^3He/^4He$ hotspots (≥9 R_A), rather than near the lower end of this range (<7 R_A).

Regional variability—Southeast Indian Ridge. The Southeast Indian Ridge (SEIR) is an ideal location for investigating the geochemical consequences of along-axis variation in mantle temperature, including variations in noble gas isotope composition. From 88°E to 120°E along the SEIR the spreading rate is constant, yet there is an increase in ridge axis depth that implies a gradient in mantle temperature of ~100-150°C from east to west (Sempéré et al. 1997). The hottest mantle appears to be present beneath the Amsterdam-St. Paul (ASP) plateau and the coldest mantle beneath the Australian-Antarctic Discordance (AAD). Going eastward along the SEIR there is also an overall decrease in $^3He/^4He$ and Fe_8 (Graham et al. 2001; Fig. 4). Fe_8 is the FeO content of a basaltic magma, in wt %, after a correction for crystal fractionation during cooling. The reference of 8 wt % MgO chosen for the FeO correction allows a direct comparison of the composition of parental magmas for individual basalts. The numerical value of Fe_8 determined in this way is very useful because it is proportional to the average depth of mantle melting (Klein and Langmuir 1987). Near the Amsterdam-St. Paul plateau, $^3He/^4He$ ratios extend above 14 R_A due to the presence of the ASP hotspot. In the AAD, $^3He/^4He$ ratios are as low as 6.2 R_A. The good covariation of $^3He/^4He$ and Fe_8 over much of the SEIR indicates that higher $^3He/^4He$ may be associated with a higher mean pressure of melting in the underlying Indian Ocean mantle. This type of covariation appears best explained by melting of a heterogeneous mantle, in which blobs or veins of lithologically distinct mantle are embedded within a peridotite matrix. These types of heterogeneities could occur, for example, as veins of garnet pyroxenite that have low $^3He/^4He$, if they originated from recycled crust or lithosphere that was enriched in U and Th. Such recycled components should have very low $^3He/^4He$, <1 R_A, and only a small contribution to the He sampled by the basalts is required. Garnet pyroxenite will melt preferentially to surrounding mantle peridotite because it has a lower solidus temperature and a smaller melting interval. However, the pyroxenite contribution to a magma will be less for melts that begin to form deeper, because the pyroxenitic melts become more effectively diluted by partial melts of peridotite (Hirschmann and Stolper 1996). Therefore, hotter mantle begins to melt deeper and, if pyroxenite is present, these two effects may lead to aggregated MORB melts that have higher values of Fe_8 and $^3He/^4He$.

There are also several peaks in $^3He/^4He$ and Fe_8, ranging between 200 and 500 km in basal width, superposed on the overall gradients along the SEIR (Fig. 4). These peaks are most prominent near the ASP plateau, and at along-axis distances of 910, 1800 and ~2850 km, respectively. The last three peaks occur near the centers of the regional segmentation of the ridge defined by fracture zone anomalies in satellite gravity data. This segmentation reveals several coherent tectonic units, up to ~900 km in along-axis width, that have been stable since the reorientation of the SEIR when it migrated over the Kerguelen hotspot at 38 Ma. Several length scales are therefore discernible in the $^3He/^4He$ variations, including a long (3000 km) gradient, a short

length scale variation of ~150 km especially prominent near the ASP hotspot, and a length scale that roughly coincides with the tectonic segmentation having a half-width of ~450 km. This last scale resembles that for hypothetical, secondary convective cells in the underlying mantle (so-called "Richter rolls"; Richter and Parsons, 1973) that have been proposed on the basis of undulations in the oceanic geoid. This led Graham et al. (2001) to suggest that there can be a strong connection between the length scale of helium isotope variations along an ocean ridge and the length scale of convection in the uppermost mantle, even in the absence of a mantle plume.

Popping rocks. The singular case of the Mid-Atlantic Ridge popping rock should be mentioned. These are rare, glassy mid-ocean ridge basalts that contain large amounts of magmatic gas. They are named for their active 'popping' on the ship's deck just after they have been recovered, due to the rapid release of the gas that was trapped at seafloor pressures of >250 bars. The popping rock from 14°N on the Mid-Atlantic Ridge has been a particular focus of study (Staudacher et al. 1989; Sarda and Graham 1990; Javoy and Pineau 1991; Pineau and Javoy 1994; Burnard et al. 1997; Moreira et al. 1998). It has the highest noble gas and carbon dioxide concentrations of any MORB glasses found to date, and is often considered to most closely represent the noble gas isotope signature of the upper mantle, because the highest analytical precision is obtained from its analyses.

The $^3He/^4He$ ratio of this popping rock is 8.14±0.06 R_A (Sarda and Graham 1990), typical for N Atlantic MORB (Table 2). Helium concentrations are between 50-90$\times10^{-6}$ std cm^3/g (Staudacher et al. 1989; Sarda and Graham 1990; Moreira et al. 1998), which is 5-10 times larger than the mean concentration in other MORB glasses. The popping rock is also notable for having an extreme vesicularity, up to 17%, and vesicle size distributions consistent with continuous nucleation and growth and no significant bubble loss. The measured $^4He/^{40}Ar$ ratios of 1.3-1.8 are the lowest in MORB glasses and are close to the expected radiogenic production ratio for the upper mantle (~3 when integrated over 10^9 years). This is a further indication that no significant bubble loss has occurred, otherwise there would be a very strong enrichment of Ar relative to He based on vapor/melt partitioning predicted from experimentally measured solubilities (see *Argon-Helium Systematics*). The popping rock is usually taken as an analog for a relatively undegassed MORB magma. The degassing flux of He at ridge crests, computed from the MORB helium deficit relative to the popping rock and from the crustal production rate by seafloor spreading (2-4$\times10^{16}$ g y^{-1}), is similar to that derived from the ^3He inventory of the deep ocean (Sarda and Graham 1990; see below).

Ridge helium flux. Because He is lost from the atmosphere, it is not possible to determine its integrated degassing history over geological time. However, an 'instantaneous' picture of the degassing at ridge crests can be obtained from the excess ^3He in the abyssal ocean and the upwelling rate as estimated from a ^{14}C box-model age (~1000 years for the deep Pacific; Craig et al. 1975). The ^3He flux estimated in this way is ~4±1 atoms cm^{-2} sec^{-1} (~1100 mol y^{-1}). In principle, this also provides a means to determine the flux of other elements at ridge crests using elemental/^3He ratios in hydrothermal vent fluids and MORB glasses (e.g., Edmond et al. 1982; Des Marais and Moore 1984; Marty and Jambon 1987; Sarda and Graham 1990; Graham and Sarda 1991), and to corroborate estimates for convective heat loss at ridge crests using vent fluid ^3He-temperature relationships (e.g., Jenkins et al. 1978; Lupton et al. 1989).

The value of the deep ocean He flux allows limits to be placed on the amount of U and Th in that part of the mantle which is being outgassed at ridges. If the production rate of ^4He by radioactive decay equals its loss rate from a mantle reservoir, then the reservoir is at steady-state and the short-term approximation applies (i.e., $t << 1/\lambda$ and $e^{\lambda t}-1 \approx \lambda t$). If the reservoir has a homogeneous $^3He/^4He$ ratio (a good approximation for the upper mantle MORB source), then the accompanying flux of ^3He is given by

$$F_3 = \{8\lambda_{238} + (7/137.88)\lambda_{235} + 6\lambda_{232}\} ([U]/238) M (^3He/^4He) \quad (2)$$

where M is the mass of the reservoir. Estimates for upper mantle λ are ~2.5 based on U-series studies of MORBs (e.g., Allègre et al. 1986; O'Nions and McKenzie 1993). The [U] of the upper mantle is ~5 ppb (5$\times10^{-9}$ g/g rock) based on models for the transfer of heat producing elements to the continental crust over time (O'Nions et al. 1979). Assuming the mantle above the 660 km seismic discontinuity (M = 1.1$\times10^{27}$ g) has $^3He/^4He$ = 1.2$\times10^{-5}$ (the mean MORB value of 8.7 R_A from Table 2) and these U and Th contents, the calculated ^3He flux is ~520 mol y^{-1}. Obviously a larger proportion of depleted mantle (M = 2.2$\times10^{27}$ g or ~50% of the whole mantle) could bring this calculation in line with the observed flux of 1100 mol y^{-1} at ridge crests. However, the total oceanic heat flux of 20$\times10^{19}$ cal y^{-1} needs to be considered as well. The ^4He/heat production ratio at secular equilibrium is ~4$\times10^{12}$ atom ^4He/cal. A ^3He flux of 1100 mol y^{-1} corresponds to a ^4He flux of 9.3$\times10^7$ mol y^{-1}, and a heat flux of 1.4$\times10^{19}$ cal y^{-1}. Therefore, the amount of radiogenic production supplying the ^4He flux at ridges supplies a maximum of 7% of the observed heat flux (O'Nions and Oxburgh 1983; van Keken et al. 2001). Much of the ^4He flux at ridges appears to be sustained by radiogenic production in the upper mantle, but most of the ^3He and heat fluxes appear to ultimately derive from either a deep mantle reservoir (O'Nions and Oxburgh 1983) or perhaps from the core (Porcelli and Halliday 2001). This concept has directly led to steady-state models for the upper mantle (Kellogg and Wasserburg 1990; O'Nions and Tolstikhin 1994, 1996; Porcelli and Wasserburg 1995a,b; Porcelli and Ballentine 2002) that critically depend on the noble gases measured in MORBs and OIBs.

Cosmic dust. Anderson (1993) argued that subduction of interplanetary dust particles (IDPs) in marine sediments could have supplied a significant amount of ^3He to the mantle over geologic time. However, extraordinarily high fluxes of IDPs in the Archean would be required to account for the amount of ^3He that is degassing at ocean ridges today (see above discussion). The terrestrial supply of ^3He from cosmic dust also depends critically on the size distribution of IDPs that survive atmospheric entry, because this controls the amount of ^3He retained during frictional heating and ablation (Trull 1994; Farley et al. 1997). Furthermore, the Anderson model requires insignificant diffusive loss of ^3He from IDPs during sediment subduction, despite experimental evidence that such loss is complete at subduction zone depths <25 km and temperatures <200°C (Hiyagon 1994b). Therefore, compared to volcanic degassing,

this source of ^{3}He is unimportant from a mantle geochemistry viewpoint.

Relation to major volatiles. The major volatile species in oceanic basalts are carbon dioxide and water. Carbon dioxide has a lower solubility than water in basaltic melts, and it often reaches saturation levels even when eruption occurs at water depths of 4 to 5 km, which makes CO_2 the dominant gas species contained in vesicles. Because noble gases have relatively low solubilities they also tend to be concentrated in vesicles. Based on a global survey of MORB glasses, the helium in vesicles appears to be in Henry's Law equilibrium with the melt (Kurz and Jenkins 1981). This is not generally true of CO_2, which can be saturated or even over-saturated at the pressure corresponding to the eruption depth (e.g., Stolper and Holloway 1988: Dixon et al. 1988; Kingsley and Schilling 1995). This has been attributed to very rapid rise of magma, from depths in the crust at which it was last saturated with CO_2, to the site of eruption and quenching on the seafloor.

Since the seminal paper by Marty and Jambon (1987), the C/^{3}He ratio has been a parameter of considerable interest in chemical geodynamics of the mantle. The CO_2/^{3}He ratio of MORBs varies over a relatively narrow range. Marty and Jambon (1987) suggested that the best estimate of the upper mantle ratio was 2×10^9, on the basis of a small data set for MORB glasses. More detailed work by Marty and Zimmerman (1999) revealed that the range of values is from ~3×10^8 to ~8×10^9, but the mean is still similar to the original estimate. In this latter study the measured CO_2/^{3}He ratio was corrected for potential atmospheric contamination and gas loss, using the He and Ar concentrations and isotope compositions measured in the same samples along with experimentally determined He and Ar solubilities for basalt melts, and assuming that the magma originally had the radiogenic production ratio of ^{4}He/^{40}Ar that is appropriate for the mantle (see the section *Argon-Helium Systematics* for more discussion of this approach). Ocean ridge basalts from more enriched mantle sources, as indicated by ^{87}Sr/^{86}Sr or K/Ti ratios, generally have higher CO_2/^{3}He (Kingsley and Schilling 1995; Marty and Zimmerman 1999). These variations in CO_2/^{3}He probably reflect heterogeneities in mantle-source composition, perhaps as a result of subduction zone recycling of surface-derived carbon.

Overview. The amplitude and length scales of ^{3}He/^{4}He variations along ridges appear to be fundamentally related to the scales of solid state mixing in the uppermost parts of the mantle, and have been especially useful for investigating chemical geodynamics of mantle plume-spreading ridge interactions. The helium isotope composition of the MORB mantle source away from the influence of hotspots and plumes is best described by a relatively narrow range in ^{3}He/^{4}He, with >90% of those ridge basalts lying between 6.5-9.5 R_A. The median ^{3}He/^{4}He ratio is similar for MORBs from each ocean basin (8.08 to 8.24 R_A; Table 2). Values above 11 R_A are observed near the Iceland hotspot (up to 18 R_A along the Reykjanes Ridge and 13 R_A along the Kolbeinsey Ridge; Fig. 3), along the Easter Microplate (12 R_A), near the Shona-Discovery-Bouvet hotspots (up to 15 R_A) in the South Atlantic, in the Red Sea and Gulf of Tadjoura (15 R_A) near the Ethiopian mantle plume, and along the Southeast Indian Ridge near the Amsterdam-St. Paul plateau (14 R_A; Fig. 4). In the singular case of the super-fast spreading region of the southern East Pacific Rise, relatively high ^{3}He/^{4}He ratios (up to 11 R_A) are observed between 16 and 18°S despite the absence of a nearby ocean island hotspot. In this region other isotopic and geochemical anomalies are also observed, suggesting the presence of either an (as yet) undetected hotspot, or a mantle 'blob' that was embedded in the upper mantle flow (Mahoney et al. 1994). The lowest ^{3}He/^{4}He ratios along the global ridge system are also found in areas of geochemical anomalies, such as along the southern Chile Rise (down to 3.5 R_A), within the Australian-Antarctic Discordance (6.2 R_A), and at 33°S on the Mid-Atlantic Ridge (6.2 R_A), the latter being another region suggested to be affected by a mantle 'blob' or heterogeneity (Michael et al. 1994). In the singular case of Axial Volcano on the Juan de Fuca Ridge, ^{3}He/^{4}He lies within the range of ~8-9 R_A (Lupton et al. 1993), despite bathymetric, morphological, and isotopic evidence for the presence of a relatively weak hotspot (e.g., Eaby et al. 1984; Hegner and Tatsumoto 1989).

The fact that the range of ^{3}He/^{4}He variation along ridges is small in comparison to the global range including ocean islands certainly implies that mixing rates in the upper mantle MORB source are relatively rapid. Nevertheless, the range in MORBs is significant, and it results from a combination of (1) input of high ^{3}He/^{4}He material from deeper in the mantle, (2) radiogenic ingrowth in the upper mantle, (3) input of subducted crust and lithosphere that is enriched in U and Th (perhaps directly to the upper mantle or perhaps though mantle plumes), and (4) partial melting of upper mantle that is chemically or mineralogically heterogeneous.

A comparison of observed and calculated helium and heat fluxes at ocean ridges suggests that a deep mantle reservoir supplies most of the ^{3}He and heat to the upper mantle (O'Nions and Oxburgh 1983; Kellogg and Wasserburg 1990). The involvement of such a deep reservoir in the upper mantle heat and mass balance appears to make it inescapable that some form of stratification is present within the mantle, and that the mantle source of some ocean islands, such as Hawaii and Iceland, lies below the mantle source for ocean ridges.

Ocean island basalts

The highest magmatic ^{3}He/^{4}He ratios are found at ocean island localities such as Hawaii and Iceland, where they extend to values above 30 R_A. (The highest values to date are 35-43 R_A, found in the Miocene alkali basalts of northwest Iceland; Breddam and Kurz 2001). Other prominent, high ^{3}He/^{4}He localities include Galápagos, Samoa, Réunion, Easter, Juan Fernandez, Yellowstone and the Ethiopian Rift. The presence of such high ^{3}He/^{4}He ratios at these sites of extensive volcanism is consistent with the existence of mantle plumes or thermal upwellings from regions deep in the Earth. Parts of these deep regions may have remained more effectively isolated over geological time. They are thereby less degassed, and have lower time-integrated (U+Th)/^{3}He compared to the shallower mantle source regions for MORB. (Further support for deep, relatively undegassed regions of the mantle comes from the Ne isotope composition of MORBs and OIBs, as discussed in the section *Ne Isotopes*). Significant spatial and temporal variability in ^{3}He/^{4}He also occurs at ocean islands. This variability may be related to distance from the center of the mantle upwelling beneath an island, or to the

stage of a volcano's evolution (e.g., seamount, shield or post-erosional). This variability can often be accounted for by variability in mixing between plume-derived material and material derived from the upper mantle, or by isotopic heterogeneity within the plume itself.

Global variability—relation to geologic and tectonic conditions. One might expect some systematic, global relationships between $^3He/^4He$ and other geological parameters. For example, interaction between a plume-derived magma and oceanic lithosphere may serve to lower $^3He/^4He$ ratios by shallow-level addition of radiogenic He (Hilton et al. 1995). As a consequence, the $^3He/^4He$ variability and the transition to lower $^3He/^4He$ at some localities might then be related to the speed of the overlying plate or to the magma supply rate (e.g., Kaneoka and Takaoka 1991). At the present time it is difficult to generalize about these issues, given the limited number of well studied ocean island hotspots and the fact that each one is somewhat unique in its setting. Key geological parameters of interest include the depth of plume origin, the plume mass flux, the extent and depth of partial melting, the proximity of a hotspot to a plate boundary (e.g., spreading ridge, continental margin, island arc), and the velocity and age (thickness) of the overlying plate. Some of these parameters, such as the depth of plume origin, are not readily quantified; others, such as depth and extent of partial melting, are relatively uncertain or show a large range. The $^3He/^4He$ ratios observed at ocean islands are compared on the basis of plume flux, lithosphere age and plate speed in Figure 5a-c.

The Hawaiian hotspot represents, by far, the largest plume mass flux (Fig. 5a). It is situated beneath a fast moving plate (100 mm/y) and old (mid-Cretaceous) lithosphere far from any plate boundaries. The highest $^3He/^4He$ ratios at Hawaii, up to 35 R_A, are found at Loihi Seamount, the youngest active volcano in the island chain (Kurz et al. 1982a, 1983; Rison and Craig 1983; Kaneoka et al. 1983; Hiyagon et al. 1992; Honda et al. 1993b; Valbracht et al. 1997; Hilton et al. 1997). High $^3He/^4He$ ratios persist throughout most of the tholeiitic shield building stage at Hawaiian volcanoes, and tend to show a rapid decrease near the end of this stage to values near 8 R_A characteristic of the ambient upper mantle (e.g., Kurz 1993; Kurz et al. 1983, 1987, 1996; Kurz and Kammer 1991; Rison and Craig 1983; Kaneoka 1987; Kaneoka and Takaoka 1978, 1980; Vance et al. 1989; Honda et al. 1993b; Roden et al. 1994; Mukhopadhyay et al. 1996).

The Iceland hotspot is ridge-centered, has a moderate plume flux (Fig. 5a), and shows a large spatial variability in basalt $^3He/^4He$, from high ratios (>40 R_A) to values lower than those typically found along spreading ridges (down to 5 R_A: Condomines et al. 1983; Kurz et al. 1985; Poreda et al. 1992; Burnard et al. 1994b; Marty et al. 1991; Hilton et al. 1990, 1998, 1999; Harrison et al. 1999; Breddam et al. 2000; Dixon et al. 2000; Moreira et al. 2001; Breddam and Kurz 2001). Much lower values (down to 0.07 R_A) are found in silicic and highly evolved volcanic rocks in Iceland, but lower crustal melting is involved in their petrogenesis and their $^3He/^4He$ ratios do not carry useful information about the underlying mantle (Condomines et al. 1983). The very high $^3He/^4He$ values are known to have persisted since the inception of the Iceland plume (Graham et al. 1998; Marty et al. 1998; Stuart et al. 2000; Kirstein and Timmerman 2000). The spatial and temporal variations at Hawaii and Iceland are usually interpreted to result from mixing, between a plume source and ambient upper mantle or lithosphere.

Samoa, like Iceland, has a moderate plume flux, but it is located on a fast moving plate near the Tonga Trench. It shows high, but variable, $^3He/^4He$ ratios (11-24 R_A) during its alkalic shield-building stage (Farley et al. 1992; Poreda and Farley 1992). These variations have been attributed to mixing between a plume source and recycled components derived from the nearby subduction zone (Farley 1995).

The Canary Island hotspot (including Madeira) in the eastern Atlantic has a small plume flux (Fig. 5a) and is situated on the oldest lithosphere in the ocean basins (Jurassic, >170 Ma; Fig. 5b), and adjacent to a continent on the very slowly moving African plate (≤5 mm/y; Fig. 5c). Its lavas show a $^3He/^4He$ range of 5.5 to 8.9 R_A (Graham et al. 1996c; Hilton et al. 2000a).

Other ocean island areas that have been studied in some detail for $^3He/^4He$ that should be mentioned in the context of tectonic setting include Réunion, the Galápagos archipelago, the Azores, the Amsterdam-St. Paul plateau, Juan Fernandez, and Heard Island (Fig. 5). Réunion is an intraplate hotspot located on a slow moving plate (15 mm/y). It shows relatively homogenous $^3He/^4He$ ratios (11-13 R_A) for long time periods during its volcanic shield-building stage (Staudacher et al. 1986, 1990; Kaneoka et al. 1986; Graham et al. 1990; Marty et al. 1993a; Hanyu et al. 2001). This stage is followed by MORB-like ratios during the very latest stages of island volcanism, such as in Recent lavas from Mauritius (Hanyu et al. 2001), making it similar in this regard to Hawaii. The Galápagos and Amsterdam-St. Paul (ASP) hotspots are each near a spreading ridge that is migrating away from the hotspot. These two hotspots have different plume fluxes (moderate at Galápagos and low at ASP), and they are located beneath plates having very different velocities (40 mm/y at Galápagos and 6 mm/y at ASP). Values of $^3He/^4He$ in the Galápagos archipelago range up to 30 R_A (Graham et al. 1993; Kurz and Geist 1999). Although no island lavas from Amsterdam or St. Paul have yet been analyzed, the influence of the ASP hotspot is evident on the nearby spreading ridge, with $^3He/^4He > 14$ R_A.

Spatial variability. There are significant spatial variations in $^3He/^4He$ at some ocean islands. The best-studied examples are the Canary Islands, the Azores, the Galápagos Islands, Juan Fernandez and Heard Island.

The Canary Islands are one of the most interesting localities for studying spatial variations in $^3He/^4He$, because young volcanism has occurred at all the islands except Gomera. Olivine and clinopyroxene phenocrysts separated from volcanic rocks show a range in $^3He/^4He$, between 5.5 to 8.9 R_A (Fig. 6). This range includes all historical and Quaternary lavas, the Pliocene lavas from Gomera, and the Miocene (shield) and Pliocene lavas of Gran Canaria (data from Vance et al. 1989; Graham et al. 1996c; Hilton et al. 2000a). The highest $^3He/^4He$ ratios are from the Pliocene series of Taburiente caldera on La Palma, where they extend up to 8.9 R_A (Graham et al. 1996c;

Hilton et al. 2000a). A value of 9.5 R_A, higher than any value found in the lavas, is reported for a cold mineral spring inside Taburiente caldera (Perez et al. 1994; Hilton et al. 2000a). Hilton et al. (2000a) interpret this as evidence that the Canaries are derived from a high-$^3He/^4He$ plume source, similar to that at Hawaii and Iceland. This is somewhat of a controversial point because the highest $^3He/^4He$ values found in the Canary Islands are within the upper limit of the MORB range (Table 2), although it is difficult to precisely define a limiting value for depleted MORB. Certainly this upper limit includes the highest values of 8.9 R_A as measured in Canary lavas. Values as high as 9.7 R_A are found in some MORB glass samples with very depleted isotopic signatures (e.g., ε_{Nd} up to +11; Mahoney et al. 1994), and in areas away from any known plume influence (Graham et al. 2001), suggesting the possibility that the groundwater value of 9.5 R_A seen at La Palma originates from a depleted MORB mantle source. More comparative work of volcanic rocks and associated fluids is needed to resolve this issue.

The Galápagos archipelago represents an ideal case for investigating spatial geochemical variability, because coeval volcanism has occurred over a lateral distance of ~500 km. It forms an interesting contrast to the Canary Islands, given their similar plume fluxes. In the Galápagos, $^3He/^4He$ ratios show extreme spatial variability, from high values in the west and south (up to 30 R_A at Fernandina), to MORB-like values in the east (Fig. 7; Graham et al. 1993; Kurz and Geist 1999). The variations are likely related to entrainment of upper mantle by a sheared mantle plume (White et al. 1993; Harpp and White 2001). In contrast, $^3He/^4He$ ratios above 9 R_A appear to be absent along the Galápagos Spreading Center (Detrick et al. 2002; Graham, unpublished data), despite unambiguous geochemical and geophysical evidence for the plume's influence there (e.g., Schilling et al. 1982; Verma and Schilling 1982). Either the plume material feeding the sub-ridge mantle is derived from the outer portions of the plume stem where the Sr-Nd-Pb isotopic enrichment is associated with lower $^3He/^4He$ ratios, or any high $^3He/^4He$ plume material that reaches the melting region below the ridge has undergone significant helium loss during an earlier stage of melting or degassing (Graham et al. 1993).

In the Juan Fernandez Islands, $^3He/^4He$ ratios show a significant variation despite relatively constant Sr and Nd isotopes. At Mas a Tierra, $^3He/^4He$ ranges between 11-18 R_A, while at Mas Afuera, values are lower and in the MORB range between 7.8 and 9.5 R_A. (Farley et al. 1993). The Mas a Tierra lavas can be further subdivided into two groups that show no overlap in He isotope composition; the alkalic and tholeiitic shield group has $^3He/^4He$ = 14.5-18.0 R_A, and the post-shield basanite group has $^3He/^4He$ = 11.2-13.6 R_A. Farley et al. (1993) interpret the $^3He/^4He$ variations as the result of mixing between plume and upper mantle sources. The relatively constant $^{87}Sr/^{86}Sr$ and $^{143}Nd/^{144}Nd$ at the islands then requires that the plume component initially had a heterogeneous distribution of volatiles, or that it underwent extraction of small degree partial melts, lowering its He/Sr and He/Nd ratios prior to the mixing event.

At Heard Island, on the Kerguelen Plateau in the southern Indian Ocean, $^3He/^4He$ ratios show a bimodal distribution that is geographically controlled (Hilton et al. 1995). The Laurens Peninsula volcanic series has a relatively narrow range of $^3He/^4He$, 16.2-18.3 R_A. The Big Ben series lavas, which erupted from the main volcano of the island, have $^3He/^4He$ ratios between 5 and 8.4 R_A. The high $^3He/^4He$ ratios on the peninsula are surprising, because the center of the plume is thought to be on the northwest margin of the Kerguelen Plateau ~550 km away. The high $^3He/^4He$ ratios might be explained by either a fossil remnant of the plume that was embedded in the lithosphere and reactivated by magmatism associated with Big Ben volcano, or by the existence of two plumes beneath the plateau (Hilton et al. 1995).

Temporal variability. The best examples of temporal change are for tholeiitic lavas from the shield building stage of Mauna Loa and Mauna Kea on the island of Hawaii, and for the alkalic shield stage lavas from Tutuila (American Samoa).

Dated lavas from Mauna Loa show a decrease in $^3He/^4He$ with time, with a transition from ~15 R_A to ~8-9 R_A near 14,000 years ago (Kurz and Kammer 1991). The decrease has been suggested to be the result of melting and mantle processes, rather than of magma chamber or metasomatic effects that selectively involve gaseous elements, because there is some coherent behavior between He and the other isotopic tracers during the transition. According to this model, the He, Pb, Sr and Nd isotope changes result from a diminishing plume contribution to Mauna Loa shield volcanism through time. A subsequent He isotope investigation of Mauna Kea volcanism, through the Hawaii Scientific Drilling Project (HSDP), shows a similar change near the end of the shield building stage at Mauna Kea (Fig. 8), also with He and Nd isotope evidence for less plume involvement through time (Kurz et al. 1996; Lassiter et al. 1996). Lavas from the upper section of the HSDP core, between 240-270 m, were erupted from Mauna Loa and have $^3He/^4He$ between 13.9–15.8 R_A, similar to values found in Mauna Loa subaerial lavas that are >30,000 years old. The upper section of the Mauna Kea sequence, between 290-620 m, has $^3He/^4He$ between 6.8-7.0 R_A, similar to MORB values (Fig. 8). A single sample from this section has $^3He/^4He$ of 6 R_A, among the lowest values found at Hawaiian volcanoes. Some later-stage radiogenic He addition may be involved, but its origin is unclear. At depths below 620 m, higher $^3He/^4He$ values are found, ranging up to 12.5 R_A. The transition from high $^3He/^4He$ to MORB–like values occurs within the end of the tholeiitic shield stage of Mauna Kea (Kurz et al. 1996).

In contrast, the stratigraphic section from Tutuila (American Samoa) shows a large variation in $^3He/^4He$, between 11-24 R_A (Fig. 9). There are large excursions in isotope composition over relatively short time periods, and no systematic trend though time (Farley et al. 1992). The variations appear to represent mixing of two isotopically extreme mantle components. The highly enriched component is characterized by radiogenic $^{87}Sr/^{86}Sr$ and low $^3He/^4He$, and may originate from recycled crustal material injected into the rising plume from the nearby subduction zone (Farley et al. 1992; Farley 1995). The high $^3He/^4He$ component has intermediate Sr, Nd and Pb isotope ratios compared to the full range of OIBs and MORBs. The rapid temporal variations in He, Sr, Nd and Pb isotopes at Samoa, without a systematic trend, indicate that the hypothesized mixing process must be erratic. This might occur when a deep rising

plume intercepts and melts recycled crustal material trapped at a boundary layer in the mantle (Farley et al. 1992).

Relation to major volatiles. Studies of the $CO_2/^3He$ ratio have received the most attention in terms of the relations between helium and major volatiles at ocean islands. Investigations have included basalt glasses, ultramafic xenoliths, vent fluids and fumarole gases. The initial work by Marty and Jambon (1987) used previously published analyses for Loihi basalt glasses, and for Kilauea and Iceland fumaroles, arriving at a mean $CO_2/^3He$ of ~4 $\times 10^9$ for high $^3He/^4He$ island localities. This value appears to be slightly higher than for MORBs, but as suggested by Marty and Jambon (1987), it should be used with care. CO_2 and He have different solubilities in aqueous fluids and so it is possible that some of the variation stems from using vent fluid data, although there is no evidence to date that hydrothermal processes fractionate CO_2 from He to a significant degree. The mean $CO_2/^3He$ ratio in Kilauea summit fumaroles is now better constrained to be ~7×10^9 (Hilton et al. 1997), near the upper end of the MORB range. Subsequent work by Hilton et al. (1998a) also showed that large variations, from 6×10^8 to 5×10^9, occur over time periods of months in Loihi vent fluids. They suggest that these changes are related to C-He fractionation during a magmatic degassing event associated with seismic tremor and a possible summit eruption in 1996 (Garcia et al. 1998).

Considerable insight into OIB C-He relations has been gained from studies of ocean island xenoliths. Of special note are the laser extraction studies performed on ultramafic xenoliths from Réunion and Samoa by Burnard et al. (1994a, 1998). Much of the range in $CO_2/^3He$ at ocean islands (~1-20$\times 10^9$; Trull et al. 1993) can be observed at microscopic scales in a single magmatic cumulate nodule of dunite from Réunion ($CO_2/^3He$ = 1-10$\times 10^9$; Burnard et al. 1994a). The $CO_2/^3He$ ratio does not show any systematic variation as a function of fluid inclusion morphology or generation (e.g., primary vs. secondary). The observed variations may be related to the presence of immiscible melts having very different C solubilities, because there are rare examples of highly alkaline glassy inclusions preserved in Réunion lavas. The Samoan xenolith studied by Burnard et al. (1998) using laser extraction is even more complex than the Réunion xenolith, having numerous stages of melt and fluid inclusion growth. Very high $CO_2/^3He$ ratios were measured in this sample, between 11-41$\times 10^9$, but this sample may have suffered considerable diffusive loss of He, because many of the Samoan xenoliths have anomalously low $^4He/^{40}Ar^*$ ratios (~0.1) compared to the expected mantle production ratio (~1.5-4.0; see *Argon-Helium Systematics* for further discussion on using $^4He/^{40}Ar^*$).

The range of values of $CO_2/^3He$ for MORBs and OIBs is strikingly similar to the range of chondritic values estimated by Marty and Jambon (1987). Trull et al. (1993) showed that, while there was overlap between the $CO_2/^3He$ ratios of MORBs and OIBs, the basalts and xenoliths from high $^3He/^4He$ ocean islands also have considerably higher $CO_2/^4He$ ratios (the OIB range is 4-40$\times 10^4$ compared to the MORB range of 0.5-7$\times 10^4$). Trull et al. (1993) suggested that the roughly similar $CO_2/^3He$, but lower $^3He/^4He$ and $CO_2/^4He$ for MORBs compared to OIBs, was produced by radiogenic ^4He production in the upper mantle, consistent with the steady-state upper mantle model for helium proposed by Kellogg and Wasserburg (1990). Preferential carbon recycling to the upper mantle would lead to a higher $CO_2/^3He$ in MORBs compared to OIBs. The similarity of $CO_2/^3He$ between mid-ocean ridges and ocean islands having high $^3He/^4He$ appears to require carbon recycling to the OIB mantle source (Trull et al. 1993).

He-Sr-Nd-Pb isotope relations. Helium isotopes for MORBs and OIBs are plotted against $^{87}Sr/^{86}Sr$, $^{143}Nd/^{144}Nd$, $^{206}Pb/^{204}Pb$ and $^{208}Pb^*/^{206}Pb^*$ in Figure 10a-d. The highest $^3He/^4He$ ratios occur at intermediate values of Sr, Nd and Pb isotopes (Kurz et al. 1982a; Farley et al. 1992; Graham et al. 1993; Hanan and Graham 1996; Hilton et al. 1999). There is some covariation between He and the other isotope systems, particularly when data from individual localities are considered alone; but there are no simple global systematics. Mixing between MORB and OIB 'components' is usually invoked to explain much of the isotopic variation in oceanic basalts. However, the relationships between OIB mantle components and mantle reservoirs, if there are any, is unclear. At least 5 mantle components, including the MORB mantle, can be identified from the multi-isotopic approach (White 1985; Zindler and Hart 1986b). Some of the helium isotope variation in OIBs, and its relation to Pb, Nd and Sr isotope variations, appears to be adequately explained by mixing between high-$^3He/^4He$ plume material and MORB mantle. Ancient melting events are primarily responsible for the evolution of the MORB mantle to low $^{87}Sr/^{86}Sr$ and high $^{143}Nd/^{144}Nd$ ratios. In contrast, recycling of crust or lithosphere appears to play a dominant role in the Sr-Nd-Pb isotopic signatures of many OIBs, especially for the Kerguelen and Society island sources having $^{87}Sr/^{86}Sr>0.705$ (White 1985).

It is important to continually bear in mind that crustal material should have extremely low $^3He/^4He$ (~0.1 R_A) if it is degassed and more than 10-100 million years old. Yet the lowest $^3He/^4He$ ratios observed at ocean island localities suggested to contain such recycled components are about 3-5 R_A, or 300-500 times larger than the expected value. If recycled material is present in an OIB mantle source region, then the fraction of He from such a component must be extremely low for any of the island systems studied so far (e.g., Farley 1995).

The islands of Tristan da Cunha and Gough in the South Atlantic are notable because they have Pb, Nd and Sr isotope characteristics similar to hypothetical values for the bulk silicate Earth. Kurz et al. (1982a) showed that $^3He/^4He$ was 5-6 R_A at these islands, lower than MORB values (Fig. 10a), indicating that a primitive mantle reservoir is not involved. On this basis, Kurz et al. (1982a) suggested that recycled crust was present in the Tristan and Gough mantle source regions.

In the Azores, $^3He/^4He$ ranges between 3.5 R_A and 11.3 R_A (Kurz et al. 1990; Moreira et al. 1999) and there is a good covariation of $^3He/^4He$ with Pb isotopes at the scale of the archipelago, indicating significant He isotope heterogeneity within the mantle source region (Moreira et al. 1999). The lowest $^3He/^4He$ is associated with elevated $^{207}Pb/^{204}Pb$ in basalts from Sao Miguel (which are among the highest observed at any ocean island), while the highest $^3He/^4He$ occurs in lavas from Terceira that have relatively radiogenic $^{206}Pb/^{204}Pb$ and typical OIB $^{207}Pb/^{204}Pb$. Moreira et al. (1999)

interpret these variations with a 3-component mixing model involving lower mantle (having high $^3He/^4He$) that was entrained into a mantle plume containing recycled crust (with radiogenic $^{206}Pb/^{204}Pb$). The low $^3He/^4He$ signature at Sao Miguel is attributed to shallow level mixing between the plume and km-size rafts of continental lithosphere that were delaminated into the shallow mantle during Jurassic rifting and opening of the North Atlantic.

The Cape Verde Islands show a pattern of $^3He/^4He$ and $^{206}Pb/^{204}Pb$ variation that is similar to that of the Azores, although with slightly less radiogenic Pb (Christensen et al. 2001). $^3He/^4He$ ratios in the Cape Verdes are both higher and lower than are typically found in MORBs. Values range between 3.2 and 13.8 R_A in primitive lavas from the islands of Santo Antão and Fogo, and there is no systematic variation with age. These variations appear to be broadly consistent with the 3-component model of Moreira et al. (1999) for the Azores, but in detail the lithospheric component involved in the Cape Verdes must be different (Christensen et al. 2001).

At Heard Island the $^3He/^4He$ ratios are bimodal (Hilton et al. 1995). The Laurens Peninsula volcanic series has $^3He/^4He$ between 16.2 and 18.3 R_A, while the Big Ben series lavas have $^3He/^4He$ between 5 and 8.4 R_A. Heard Island shows a range in $^{87}Sr/^{86}Sr$ and $^{206}Pb/^{204}Pb$ that is among the largest seen at a single ocean island (Barling et al. 1994), in some cases with extremely radiogenic Sr ($^{87}Sr/^{86}Sr > 0.706$). The Laurens Peninsula lavas are relatively homogeneous in Sr-Nd-Pb isotopes, while the Big Ben series is heterogeneous. Strongly curvilinear Pb-Nd and Pb-Sr isotope arrays, and linear Pb-Pb arrays, indicate that the genesis of Heard lavas involves binary mixing (Barling and Goldstein 1990). The bimodal distribution of $^3He/^4He$ does not follow this simple relationship, however, and Hilton et al. (1995) suggested that the low $^3He/^4He$ ratios were derived by contamination from radiogenic He in the Kergeuelen lithosphere, which may partly have a continental origin (Barling et al. 1994). Based on the He isotope results for Heard Island, Hilton et al. (1995) called into question whether the low $^3He/^4He$ seen at other ocean islands, such as Tristan da Cunha, Gough and St Helena could have an origin from recycled material, because those islands are characterized by relatively few He isotope analyses, and some of the phenocrysts have low He contents which could make them more susceptible to contamination by radiogenic He.

Relatively low $^3He/^4He$ ratios also typify islands with the most radiogenic $^{206}Pb/^{204}Pb$ ratios (the 'HIMU' component, or high μ, where $\mu = {}^{238}U/^{204}Pb$) such as St. Helena and the Cameroon Line in the South Atlantic, and the Cook-Austral islands in the South Pacific (Graham et al. 1992a; Hanyu and Kaneoka 1997; Barfod et al. 1999). The HIMU component has been variably interpreted to originate from recycled ocean crust (Hofmann and White 1982; Zindler et al. 1982; Chauvel et al. 1992; Hanan and Graham 1996; Hanyu and Kaneoka 1997), carbonatite metasomatism (Tatsumoto 1984), intra-mantle differentiation by silicate melts (Halliday et al. 1990; Barfod et al. 1999), recycled and metasomatized continental lithosphere (McKenzie and O'Nions 1995), and recycled oceanic lithosphere (Moreira and Kurz 2001). The significance of low $^3He/^4He$ values at these ocean island localities is further complicated, because low ratios might also be produced by interaction with the oceanic lithosphere through which OIB magmas ascend, or by prolonged storage of degassed magma at crustal levels (Zindler and Hart 1986a; Graham et al. 1988). Thorough studies of "low-$^3He/^4He$" islands are needed to resolve many of these issues.

At the present time, the myriad of mantle components inferred from the Sr-Nd-Pb isotopes cannot be adequately placed into a reservoir framework within the mantle. Many of the components appear to be ubiquitous. For example, the enriched type of mantle present at some ocean islands also appears to comprise a worldwide pollutant of the MORB mantle (Hanan and Graham 1996). Furthermore, while it is obvious that the MORB mantle is well characterized for $^3He/^4He$, it is currently not possible to identify a single value of $^3He/^4He$ (or even a narrow range of values) that characterize each of the OIB isotopic end-members. One possible exception to this is the relatively uniform and low $^3He/^4He$ ratios (<7 R_A) of HIMU lavas, which suggests that this may be a general characteristic of this mantle source type (Graham et al. 1992; Hanyu and Kaneoka 1997).

In a global context, there is a convergence of individual ocean island isotopic arrays on a roughly similar composition that lies internal to the OIB end-members (Hart et al. 1992; Farley et al. 1992; Hauri et al. 1994; Hanan and Graham 1996). This convergence implies the presence of a distinct mantle reservoir with approximately the following characteristics; $^{87}Sr/^{86}Sr = 0.703\text{-}0.704$, $^{143}Nd/^{144}Nd = 0.51285\text{-}0.51295$ (ε_{Nd} = 4-6) and $^{206}Pb/^{204}Pb = 18.5\text{-}19.5$. This is a large range. Nevertheless, $^3He/^4He$ of individual OIB suites often shows an increasing trend toward these intermediate compositions (Farley et al. 1992; Graham et al. 1993). Indeed, the highest measured $^3He/^4He$ in a lava for which Sr, Nd and Pb isotope data are also available, from Selardalur in northwest Iceland (Hilton et al. 1999), lies in this range (see Fig. 10). From the MORB viewpoint, the patterns of He isotope convergence appear to be different for the Mid-Atlantic Ridge (geochemical anomalies at 14°N and 33°S) compared to the East Pacific Rise (geochemical anomalies at 17°S and the Easter Microplate). In the Atlantic cases an increasingly radiogenic Pb signature, indicating more of the common material, is accompanied by a stronger radiogenic He signal (lower $^3He/^4He$), while in the Pacific the opposite appears to be true. Hanan and Graham (1996) inferred from this contrast that this material originates from a boundary layer within the mantle, below which the high $^3He/^4He$ reservoir is located. The common material with low $^3He/^4He$ was taken to originate from recycled material trapped in this layer, while the high $^3He/^4He$ in the Pacific cases implies a slightly larger mass transfer in that region from the underlying reservoir. This could further imply that the regional distribution of recycled crust trapped in the mantle accounts for the contrast in He and Pb isotope covariations.

Subduction of crust and lithosphere is a major mechanism for creating mantle heterogeneity. It is possible that recycled materials form distinct reservoirs that contribute to the large-scale structure of mantle, such as trapped megaliths (Ringwood 1982) or as large, coherent downgoing slabs that are impeded at deep boundary layers (Kellogg et al. 1999). As yet, however, no unequivocal evidence for this notion exists

in the global isotope systematics. In fact, where the mixing relationships are best defined for individual island localities, through strongly hyperbolic arrays in Sr-Nd-Pb isotope relations such as those observed at Heard Island (Barling and Goldstein 1990), the individual island components do not correspond to the extreme mantle end-members defined from the global data set. This indicates that OIB source reservoirs often have intermediate isotopic compositions that were created by prior differentiation or mixing events (Barling and Goldstein 1990; Hart et al. 1992; Hanan and Graham 1996).

The comparisons in Figure 10 do indicate that some OIB source (deep mantle) regions have $^{3}He/^{4}He \geq 40$ R_A. These mantle regions also have Δ_{Pb} values near 3.9-4.0 in some cases (Fig. 10d), consistent with a long-term history of quasi-isolation. Such Δ_{Pb} values are present in the mantle source of high-$^{3}He/^{4}He$ tholeiitic basalts from the shield stage of many Hawaiian volcanoes, where a remarkable and internally consistent relationship between $^{3}He/^{4}He$ and $^{208}Pb/^{206}Pb$ was discovered (Eiler et al. 1998). For these Hawaiian shield lavas, Eiler et al. (1998) showed that it is possible to predict the $^{3}He/^{4}He$ ratio to ±2 R_A based only on Pb isotope systematics. This also suggests that some of the observed isotopic variations at ocean islands are related to internal heterogeneity within their mantle source regions.

He-Os isotope relations. An emerging area of investigation is the relationship between $^{3}He/^{4}He$ and $^{186}Os/^{188}Os$ in ocean island basalts. ^{186}Os is produced by long-lived radioactive decay of ^{190}Pt, and the Earth's outer core is thought to be enriched in Pt/Os, making the $^{186}Os/^{188}Os$ a potential tracer for the involvement of very deep Earth material in the origin of some OIBs (Walker et al. 1995; Brandon et al. 1998). Os isotopes in olivine-rich basalts from Hawaii can be explained by the involvement of ~1% of outer core material admixed with the Hawaiian mantle source, and there is a correlation showing that higher $^{3}He/^{4}He$ is associated with higher $^{186}Os/^{188}Os$ in Hawaiian picrites (Brandon et al. 1999). However, a reconnaissance sampling of picrites from Iceland shows that elevated $^{186}Os/^{188}Os$ is not associated with high $^{3}He/^{4}He$ (Brandon et al. 2001). More work on the He-Os isotope systematics will provide important constraints on possible involvement of material from the core-mantle boundary in the noble gas signature of ocean island basalts.

Overview. There does not seem to be any direct relationship between plate speed or plume flux and the value of $^{3}He/^{4}He$ measured at ocean islands. It does seem possible that somewhat more variable $^{3}He/^{4}He$ ratios may be found on old oceanic lithosphere or near continental margins/subduction zones, but this cannot be firmly concluded based on the available evidence (Fig. 5). Buoyancy flux, plate speed and lithosphere age may serve to modulate the $^{3}He/^{4}He$ signal at ocean islands, but it is clear that they do not control it.

The high $^{3}He/^{4}He$ ratios at localities such as Hawaii, Iceland, Galápagos and Samoa are consistent with the idea that some deep Earth regions have remained more effectively isolated and are less degassed than the upper mantle MORB source. The relations of Sr, Nd and Pb with He isotopes clearly identify two distinct reservoirs, namely, the depleted MORB mantle and a high $^{3}He/^{4}He$ mantle source for ocean islands such as Hawaii and Iceland. OIBs with the highest $^{3}He/^{4}He$ ratios show more enriched Sr and Nd isotope compositions compared to MORBs. Nevertheless, these OIBs are not characterized by primitive or 'bulk Earth' Sr and Nd isotope compositions ($^{87}Sr/^{86}Sr = 0.705$, $^{143}Nd/^{144}Nd = 0.51264$). Instead, they have depleted isotope signatures, indicating some earlier episode of melting in the history of their mantle sources. These isotope systematics might be explained by mixing of a very small amount (less than a few percent) of primitive, gas-rich mantle with differentiated mantle reservoirs. However, any self-consistent and detailed mass balance model that attempts to fully account for all the isotopic observations is likely to be non-unique, due to the range of crustal and lithospheric materials that have been recycled to the mantle.

At regional and local scales, the relationship of $^{3}He/^{4}He$ to other isotopic tracers is often consistently explained in terms of mantle or magma mixing processes. There are some cases that may need to be explained by plume heterogeneity in $^{3}He/^{4}He$, by magma degassing and radiogenic ingrowth of He, or by wallrock reaction/metasomatic effects during magma transport, but detailed studies have yet to be carried out that firmly establish cause and effects. Perhaps of most significance to characterizing reservoirs within the Earth, it is unclear whether the intermediate $^{3}He/^{4}He$ ratios (~10 to 30 R_A) often found at ocean islands are always due to mixing between high $^{3}He/^{4}He$ plume material and upper mantle or recycled components. The best example is along the Réunion hotspot track, where values of 11-13 R_A appear to persist for 65 Ma (Staudacher et al. 1990; Graham et al. 1990; Marty et al. 1993a; Basu et al. 1993; Hanyu et al. 2001). The constancy of intermediate $^{3}He/^{4}He$ for such long time periods is not readily explained by mixing, and suggests the possibility for deep mantle reservoirs having variable $^{3}He/^{4}He$.

NEON

Significance

Early neon isotope measurements indicated that the Ne isotope composition of the Earth's mantle differs from that of the atmosphere (Craig and Lupton 1976; Poreda and Radicati di Brozolo 1984), but confidence in the early results was limited by the low analytical precision. Once some of the analytical obstacles were overcome, the work by Honda et al. (1987) and Ozima and Zashu (1988) on diamonds, and by Sarda et al. (1988) on submarine volcanic glasses from ridges and islands, showed conclusively that the mantle is characterized by elevated ratios of $^{20}Ne/^{22}Ne$ and $^{21}Ne/^{22}Ne$ compared to the atmosphere. The relatively high $^{20}Ne/^{22}Ne$ in MORBs and OIBs indicates that the connection between the Earth's atmosphere and mantle is not a simple, complementary relationship. The different correlations between $^{20}Ne/^{22}Ne$ and $^{21}Ne/^{22}Ne$ in MORBs and OIBs each pass through the composition of air (Fig. 11), due to the ubiquitous presence of an atmospheric component. Key questions arise from the Ne isotope data, especially about the origin of the atmosphere. The chapters by Porcelli and Ballentine (2002) and Pepin and Porcelli (2002) discuss these questions in more detail. Of special note is the observation that the $^{20}Ne/^{22}Ne$ ratio in mantle-derived rocks approaches the solar-like composition while in the atmosphere it is much lower. This suggests that Ne

in the Earth's atmosphere has been substantially fractionated from its terrestrial primordial composition (e.g., Porcelli and Pepin 2000) or that it was added as a late veneer (Marty 1989).

Precise Ne isotope analyses of mantle-derived rocks are still somewhat limited in number. The inherently low abundance of Ne in mantle melts makes atmospheric contamination a potential problem, and corrections for isobaric interference during the mass spectrometer analysis (e.g., doubly charged species $^{40}Ar^{++}$ and $^{12}C^{16}O_2^{++}$) always need to be determined. In general, the most reliable Ne isotope analyses today are produced by the stepwise release of gases (as they are for Ar and Xe isotopes), either by incremental crushing or incremental heating of a sample in vacuum.

Nucleogenic production

MORBs and OIBs are systematically different in their Ne isotope composition (Sarda et al. 1988; Honda et al. 1991, 1993a,b; Moreira et al. 1995; Moreira and Allègre 1998). This difference results from differences in the dilution, by primordial Ne, of the nucleogenic ^{21}Ne that is produced in their mantle sources. Even a small amount of nucleogenic production can markedly shift the mantle $^{21}Ne/^{22}Ne$ ratio because ^{21}Ne is so scarce. The nucleogenic production rate of Ne depends on several factors, including the elemental and isotopic compositions of the target elements within the source rocks, the neutron and α-particle energy spectrum, the neutron/α-particle production ratio, and the Ne isotope yields from the nuclear reaction (e.g., Kyser and Rison 1982; Yatsevich and Honda 1997; Leya and Wieler 1999). The most important pathways for ^{21}Ne production, often referred to as the Wetherill reactions (Wetherill 1954), are $^{18}O(\alpha,n)^{21}Ne$ and $^{24}Mg(n,\alpha)^{21}Ne$, with the former reaction being the dominant one for the Earth's mantle (Yatsevich and Honda 1997). In these reactions the α-particles and neutrons interact with target atoms of ^{18}O and ^{24}Mg. The α-particles are derived from U and Th decay, while the neutrons are produced from particle collisions with other elements such as oxygen. The production of radiogenic ^4He (α-particles) and nucleogenic ^{21}Ne in the mantle is therefore strongly coupled.

A good estimate of the $^{21}Ne/^{22}Ne$ ratio of the mantle source can be determined from the realization that Ne in a volcanic rock is a binary mixture between air and mantle (e.g., Moreira et al. 1995). This estimate is similar to that determined by a ternary deconvolution using $^{20}Ne/^{22}Ne$ and $^{21}Ne/^{22}Ne$ ratios for air, primordial (here assumed to be solar for illustration) and nucleogenic end-members (e.g., Honda et al. 1993a), because the nucleogenic ^{22}Ne production is minor compared to ^{21}Ne. The extrapolated $^{21}Ne/^{22}Ne$ corresponding to a solar $^{20}Ne/^{22}Ne$ ratio, $^{21}Ne/^{22}Ne_E$, can be determined for a line that passes through the air and any data point on the Ne three-isotope diagram, as illustrated in Figure 12. Its numerical value is given by

$$^{21}Ne/^{22}Ne_E = (^{21}Ne/^{22}Ne_M - {}^{21}Ne/^{22}Ne_A)/f_{22} + {}^{21}Ne/^{22}Ne_A \qquad (3)$$

where E, S, A and M refer to extrapolated, solar, air and measured values, respectively, and where f_{22} is the proportion of mantle-derived Ne in a sample, i.e.,

$$f_{22} = \frac{(^{20}Ne/^{22}Ne_M - {}^{20}Ne/^{22}Ne_A)}{(^{20}Ne/^{22}Ne_S - {}^{20}Ne/^{22}Ne_A)}.$$

(Note: $^{20}Ne/^{22}Ne_S$ = 13.8, $^{21}Ne/^{22}Ne_S$ = 0.0328, $^{20}Ne/^{22}Ne_A$ = 9.8 and $^{21}Ne/^{22}Ne_A$ = 0.029).

Mid-ocean ridge basalts

In a diagram of $^{20}Ne/^{22}Ne$ vs. $^{21}Ne/^{22}Ne$, ocean ridge basalts form a well defined array that passes through the composition of air and extends to values of $^{20}Ne/^{22}Ne \geq 12.5$ and $^{21}Ne/^{22}Ne \geq 0.07$ (Fig. 11). This array is usually interpreted as a mixing line between upper mantle Ne and air Ne. How and when this contamination by air occurs is conjectural. Some investigators propose that it takes place during magma ascent and eruption (e.g., Farley and Poreda 1993), or that it was introduced by ancient subduction (e.g., Sarda et al. 2000); others argue that it is largely an artifact introduced during sample preparation (e.g., Ballentine and Barfod 2000). The variability of repeat analyses by stepwise heating makes it evident that some allowance should be made for the effects of air contamination in every analysis, and the measured Ne isotope ratio should always be taken as a minimum estimate for the mantle source composition.

Global variability. In general, the Ne isotope measurements have relatively large and correlated analytical uncertainties. The scatter about the MORB Ne isotope array therefore makes it difficult to determine whether the upper mantle is characterized by a single Ne isotope composition. It seems likely that the whole mantle is characterized by a uniform value of $^{20}Ne/^{22}Ne$, but this is an unproven assumption. Because there are no known reactions that produce ^{20}Ne to a significant extent, variable $^{20}Ne/^{22}Ne$ in the mantle seems implausible unless nucleogenic production of ^{22}Ne is significant and spatially variable. Two MORB suites, from the southern East Pacific Rise (Niedermann et al. 1997) and the southern Mid-Atlantic Ridge (Moreira et al. 1995), each show a decrease in $^{20}Ne/^{22}Ne$ with increasing $^{21}Ne/^{22}Ne$, with a vector that points approximately to the solar Ne isotope composition (especially for the southern Mid-Atlantic Ridge samples with higher $^3He/^4He$ ratios near the Shona hotspot; see Fig. 11). Based on this evidence, Niedermann et al. (1997) speculated that the mantle could vary spatially in the production of ^{22}Ne (and consequently in its $^{20}Ne/^{22}Ne$ ratio), due to a heterogeneous distribution of fluorine and ^{22}Ne production via the reaction $^{19}F(\alpha,n)^{22}Na(\beta^+)^{22}Ne$. However, the recent estimates by Yatsevich and Honda (1997) indicate that ^{22}Ne production in the mantle is <2% of that for ^{21}Ne. It therefore seems more likely that the data trends in Figure 11 for the southern EPR and MAR basalts are better explained by partial melting of upper mantle into which some less degassed OIB material, having higher $^{20}Ne/^{22}Ne$ and lower $^{21}Ne/^{22}Ne$, had been admixed.

The most precise Ne isotope analyses of volcanic rocks yet available are for the MAR popping rock (Moreira et al. 1998). These stepwise crushing analyses display a very tight Ne isotope correlation that is usually taken as a precise definition of the upper mantle trend for the $^{20}Ne/^{22}Ne$ - $^{21}Ne/^{22}Ne$ diagram, illustrated by the MORB line in Figure 11.

Local variability. In comparison to helium, much less work has been carried out on the spatial variation of Ne isotopes along ridges, largely due to the difficult nature of the analyses. The most detailed studies to date are from the southern East Pacific Rise (Niedermann et al. 1997), the southern Mid-Atlantic Ridge in the vicinity of the Shona and Discovery mantle plumes (Moreira et al. 1995; Sarda et al. 2000), and the spreading center in the Manus back-arc basin of the southwest Pacific (Shaw et al. 2001). In the first two of these cases, less nucleogenic Ne (lower $^{21}Ne/^{22}Ne$) is found in regions of higher $^{3}He/^{4}He$ ratios and bathymetric anomalies, although there is not a strict 1:1 relation between He and Ne isotopes. For the Shona and Discovery areas the observed Ne and He isotope variations are consistent with plume material feeding into the sub-ridge mantle from nearby hotspot sources, as suggested from other geophysical and geochemical data (Small 1995; Douglass et al. 1999). There are no prominent ocean island hotspots or seamounts near the southern EPR between 14-19°S, but the bathymetric and geochemical anomalies along this section of the ridge also suggest an origin from hotspot-derived material, perhaps as a mantle blob that was entrained into the upper mantle flow (Mahoney et al. 1994).

There is evidence that some MORB suites show a different Ne isotope trend from the popping rocks. Basalts from the northern Chile Ridge lie to the right of the well-defined popping rock line in the Ne three-isotope diagram (Fig. 11), indicating a stronger component of nucleogenic Ne in their mantle source. Niedermann and Bach (1998) suggest that this could be the result of a prior melting event that fractionated the U/Ne ratio of the residual mantle. Assuming Ne is more incompatible than U, the mantle residue from an earlier melting event would acquire a higher value of $^{21}Ne/^{22}Ne$ through time compared to more fertile mantle. The time scale required is 10-100 Ma, consistent with the formation history of the northern Chile Ridge and westward mantle transport from a region of earlier melting beneath the East Pacific Rise. Some of these northern Chile Ridge basalts also have $^{3}He/^{4}He$ ratios at the low end of the MORB range (<7 R_A), which is consistent with a model residual mantle having elevated $U/^{3}He$. However, a few of the lavas have $^{3}He/^{4}He$ above 8 R_A, suggesting that some $^{3}He/^{22}Ne$ fractionation may also have occurred during the proposed earlier melting event.

Significant decoupling of He and Ne isotopes does appear to occur in some cases, and is best exemplified by the spreading ridge basalts from the Manus Basin (Shaw et al. 2001). Manus Basin basalts have $^{3}He/^{4}He$ ratios up to 15 R_A, yet they show a Ne isotope slope that is less than the MORB trend as defined by the popping rocks (Fig. 11). Shaw et al. (2001) considered several possible explanations for the discrepancy, ruling out crustal contamination, fluid addition from the subducting plate, or addition of Ne from ancient slabs that were recycled to the mantle. They conclude that either He was fractionated from Ne in the back-arc mantle by melting and degassing during the last 10 Ma, or that the Earth's mantle has maintained some record of primordial heterogeneity in its $^{3}He/^{22}Ne$ ratio.

Ocean island basalts

In comparison to MORBs, some OIBs show a much steeper correlation in the Ne three-isotope diagram (Fig. 11). This is especially true for the cases of Hawaii, Iceland and Réunion (Fig. 11; Honda et al. 1991; Valbracht et al. 1997; Trieloff et al. 2000; Dixon et al. 2000; Moreira et al. 2001; Hanyu et al. 2001). These steep trends reveal that these OIB mantle sources have less nucleogenic Ne (lower $^{21}Ne/^{22}Ne$) than the MORB mantle source. Because MORBs also show more radiogenic He than OIBs from Hawaii, Iceland and Réunion, the mantle source for MORBs must be characterized by lower time-integrated $^{3}He/(U+Th)$ and $^{22}Ne/(U+Th)$ than the mantle source for those OIBs. Because the MORB mantle source is also trace element-depleted compared to the source for many OIBs, the OIB mantle source, at least for cases such as Hawaii, Iceland and Réunion, must be less degassed (i.e., it has higher ^{3}He and ^{22}Ne concentrations) than the upper mantle source of MORBs.

Because nucleogenic ^{21}Ne production is coupled to radiogenic ^{4}He production, one expects *a priori* that OIBs with a steeper slope on the Ne three-isotope diagram will have higher $^{3}He/^{4}He$ ratios. If He and Ne were perfectly coupled in the Earth (i.e., if no He/Ne fractionation occurred), the $^{3}He/^{4}He$ ratio at any locality could be predicted from the slope on the Ne isotope diagram, assuming the initial He and Ne isotope compositions are known (e.g., Honda et al. 1993a). A detailed comparison of the Ne isotope correlations for Iceland, Loihi, Réunion and the MAR popping rock is insightful in this context (see Fig. 11). The three ocean islands are characterized by relatively high $^{3}He/^{4}He$ (>30 R_A for some basalts from Iceland and Hawaii, and ~13 R_A for Réunion), while the popping rock, taken to exemplify the MORB mantle, has a $^{3}He/^{4}He$ ratio of 8 R_A. The isotope characteristics of the Réunion island source ($^{3}He/^{4}He$ = 13 R_A and an intermediate slope on the Ne three-isotope diagram and $^{87}Sr/^{86}Sr > 0.704$) cannot be explained by mixing of either recycled crust or MORB mantle with a high $^{3}He/^{4}He$-source such as that for Loihi or Iceland. Hanyu et al. (2001) suggest that the Réunion plume source is therefore distinct from the Iceland and Loihi sources, and that the mantle contains more than one relatively undegassed reservoir, each having elevated but different $^{3}He/^{4}He$ ratios. This is an intriguing hypothesis that warrants further consideration, especially in light of developing models for deep mantle stratification that involve large domains having a complex topography that responds to convection and pressure from subducting slabs (e.g., Kellogg et al. 1999). Another possibility to bear in mind, however, is that some decoupling of He and Ne isotopes may occur if the mantle He/Ne ratio is fractionated during melting processes.

Solar hypothesis. The steep OIB correlations on the three-Ne isotope diagram, especially for basalts from Iceland and Loihi Seamount, trend toward Ne isotope compositions resembling either solar wind or the solar component commonly found in meteorites (Ne-B). It is not possible at the present time to distinguish unambiguously between these two possibilities, and the implications for early Earth evolution are quite different. The highest values of $^{20}Ne/^{22}Ne$ yet measured are ~12.5 for terrestrial lavas from several localities, including Loihi Seamount, Iceland and the popping rocks. This led Trieloff et al. (2000) to suggest that the Earth's initial Ne is best described by Ne-B, a component produced in meteorites by irradiation from the solar wind. Following this reasoning, Trieloff et al. (2000) argued that the Earth acquired its Ne while the young sun was still very active, during which time small planetesimals were thoroughly irradiated prior to their assembly to form the Earth. In contrast, Ballentine et al. (2001)

argued that, because all basalt analyses can be expected to contain some air neon, a solar Ne isotopic composition ($^{20}Ne/^{22}Ne$ of ~13.8) best represents the Ne trapped within the Earth. This conclusion is based on the correlation between Ne and Ar isotopes seen in step crushing analyses of the MAR popping rock (Moreira et al. 1998; see Fig. 14, below) and its extrapolation to the very high $^{40}Ar/^{36}Ar$ measured by laser extraction from individual bubbles in the same lavas (Burnard et al. 1997), for which precise Ne isotope measurements were not possible. Following this reasoning, the Earth would have solar Ne isotope composition, and gravitational capture of a dense primitive atmosphere within the solar nebula during Earth accretion is a logical model (Mizuno et al. 1980).

ARGON

Significance

Argon isotopes can provide powerful constraints on the formation of the atmosphere, and on geodynamics and isotopic evolution of the mantle. Unlike He which is lost from the atmosphere, Ar has accumulated over Earth history. The primordial $^{40}Ar/^{36}Ar$ ratio is also extremely low, so the amount of ^{40}Ar initially present in the Earth can be reasonably taken as zero. Transport of ^{40}Ar to the atmosphere involves volcanic degassing, hydrothermal circulation through the crust, and erosion of continental crust that releases radiogenic Ar generated by decay of ^{40}K. The half-life of ^{40}K (1.25 Gy) is relatively short compared to the age of Earth, making the abundance of Ar in the atmosphere along with the $^{40}Ar/^{36}Ar$ of the atmosphere and upper mantle useful parameters for unraveling the history of degassing and plate tectonic recycling (e.g., Turekian 1959; Hamano and Ozima 1978; Fisher 1978; Sleep 1979; O'Nions et al. 1979; Hart et al. 1979; Sarda et al. 1985; Allègre et al. 1986/1987; Turner 1989; Albarède 1998; Coltice et al. 2000; Porcelli and Ballentine 2002). As one example, in the limiting case where all the ^{40}Ar generated in the crust has been released to the atmosphere, 30% of the Ar in the atmosphere would be from the crust and 70% from the mantle (Turcotte and Schubert 1988). Under these circumstances, only one-quarter of the whole mantle would be outgassed. As another example, under assumptions of a layered mantle (in which the 660 km seismic discontinuity represents the boundary) with known K content, about one-half of the terrestrial ^{40}Ar inventory is still retained in the deep Earth (Allègre et al. 1996). These conclusions depend directly on the K concentration of the Earth; a lower K/U ratio than commonly assumed leads to the conclusion of a more degassed deep Earth (Davies 1999).

Radiogenic production

In a closed system, the amount of radiogenic ^{40}Ar produced over time t is given by

$$^{40}Ar^* = a \cdot b \cdot K \, (e^{\lambda_{40} t} - 1) \qquad (4)$$

where a is the natural abundance of ^{40}K (0.0117%), b is the branching ratio of ^{40}K decay to ^{40}Ar by electron capture (0.1048), K is the amount of potassium present, and λ_{40} is the total decay constant (0.554 Gy^{-1}).

Atmospheric contamination

Obtaining meaningful Ar isotope analyses on basalts is analytically challenging, because contamination by atmospheric components is notorious. Potential sources of this contamination include seawater, altered wall rock, or air itself. Basalt glasses may show complicated variations within an individual glassy rim, with lower $^{40}Ar/^{36}Ar$ in both the outermost glassy part as well as in the more crystalline interior (Kumagai and Kaneoka 1998). The atmospheric contaminant in MORBs appears to be significantly less in vesicles, because all measurable ^{36}Ar in the popping rock is accounted for by the amount released during the analysis of vesicle-free glass (Burnard et al. 1997), and there is no correlation between ^{3}He and ^{36}Ar from basalt crushing analyses (Ballentine and Barfod 2000). This suggests that for MORBs the contamination may not be occurring by crustal assimilation, but rather by adsorption or entrapment following eruption. In the case of many ocean islands, phenocrysts are separated from subaerially erupted lavas for noble gas analysis. Such samples usually show a large range in measured $^{40}Ar/^{36}Ar$ due to variable proportions of atmospheric and magmatic components (Farley and Craig 1994). The air component is not readily removed by physical or chemical treatment. It is also present to a large extent in fluid inclusions, along with the magmatic gas, as revealed by laser fusion analyses (Farley and Craig 1994; Burnard et al. 1994a). This indicates that the contamination may also occur by assimilation of crust, or by direct addition of seawater or air to a magma (Farley and Craig 1994). Argon isotope ratios in OIBs that resemble air are most likely due to contamination, and should not be taken as evidence for a deep mantle reservoir having near-atmospheric Ar isotope composition (Patterson et al. 1990). In fact, where OIBs have been analyzed that have high $^{3}He/^{4}He$, they can range to moderately high $^{40}Ar/^{36}Ar$ ratios, up to ~8000 (Farley and Craig 1994; Burnard et al. 1994a,b; Trieloff et al. 2000).

Ballentine and Barfod (2000) reviewed the effects of atmospheric contamination in MORBs and OIBs in detail. Intriguingly, they showed that the modern air contaminants released during crushing are preferentially located in sites that are more easily ruptured than those containing magmatic gas. This suggests that much of the contamination occurs through the annealing of microfractures, following air entrapment that occurs either during sample recovery from seafloor depths or during sample preparation in the laboratory. This contaminant gas should, in principle, be separable from magmatic gas by stepwise crushing or heating, although a diagnostic test of when it is completely removed remains to be fully developed. Measured $^{40}Ar/^{36}Ar$ ratios should always be considered minimum values in young basalts.

It is commonly assumed that all ^{36}Ar present in a MORB or OIB sample could be derived from air contamination. This is a reasonable assumption provided that the $^{40}Ar/^{36}Ar$ is >3000, as seems likely for mantle source regions. This assumption allows a minimum estimate for the amount of magmatic ^{40}Ar present in a sample. This amount of radiogenic Ar derived from the mantle, denoted $^{40}Ar^*$, is given by

$$^{40}Ar^* = \left(^{40}Ar/^{36}Ar_M - ^{40}Ar/^{36}Ar_A\right) {}^{36}Ar_M \qquad (5)$$

where M designates the measured ratio and A the air ratio ($^{40}Ar/^{36}Ar_A = 295.5$). There is no straightforward way to estimate a sample's complement of primordial ^{36}Ar derived from the mantle. For example, if one assumes a mantle $^{40}Ar/^{36}Ar$ ratio (such as $^{40}Ar^*/^{36}Ar_P = 40{,}000$, where p refers to primordial Ar), any correlation involving $^{36}Ar_P$ (such as $^3He/^{36}Ar_P$) will be inherently the same as one involving $^{40}Ar^*$, since both are directly correlated by the assumed $^{40}Ar^*/^{36}Ar_P$ ratio.

Mid-ocean ridge basalts

Global variability. The mantle $^{40}Ar/^{36}Ar$ ratio is variable due to time-integrated variations in $K/^{36}Ar$. MORBs show $^{40}Ar/^{36}Ar$ ratios that range up to 40,000. The very highest values have been measured using a laser to rupture individual vesicles in the MAR popping rock (Burnard et al. 1997). Values up to 28,000 have been measured for these same samples by incrementally heating or crushing bulk samples of the glass in vacuum (Staudacher et al. 1989; Moreira et al. 1998). Very high ratios, with relatively large uncertainties, have also been measured in glassy basalts from the Mid-Atlantic Ridge ($^{40}Ar/^{36}Ar = 42{,}400 \pm 9700$; Marty and Humbert 1997) and from 10°S on the southern East Pacific Rise ($^{40}Ar/^{36}Ar > 35{,}000$, limited by the absence of detectable ^{36}Ar; Fisher 1994). Ratios above 25,000 have also been measured in MORB glasses from the MAR near the Kane transform (Sarda et al. 1985), from the South Atlantic (Sarda et al. 2000), and from the N Chile Ridge in the eastern Pacific (Niedermann and Bach 1998). It is tempting to suggest that the whole upper mantle might be characterized by a $^{40}Ar/^{36}Ar$ value near 30,000 based on this similarity. However, individual analyses of the popping rock show the highest measured $^{40}Ar/^{36}Ar$ (>20,000) during the last two steps of crushing which release the lowest amounts of ^{36}Ar ($<1.5 \times 10^{-10}$ std cm^3; Moreira et al. 1998), indicating that even in these most gas-rich samples, atmospheric contamination is significant for Ar isotope analyses. The value of 40,000 measured by Burnard et al. (1997) using a laser probe should probably be taken as a minimum estimate for the upper mantle.

There is no systematic behavior between $^{40}Ar/^{36}Ar$ and $^3He/^4He$ for the upper mantle based on the MORB analyses. $^{40}Ar/^{36}Ar$ ratios for MORBs are quite variable, ranging by 2 orders of magnitude, while $^3He/^4He$ varies by about a factor of 2 (Fig. 13). For the case of the popping rock, the highest $^{40}Ar/^{36}Ar$ ratios are also associated with the highest measured $^{20}Ne/^{22}Ne$ (Fig. 14), consistent with the lowest degree of atmospheric contamination in those analyses. Moreira et al. (1998) inferred that the maximum $^{40}Ar/^{36}Ar$ of the MORB mantle is 44,000, based on extrapolation of the popping rock $^{40}Ar/^{36}Ar$-$^{20}Ne/^{22}Ne$ trend to solar $^{20}Ne/^{22}Ne = 13.8$ (Fig. 14). High $^{40}Ar/^{36}Ar$ ratios are also found in other samples with lower $^{20}Ne/^{22}Ne$, such as from the N Chile Ridge and southern MAR. Much of the variation observed in Figure 14 must be due to air contamination. Different degrees of air contamination would only produce a single trajectory however, so the scatter in the data indicates a significant variation in the Ne/Ar ratio for either, or both, of the mixing end-members (i.e., the atmosphere-derived contaminant and the magmatic gas). For example, to account for the data scatter, any binary mixing between magmatic gas and unfractionated air would require that the $^{22}Ne/^{36}Ar$ ratio of the magmatic gas ranges from an order of magnitude larger to an order of magnitude smaller than the air ratio. From a simultaneous consideration of Ne-Ar and Ne-Xe isotope systematics, Harrison et al. (2002) showed that contamination usually involves a fractionated atmospheric component having $^{22}Ne/^{36}Ar$ significantly less than air, such as might be expected if water-rich or adsorbed components play a role. This seriously complicates a full interpretation of even the best available heavy noble gas analyses. Measured $^{40}Ar/^{36}Ar$ ratios should be considered minimum estimates for their mantle source.

Regional variability. Given the strong potential effect of contamination by atmospheric components, it is difficult to quantitatively assess the spatial variability in $^{40}Ar/^{36}Ar$ along ridges. Sarda et al. (1999a) showed that the maximum $^{40}Ar/^{36}Ar$ ratio along the Mid-Atlantic Ridge, measured by step heating of basalt glasses, varies systematically with indicators of mantle heterogeneity such as Pb isotopes, with one end-member defined by the Azores hotspot. The correlations hold for the North and South Atlantic considered as a whole. Sarda et al. (1999a) reasoned that this ruled out shallow level contamination processes, and favored mixing that involved depleted upper mantle and recycled materials having low $^{40}Ar/^{36}Ar$ and radiogenic Pb. This would require that the recycled material has a $K/^{36}Ar$ ratio less than upper mantle values, i.e., that atmospheric noble gases are recycled to the mantle by subduction. Burnard (1999b) challenged this explanation however, and argued that shallow level contamination could explain the regional correlation between Ar and Pb isotopes. Radiogenic Pb signatures are typically found along axial topographic highs, where ridges are often influenced by nearby island hotspots. Low $^{40}Ar/^{36}Ar$ is also found along shallower ridge sections where degassing at shallower levels can lead to an increased susceptibility to contamination, and this can produce a correlation between $^{40}Ar/^{36}Ar$ and axial depth (Burnard 1999b; Burnard et al. 2002). Sarda et al. (1999b) suggested that such a process should produce erratic results rather than a systematic trend. Whether the regional variation in Ar isotopes along ocean ridges carries information about variations in the upper mantle is still debated. Chlorine contents in suites of MORB glasses studied for Ar isotopes could potentially resolve this debate (e.g., Michael and Cornell 1998).

Relation to other volatiles. The $N_2/^{36}Ar$ ratio varies by several orders of magnitude in MORB glasses, and is correlated with $^{40}Ar/^{36}Ar$ (Marty 1995). This means that the nitrogen abundance correlates with the amount of ^{40}Ar, due to two-component mixing between a mantle-derived end-member having high $^{40}Ar/^{36}Ar$ and an atmospheric end-member having $^{40}Ar/^{36}Ar = 295.5$. The trend of increasing $N_2/^{36}Ar$ with $^{40}Ar/^{36}Ar$ in MORB glasses can be extrapolated to an upper mantle $^{40}Ar/^{36}Ar > 30{,}000$, and gives $N_2/^{36}Ar > 2.2 \times 10^6$ (Marty 1995), which is two orders of magnitude higher than the value in the modern atmosphere. This could mean that small amounts of nitrogen have been recycled to the volatile-depleted upper mantle. Marty and Humbert (1997) and Marty and Zimmerman (1999) subsequently showed that the high $^{40}Ar/^{36}Ar$ ratios of the upper mantle are accompanied by a depleted ^{15}N signature relative to air, with $\delta^{15}N = -3$ to -5 ‰. This indicates that only a very limited amount of nitrogen recycling could have occurred, and that atmospheric nitrogen is not derived solely by outgassing of the upper mantle. Instead, it seems possible that the early atmosphere underwent volatile

fractionation of N relative to ^{36}Ar. The high degree of correlation between N_2 and ^{40}Ar abundances in MORB glasses would then indicate some parallel degassing of N_2 and ^{40}Ar over geologic time (Marty 1995). A detailed model of mantle degassing, early atmospheric dissipation and fractionation, and recycling fluxes using combined He, Ne, Ar and N isotope constraints from oceanic basalts has been presented by Tolstikhin and Marty (1998).

Solar hypothesis. Ratios of noble gas isotopes that have only a primordial component, such as ^{38}Ar/^{36}Ar, are key in any attempt to identify potential solar components within the Earth. Anomalously low ^{38}Ar/^{36}Ar was first recognized by Niedermann et al. (1997) in their measurements of East Pacific Rise basalts. They did not place much significance on those results given that only a few of them were outside the 2-sigma uncertainty of the air ratio (air ^{38}Ar/^{36}Ar = 0.188). Low ratios, down to ^{38}Ar/^{36}Ar =0.185, were also measured for the deeply erupted glassy basalts at Loihi Seamount (Valbracht et al. 1997). The low ^{38}Ar/^{36}Ar ratios at Loihi were correlated with non-atmospheric and elevated ^{20}Ne/^{22}Ne, providing preliminary evidence for a solar Ar component in the mantle. (The mean value of ^{38}Ar/^{36}Ar is 0.175 in solar wind). Subsequently, Pepin (1998) took the results from both the EPR and Loihi studies as promising evidence for a solar-like Ar component in the mantle, and discussed some of the implications for planetary accretion and atmospheric origin. The low ^{38}Ar/^{36}Ar ratios in the EPR samples are not correlated with high ^{40}Ar/^{36}Ar, however, as would be expected from binary mixing between air and mantle components (Kunz 1999). Indeed, some of those low ^{38}Ar/^{36}Ar ratios were measured simultaneously with atmospheric ^{40}Ar/^{36}Ar ratios. It should also be recognized that very small analytical artifacts in the original studies might be the cause for the low ^{38}Ar/^{36}Ar ratios. Mass fractionation effects during gas extraction or analysis must be completely removed, and this is especially difficult to verify in the presence of relatively large amounts of ^{40}Ar. At this point in time it seems *possible* that a solar Ar component is present within the mantle, but the analytical evidence is weak and it remains unproven.

Ocean island basalts

The highest ^{40}Ar/^{36}Ar ratios at ocean islands are found in xenoliths from Samoa, where values range up to 21,500 (Farley et al. 1994). The origin of the high ^{40}Ar/^{36}Ar in these xenoliths is unclear, however, because the fluid inclusions show strong metasomatic overprints that occurred in the upper mantle (Burnard et al. 1998). The highest ^{40}Ar/^{36}Ar ratios obtained on ocean island basalt glasses are from Loihi Seamount, where they range up to 8300 (Trieloff et al. 2000). In the most detailed study of Ar isotopes at a single ocean island, Farley and Craig (1994) obtained a maximum ^{40}Ar/^{36}Ar of 8000 for olivine phenocrysts from Juan Fernandez, a high ^{3}He/^{4}He hotspot. Bulk crushing and laser fusion of individual crystals were carried out for forty splits of olivine from a single lava, and a variety of chemical and physical pre-treatments were attempted.

The relation between ^{40}Ar/^{36}Ar and ^{3}He/^{4}He or ^{20}Ne/^{22}Ne in ocean island basalts and xenoliths is generally poor (Figs. 13 and 14). The apparent difference in ^{40}Ar/^{36}Ar–^{3}He/^{4}He systematics between MORBs and OIBs was suggested by Kaneoka (1983, 1985) to indicate a layered mantle structure, in which OIB sources have higher ^{3}He/^{4}He and ^{40}Ar/^{36}Ar ratios that are nearly the same as the atmosphere. More recent data showing ^{40}Ar/^{36}Ar up to ~8000 in OIBs now makes a model involving OIB source reservoirs of near atmospheric composition untenable. High ^{40}Ar/^{36}Ar values, particularly in the Loihi glasses (Trieloff et al. 2000), are associated with ^{20}Ne/^{22}Ne ratios comparable to the highest values obtained in terrestrial basalts, evidence that these Loihi analyses are not very strongly affected by air contamination. The mantle source for OIBs from localities such as Iceland, Hawaii and Réunion clearly has a ^{40}Ar/^{36}Ar ratio higher than the atmosphere (Trieloff et al. 2000; Burnard et al. 1994b). It is not possible to assume that all air contamination has been eliminated even in these first rate analyses. A ratio of ^{40}Ar/^{36}Ar $\geq$ 8000 is arguably the best estimate for the mantle source of these OIBs (Fig. 14), although it is not currently possible to rule out the presence of a deep OIB source reservoir, having somewhat lower ^{40}Ar/^{36}Ar, that generates OIB magma that subsequently undergoes slight contamination by volatiles derived from the shallower MORB mantle.

KRYPTON

Krypton isotopes in oceanic basalts have not been very diagnostic of mantle processes. The Kr isotopic composition of oceanic basalts is typically the same as modern air. Minor production of ^{83}Kr, ^{84}Kr and ^{86}Kr occurs from the spontaneous fission of ^{238}U, but it has not yet been detected in young oceanic basalts, due to the small fission yields (<1% for ^{86}Kr, ≤0.1% for ^{83}Kr and ^{84}Kr) in the mass region where Kr nuclides are present in relatively high abundance (natural abundance of 11.5%, 57% and 17.3%, respectively, for ^{83}Kr, ^{84}Kr and ^{86}Kr). Even if air contamination during sample analysis could be totally eliminated, it is unclear whether such small contributions could be resolved.

XENON

Significance

Xenon isotopes in oceanic basalts provide the most basic evidence on early differentiation of our planet and on formation of the atmosphere. Several Xe isotopes are produced by extinct radioactivity, providing a method to quantify events at the very start of Earth history near 4500 million years ago to a high precision, within several tens of millions of years. The difference between ^{129}Xe/^{130}Xe of the mantle and atmosphere is fundamental evidence for their early separation (e.g., Thompson 1980; Staudacher and Allègre 1982). It is thought that formation of the atmosphere involved some early degassing of the mantle. Whether the Earth ever had a primary atmosphere is still an open question, and ultimately depends upon whether the inner planets formed in the presence of a solar nebula gas phase. The timing of these early events, the degree to which Xe isotope differences reflect variations in I/Xe and Pu/Xe of source reservoirs, and the extent to which the mantle and atmosphere are complementary, all remain points of active investigation. For example, it has become widely recognized

that the Moon may have formed by impact of a Mars-sized body on the early Earth (Hartmann 1984). The impact hypothesis is obviously relevant to models of atmosphere formation, because much of the original solid body would be left molten, and many of the lighter gas species originally present would escape the gravitational field (Pepin 1997). The Xe isotope systematics of oceanic basalts and the atmosphere indicate isotopic closure of Xe in the terrestrial system within ~10^8 years of the onset of accretion (Staudacher and Allègre 1982; Ozima et al. 1985; Podosek and Ozima 2000; Porcelli and Pepin 2000).

Radiogenic production

Several of the heavier Xe isotopes have contributions from spontaneous fission, both from decay of long-lived ^{238}U and from extinct ^{244}Pu. ^{129}Xe was also produced by the extinct β^- decay of ^{129}I (Table 1). The relative fission yields for ^{238}U are ^{129}Xe/^{131}Xe/^{132}Xe/^{134}Xe/^{136}Xe = <0.002/0.076/0.595/0.832/1, with the absolute yield of ^{136}Xe, ^{136}y = 6.3±0.4% (Ozima and Podosek 2002; Porcelli et al. 2002). As an example, for a closed system the amount of ^{136}Xe produced by decay of ^{238}U is

$$^{136}\mathrm{Xe} = (\lambda_{sf}/\lambda_{238})^{136}\mathrm{y}\ ^{238}\mathrm{U}(e^{\lambda_{238}t} - 1) \quad (6)$$

where $\lambda_{sf}/\lambda_{238}$ is the ratio of fission to total decay (5.45×10^{-7}). For the case of ^{244}Pu, the relative fission yields are ^{129}Xe/^{131}Xe/^{132}Xe/^{134}Xe/^{136}Xe = 0.048/0.246/0.885/0.939/1, with the absolute yield of ^{136}Xe = 5.6±0.6% (Lewis 1975). The amount of ^{136}Xe produced by extinct ^{244}Pu is

$$^{136}\mathrm{Xe} = (\lambda_{sf}/\lambda_{244})^{136}\mathrm{y}\ ^{244}\mathrm{Pu}_0\ e^{-\lambda_{244}(T_0-t)} \quad (7)$$

where λ_{244} is the decay constant for ^{244}Pu (8.45 Gy^{-1}), $\lambda_{sf}/\lambda_{244} = 1.25\times10^{-3}$, T_0 is the time at which the system became closed having an amount of plutonium ^{244}Pu$_0$, and (T_0 - t) is referred to as the formation interval. ^{129}Xe was also produced from I^{129}, so

$$^{129}\mathrm{Xe} = {}^{129}\mathrm{I}_0 e^{-\lambda_{129}(T_0-t)} \quad (8)$$

where λ_{129} is the decay constant for ^{129}I (40.8 Gy^{-1}).

The above considerations show that several ages may be calculated from Xe isotope systematics, provided that certain key parameters are specified. These ages may be computed as I-Xe or I-Pu-Xe ages. The different methods usually involve a comparison between planetary materials, such as meteorites and the Earth, or between different terrestrial reservoirs, such as the atmosphere and the upper mantle. The key parameters that need to be specified are the initial amounts of ^{129}I and ^{244}Pu, and the abundance of I in the Earth today. These are usually treated in terms of the ratios $(^{129}\mathrm{I}/^{127}\mathrm{I})_0$, $(^{244}\mathrm{Pu}/^{238}\mathrm{U})_0$, and $(^{127}\mathrm{I}/^{238}\mathrm{U})$, respectively. The I-Xe and I-Pu-Xe ages of the atmosphere, computed from differences between the ^{129}Xe/^{130}Xe and ^{136}Xe/^{130}Xe measured in air and in mid-ocean ridge basalts, indicate formation intervals of ~50-100 Ma (Staudacher and Allègre 1982; Ozima et al. 1985; Marty 1989). These short time scales indicate that the atmosphere and upper mantle have remained effectively separated for most of Earth's ~4500 Ma history. A comparison of the isotopic compositions of terrestrial, lunar and meteoritic Xe also provides a high resolution chronometer of early solar system events. I-Pu-Xe ages computed in this way indicate that the Earth-Moon system became closed to Xe loss ~100 Ma after the beginning of solar system formation (Wetherill 1975; Bernatowicz and Podosek 1978; Swindle et al. 1984; Lin and Manuel 1987; Ozima and Podosek 1999; Podosek and Ozima 2000).

Mid-ocean ridge basalts

One of the most remarkable findings in noble gas geochemistry to date has been the observed 'excess' ^{129}Xe in some mid-ocean ridge basalt glasses. Anomalous ^{129}Xe/^{130}Xe in MORBs was first reported by Staudacher and Allègre (1982), who measured ratios up to 7% higher than the modern atmosphere (air ^{129}Xe/^{130}Xe = 6.48). These anomalies are present in MORBs from all the major ocean basins. Small anomalies also occur in ^{134}Xe/^{130}Xe and ^{136}Xe/^{130}Xe (air ^{136}Xe/^{130}Xe = 2.17). These enrichments have been verified in subsequent MORB studies (e.g., Marty 1989; Kunz et al. 1998; Moreira et al. 1998; Sarda et al. 2000). The largest MORB ^{129}Xe/^{130}Xe ratios and ^{136}Xe/^{130}Xe, and the most precisely determined, are for the MAR popping rock, which shows ratios up to 7.73 and 2.57, respectively (Fig. 15). Moreira et al. (1998) infer that the maximum ^{129}Xe/^{130}Xe of the MORB mantle is 8.2, based on extrapolation of the popping rock ^{129}Xe/^{130}Xe-^{20}Ne/^{22}Ne trend to a solar ^{20}Ne/^{22}Ne = 13.8 (Fig. 16). Based on the ^{136}Xe/^{130}Xe-^{129}Xe/^{130}Xe correlation evident in Figure 15, this extrapolation gives ^{136}Xe/^{130}Xe = 2.7 for the upper mantle.

Excesses of ^{129}Xe in MORBs are derived from extinct radioactivity of ^{129}I, while those of ^{131,132,134,136}Xe are derived both from fission of ^{238}U and extinct ^{244}Pu. The correlation of MORB ^{136}Xe excesses with those of ^{129}Xe are best explained in terms of mixing between air and a depleted mantle component (Fig. 15). Spontaneous fission of ^{238}U and ^{244}Pu produces a vertical shift on Figure 15, while decay of ^{129}I produces a horizontal one. Some proportion of the fissiogenic component may be ^{244}Pu-derived, but the value of this proportion is sometimes a controversial point, and quantifying it requires precise analyses of ^{131,132,134,136}Xe/^{130}Xe in order to resolve small differences in the fissiogenic excesses (see the previous discussion of the production yields). Kunz et al. (1998) showed that when the most precise analyses are considered, or when the correlation lines are error weighted, the proportion of MORB fissiogenic ^{136}Xe that is ^{244}Pu-derived is 32±10%. Although the exact time scale is somewhat model dependent, this value leads to a refined I-Pu-Xe estimate for closure of the terrestrial Xe system that is ~50-70 Ma after solar system formation (Kunz et al. 1998).

Ocean island basalts

Ocean island basalts and xenoliths show much smaller anomalies in ^{129}Xe/^{130}Xe and ^{136}Xe/^{130}Xe ratios than MORBs (Fig. 15). The small excesses in radiogenic and fissiogenic Xe appear to be correlated, but it is impossible to establish this firmly given typical analytical errors of ≥10% in ^{136}Xe/^{130}Xe. It is also possible that Xe in OIB samples is sometimes contaminated by MORB-type Xe, as suggested for the Samoan xenoliths (Poreda and Farley 1992). If Xe isotope excesses are indigenous to the OIB sources, the relative fissiogenic contributions from ^{238}U and ^{244}Pu could, in principal, be different from those for the MORB mantle. One might expect from the steady-state

mantle model (Porcelli and Wasserburg 1995b) that OIBs with high $^{3}He/^{4}He$ would have lower $^{136}Xe/^{130}Xe$ compared to MORBs, due to an enhanced ^{238}U-fissiogenic Xe component in the more degassed upper mantle. At the present time, a systematic, shallower trend of OIBs compared to MORBs is not clearly resolvable in Figure 15. A shallower slope for Iceland and Loihi is evident on the $^{129}Xe/^{130}Xe$–$^{20}Ne/^{22}Ne$ diagram (Fig. 16). This trend is poorly defined, but when extrapolated to solar $^{20}Ne/^{22}Ne = 13.8$ there is the possibility that $^{129}Xe/^{130}Xe$ could be as high as ~7.2. This could be evidence for excess ^{129}Xe in those OIB mantle source regions. In contrast, if Ne-B ($^{20}Ne/^{22}Ne$ = 12.5) is the suitable choice (Trieloff et al. 2000; see discussion of the *Solar Hypothesis* for Ne isotopes) then no ^{129}Xe anomaly is apparent. Since OIBs usually erupt at shallower depths, they also degas more extensively and are more susceptible than MORB glasses to atmospheric contamination. This accounts for much of the observed scatter in Figures 15 and 16, and also makes it difficult to precisely define different trends for OIBs.

Solar hypothesis. Ratios involving the lighter Xe isotopes $^{124,126,128}Xe$ may be diagnostic of solar Xe. These nuclides are present in relatively low abundance (0.09-1.9%) and are quite difficult to measure. Consequently, no excesses of these isotopes have yet been reported in basalts. However, excesses have been found in CO_2 well gases from the southwestern US and S Australia (Caffee et al. 1999). These gases often contain a high abundance of noble gases, helping overcome some of the analytical difficulties. Excesses of $^{124,126,128}Xe$ in the well gases are correlated with excess ^{129}Xe and with $^{20}Ne/^{22}Ne$. The ultimate origin of such well gases is usually taken to be the Earth's mantle, with some additional crustal (radiogenic and nucleogenic) components (Staudacher 1987).

COUPLED RADIOGENIC/NUCLEOGENIC PRODUCTION

If the parental nuclide abundance ratios (such as K/U, Th/U, Pu/U) are known, the inter-elemental radiogenic production ratios (e.g., $^{4}He/^{40}Ar$, $^{4}He/^{21}Ne$, $^{4}He/^{136}Xe$ and ^{4}He/heat) may be predicted for all the noble gases (predictions involving Ne are possible when matrix composition is known). This is a very powerful approach to understanding Earth processes which is still being developed. The major limitation has been the few high quality measurements of all the noble gas isotopes in individual rock samples. This coupled approach provides some of the most powerful constraints on chemical heterogeneity of the mantle, the role of partial melting, and the significance of gas loss during magma ascent to the Earth's surface. Several examples are discussed below. With special treatment of the He-Ne systematics, measured concentrations of He and Ne are not needed to infer the ratio of the primordial nuclides $^{3}He/^{22}Ne$ in the mantle source, provided that the assumption of an initial isotope composition of the solid Earth, usually taken to be solar, is valid. In other treatments, the measured noble gas concentrations, after correction for atmospheric contamination, enter into estimates of the mantle source ratios (e.g., $^{3}He/^{22}Ne_S$, $^{4}He/^{21}Ne^*$, $^{4}He/^{40}Ar^*$). The ratios estimated in this way can be compared diagrammatically, and they reveal a wealth of information about physical processes in the mantle and in magma generated from it.

Neon-helium systematics

Time-integrated $^{3}He/^{22}Ne$ ratio. *A priori* one might expect the $^{3}He/^{22}Ne$ ratio to be constant over time. The time-integrated ratio (designated $<^{3}He/^{22}Ne>$) in a mantle reservoir may be inferred directly from the isotope compositions of He and Ne (Honda and McDougall 1998), without relying on measured He and Ne concentrations. This requires assumptions for the initial He and Ne isotope compositions for the Earth, such as solar values. The time-integrated ratio is given by

$$<^{3}He/^{22}Ne> = \frac{(^{21}Ne/^{22}Ne_E - {}^{21}Ne/^{22}Ne_S)}{(^{4}He/^{3}He_M - {}^{4}He/^{3}He_S)\,J_{Ne/He}} \qquad (9)$$

where $J_{Ne/He} = 4.5 \times 10^{-8}$ is the nucleogenic ^{21}Ne to radiogenic ^{4}He production ratio of the mantle (Yatsevich and Honda 1997).

Histograms for $<^{3}He/^{22}Ne>$ are compared in Figure 17. These values were estimated assuming solar Ne isotope composition ($^{20}Ne/^{22}Ne_S = 13.8$, $^{21}Ne/^{22}Ne_S = 0.0328$) and $^{3}He/^{4}He = 150\ R_A$. This choice of initial values is internally self-consistent with solar He and Ne isotope compositions deduced from analyses of the noble gases trapped in extraterrestrial materials, in particular the atmosphere of Jupiter ($^{3}He/^{4}He = 120\ R_A$; Mahaffy et al. 2000). A self-consistent choice involving Ne-B, as suggested by Trieloff et al. (2000), would require using $^{3}He/^{4}He = 280\ R_A$, similar to the value for solar energetic particles or solar wind-implanted components.

Mean values of $<^{3}He/^{22}Ne>$ for MORBs and OIBs are 8.8±3.5 (1 sd, n = 85) and 6.0±3.6 (1 sd, n = 169), respectively. These computed results are for crushing and step heating analyses for which $^{20}Ne/^{22}Ne$ was >2 above the air value. The calculated ranges in $<^{3}He/^{22}Ne>$ are large and there are sampling biases; e.g., individual samples, such as popping rocks and Loihi basalts, are included several times because they have been analyzed by different investigators using a variety of methods. This makes it difficult to say with certainty whether any apparent difference between MORBs and OIBs is real. For comparison, the ratio of $^{3}He/^{22}Ne$ in the modern-day solar wind is ~3.8 (Benkert et al. 1993). The mantle seems to have a slightly higher average ratio than this value, which might indicate that the $^{3}He/^{22}Ne$ ratio has been fractionated in the silicate Earth, with He showing a relative enrichment. Because helium is about twice as soluble as Ne in silicate melts (Jambon et al. 1986; Lux 1987), one speculative scenario proposed to account for such a fractionation is solubility controlled degassing of an early terrestrial magma ocean (Honda and McDougall 1998).

$^{4}He/^{3}He$-$^{21}Ne/^{22}Ne$ relationships. MORBs and OIBs show a generally systematic relationship between measured He isotope composition and the $^{21}Ne/^{22}Ne$ ratio of the mantle source ($^{21}Ne/^{22}Ne_E$), calculated using Equation (3) and assuming the solar hypothesis is appropriate (Fig. 18). In this He-Ne approach, it is more expedient to use the $^{4}He/^{3}He$ ratio, because it facilitates a diagrammatic comparison of hypothetical mixing and radiogenic evolution lines, and both of these processes are easily parameterized in terms of the $^{3}He/^{22}Ne$ ratio.

Higher values of $^{3}He/^{4}He$ (low $^{4}He/^{3}He$) at localities such as Loihi and Iceland are

accompanied by lower values of $^{21}Ne/^{22}Ne_E$ (Fig. 18). The He and Ne isotopic differences between the MORB and OIB mantle sources require their source regions to have remained separated for long time periods (>10^9 years). Some of the observed He-Ne isotope variation suggests that mixing, either between mantle reservoirs or between different magmas, may have occurred relatively recently. For example, the trend may be produced by interaction of OIB source material, derived from the deep mantle and having solar-like $^{21}Ne/^{22}Ne$ and low $^4He/^3He$, with MORB source material, derived from the upper mantle and having $^4He/^3He$ = 84,600 ($^3He/^4He$ = 8.5 R_A) and $^{21}Ne/^{22}Ne$ = 0.075 (Moreira and Allègre 1995; Moreira et al. 2001). If r is defined as the concentration ratio $[^3He/^{22}Ne]_{MORB}/[^3He/^{22}Ne]_{OIB}$, where the subscripts designate the end-member components on Figure 18, a mixing line which best describes the data from Iceland would have r between 1 and 10. Compared to the OIB end-member, the MORB end-member must be enriched in He relative to Ne in this instance. This could indicate that any such mixing beneath Iceland is between a MORB magma that was previously degassed (leading to a higher He/Ne ratio as predicted from solubility considerations), and an undegassed, plume-like magma (Moreira et al. 2001). However, the observed scatter in Figure 18 for oceanic basalts also indicates a significant variation in the $^3He/^{22}Ne$ ratio from one location to another, and this might be due to differences in the type of mixing. For example, the Loihi data would be better described by r values <1, which might indicate that any mixing process occurs deeper beneath Hawaii, where magma degassing is less significant.

An alternative possibility is that the Earth's mantle is characterized by heterogeneity in $^3He/^{22}Ne$ ratio. If the initial Earth is taken to have solar-like Ne and He (e.g., $^3He/^4He$ = 150 R_A or $^4He/^3He$ = 4800), then the MORB end-member shown on Figure 18 would have $^3He/^{22}Ne$ = 12, while the OIB end-members ($^3He/^4He$ = 35 R_A or $^4He/^3He$ = 20,500), represented by Iceland ($^{21}Ne/^{22}Ne$ = 0.035) and Loihi ($^{21}Ne/^{22}Ne$ = 0.042), would have $^3He/^{22}Ne$ of 3 and 12, respectively (calculated in an analogous way to Eqn. 9). If heterogeneity accounts for the full variation observed in oceanic basalts, then $^3He/^{22}Ne$ must vary by about a factor of 20 throughout the mantle (Fig. 18).

Measured $^3He/^{22}Ne_S$ and $^4He/^{21}Ne^*$. Because ^{22}Ne in young oceanic basalts carries an insignificant nucleogenic component, the amount of mantle-derived ^{22}Ne is

$$^{22}Ne_S = {}^{22}Ne_M f_{22} \quad (10)$$

where $^{22}Ne_M$ is a sample's measured amount of ^{22}Ne and f_{22} is the proportion of mantle-derived Ne present, i.e.,

$$f_{22} = \frac{(^{20}Ne/^{22}Ne_M)-(^{20}Ne/^{22}Ne_A)}{(^{20}Ne/^{22}Ne_S)-(^{20}Ne/^{22}Ne_A)}.$$

The ratio of primordial ^3He to solar ^{22}Ne is

$$^3He/^{22}Ne_S = \frac{(^3He/^4He_M)([^4He]_M)}{([^{22}Ne]_M)f_{22}} \quad (11)$$

The amount of mantle-derived nucleogenic ^{21}Ne ($^{21}Ne^*$) in a sample is therefore given by

$$^{21}Ne^* = {}^{22}Ne_S\,(^{21}Ne/^{22}Ne_E - {}^{21}Ne/^{22}Ne_S) \quad (12)$$

Note that this situation for $^{21}Ne^*$ is unlike that for $^{40}Ar^*$, in which primordial ^{40}Ar is negligible. Because the measured Ne is comprised of 3 components (primordial, atmospheric and nucleogenic), the calculation of $^{21}Ne^*$ requires deconvolution using $^{21}Ne/^{22}Ne_E$, $^{21}Ne/^{22}Ne_S$, f_{22} and $^{22}Ne_M$.

The $^3He/^{22}Ne_S$ ratio is compared to the $^4He/^{21}Ne^*$ ratio for MORBs and OIBs in Figure 19. This diagram was first presented by Valbracht et al. (1996) in a discussion of xenoliths from Kerguelen and it was further developed by Honda and Patterson (1999), forming the basis for a discussion of He and Ne fractionation at ocean ridges. All MORB samples shown in Figure 19 are submarine glasses, while OIB samples include glasses, phenocrysts and xenoliths. The $^3He/^{22}Ne_S$ and $^4He/^{21}Ne^*$ ratios range over 3 orders of magnitude, and are correlated with a slope of ~1. MORBs in general appear to be enriched in He relative to Ne, and in He relative to Ar (see below). Xenoliths from ocean islands such as Samoa and Réunion generally appear to be fractionated in the opposite sense (Fig. 19). The large ranges in both $^3He/^{22}Ne_S$ and $^4He/^{21}Ne^*$ seen in Figure 19 is evidence for significant fractionation in the He/Ne ratio. An important conclusion of this work is that the fractionations are relatively recent, otherwise there would be a much larger variation in $^3He/^{22}Ne_S$ while $^4He/^{21}Ne^*$ would approach the production ratio. These observations further underline the need for extreme caution when inferring mantle source characteristics from the measured elemental ratios of noble gases.

Samples such as the MAR popping rock contain He and Ne with the theoretical ratios. Other MORBs generally do not, indicating that the helium enrichment characteristic of the MORB data set as a whole is probably not due to an enrichment in the upper mantle. It is also notable that a few samples from high $^3He/^4He$ localities do not show a significant fractionation from expected mantle ratios. These samples are the deeply erupted glassy basalts from Loihi seamount (Hiyagon et al. 1992; Valbracht et al. 1997; Trieloff et al. 2000) and several subglacial basalt glasses from Iceland (Dixon et al. 2000; Trieloff et al. 2000; Moreira et al. 2001). With the exception of the above three sample suites, the thousand-fold variation in He/Ne observed for other mantle-derived samples makes it clear that any attempt to estimate representative noble gas concentrations for their mantle sources is nearly futile. In light of this, the so-called "helium paradox" (i.e., the observation that OIB magmas with high $^3He/^4He$ often have lower helium contents than more deeply erupted MORB magmas; Anderson 1998a), is a manifestation of shallow level processes and has little bearing on mantle source characteristics.

Argon-helium systematics

The $^4He/^{40}Ar^*$ ratio can be computed using the measured He content and $^{40}Ar^*$ calculated from Equation (5). This ratio may then be compared to theoretical values estimated for the mantle using Equations (1) and (4).

$$\frac{^4He^*}{^{40}Ar^*} = \frac{8(e^{\lambda_{238}t}-1)+(7/137.88)(e^{\lambda_{235}t}-1)+\theta(e^{\lambda_{232}t}-1)}{(K/U)1.23x10^{-5}(e^{\lambda_{40}t}-1)} \quad (13)$$

The theoretical $^4He^*/^{40}Ar^*$ ratio varies between 1.6 (for t = 4500 Ma) and 4.2 (for $t << 1/\lambda_{235}$) for typical mantle values of $\theta = 3$ and K/U (atomic) = 7.73×10^4 (K/U weight ratio = 1.3×10^4) (Jochum et al. 1983).

The measured $^4He/^{40}Ar^*$ ratio is compared to $^4He/^{21}Ne^*$ for oceanic basalts and xenoliths in Figure 20. Oceanic basalts range over 3 orders of magnitude in He/Ar, similar to variations observed from the He-Ne systematics just considered. Nearly all MORB glasses are enriched in ^4He relative to $^{40}Ar^*$, ranging upward from the production ratio by more than a factor of 50. The popping rocks have $^4He/^{40}Ar^*$ ratios of 1.2-1.8, similar to the expected production ratio for a 4.5 Gy evolution, but about a factor of 2 lower than the value expected for an upper mantle mixing time of 10^9 years. A few of the most deeply erupted and least degassed Loihi seamount glasses analyzed by Trieloff et al. (2000) approach the theoretical ratios. Notably, the basalt glasses from Iceland reported by Trieloff et al. (2000) have also preserved the $^4He/^{40}Ar^*$ ratio of their mantle source.

A similar comparison may be made between $^4He/^{40}Ar^*$ and $^3He/^{22}Ne_S$ (Fig. 21). Again the data range is large and the ratios are broadly correlated. There is overlap between OIBs and MORBs near the expected mantle values, which includes the popping rock, Loihi Seamount and Iceland glasses. Some MORB and Loihi glasses trend at high angles away from the mantle values due to gas loss effects. In contrast, xenoliths from Kerguelen, Samoa and Réunion show a less steep slope, and trend to lower $^3He/^{22}Ne_S$ and $^4He/^{40}Ar^*$ ratios. Xenoliths from ocean islands often originate as fragments of oceanic lithosphere, and their shallower trend on Figure 21 may indicate that their trapped fluid inclusions represent gases extracted from ascending and fractionating magmas (Moreira and Sarda 2000).

Magma degassing. Figures 20 and 21 are especially diagnostic for investigating the physics of magma degassing. Moreira and Sarda (2000) and Sarda and Moreira (2002) suggest that the He-Ne-Ar covariations are produced by differences in the style of degassing for different tectonic regimes. Along mid-ocean ridges they propose that degassing is predominantly through bubble loss following closed system, equilibrium vesiculation, whereas beneath oceanic islands the degassing may largely occur through Rayleigh distillation (open system, fractional degassing), during which vesiculating bubbles are continuously lost (Figs. 20 and 21). Their model accurately reproduces the observed trends, but it requires the solubility of helium to be a factor of 4 larger than its experimentally determined value, while the solubility of Ar must remain unchanged (i.e., $S_{He} = 40S_{Ar}$ in their model compared to $S_{He} = 10S_{Ar}$ measured experimentally). The possibility that different degassing mechanisms operate beneath islands and ridges has important implications for using noble gases in basalts to infer mantle characteristics. Rayleigh degassing would lead to a much more effective gas loss, especially for the heavier noble gases, making it more difficult to detect Xe isotope anomalies in OIBs.

In situ laser analyses of two MORB glasses from the Mid-Atlantic Ridge by Burnard (1999a) reveal significant differences in He/Ar and Ar/CO_2 for individual vesicles within a sample. The observed fractionations occur during bubble growth and are consistent with a solubility-controlled Rayleigh-type degassing. Two studies of MORB glasses have also shown that $^4He/^{40}Ar^*$ is broadly correlated with axial depth and lava MgO content (Marty and Zimmerman 1999; Burnard et al. 2002). This suggests that the amount of gas loss from a MORB magma is related to confining pressure and/or the degree of crystallization of the melt. Because He solubility is an order of magnitude larger than that for Ar, the He/Ar ratio of gas bubbles will be about 10 times less than that of the parental melt. Consequently, any gas loss leads to elevated $^4He/^{40}Ar^*$ in the residual magma. Variation in $^4He/^{40}Ar^*$ for MORB suites from the East Pacific Rise and Mid-Atlantic Ridge (Marty and Zimmerman 1999) and from the Southeast Indian Ridge (Burnard et al. 2002) are consistent with such a degassing process accompanying fractional crystallization at 2-6 km depth.

Partial melting. It is also possible that observed variations in $^4He/^{40}Ar^*$ and $^4He/^{21}Ne^*$ are related to fractionation during partial melting. Firmly establishing this requires a means to correct for any possible noble gas elemental fractionation during magma crystallization and degassing. The most promising method relies on stepwise crushing of basaltic glasses and requires careful attention to detail (Burnard 2001). This method is designed to extract gas from sequentially smaller bubbles for isotopic analysis. The larger bubbles, which release their gas early in the extraction, will have formed earlier in the history of a magma and trapped less fractionated volatiles, while the smaller bubbles, which release their gas later in the extraction, formed later and trapped gas with fractionated noble gas abundances. Because the $^4He/^{21}Ne$ mantle ratio can be assumed constant, the trajectories of $^4He/^{40}Ar^*$ and $^4He/^{21}Ne^*$ measured during step crushing can be used to assess fractionation of He from Ar prior to vesiculation. Using this approach on a basalt from the Mid-Atlantic Ridge, Burnard (2001) determined an initial magmatic $^4He/^{40}Ar^*$ of ~5. This elevated ratio might be explained by a kinetically-controlled He enrichment during partial melting. It might also represent the mantle source value, if the source underwent a recent, prior episode of melting which led to He and Ar loss, because the value is similar to the instantaneous production ratio of 4.2 (Eqn. 13).

Xenon-neon-helium systematics

For Xe isotopes, one could extrapolate to a mantle end-member value using the $^{20}Ne/^{22}Ne$-$^{136}Xe/^{130}Xe$ relationships. However, analytical uncertainties in Xe isotope analyses are sufficiently large to preclude doing this in a meaningful way at the present time. A simpler way to crudely estimate the amount of radiogenic ^{136}Xe in a sample is to assume that all ^{130}Xe derives from air, analogous to the way in which ^{36}Ar is used to calculate $^{40}Ar^*$.

$$^{136}Xe^* = \left(^{136}Xe/^{130}Xe_M - ^{136}Xe/^{130}Xe_A\right) {}^{130}Xe_M \quad (14)$$

where $^{136}Xe/^{130}Xe_A = 2.176$.

The theoretical $^4He^*/^{136}Xe^*$ ratio, calculated from Equations (1) and (6), is 4.5×10^8. A comparison of measured $^4He/^{136}Xe^*$ with measured $^4He/^{21}Ne^*$ is made in Figure 22. There is much less Xe isotope data available than for the other noble gases. Nevertheless, it is remarkable that once again the Iceland basalt glasses analyzed by Trieloff et al. (2000) and the MAR popping rock show values similar to the expected production ratios for the mantle.

MANTLE ABUNDANCE PATTERNS OF NOBLE GASES

The relative abundances of primordial noble gases can be calculated from the considerations in the previous sections. The exercise will be carried out here for MORB mantle represented by the popping rock, and for OIB mantle represented by Loihi and Iceland, because basalt glasses from these localities show the least fractionation of their radiogenic production ratios from expected mantle source values.

For the purposes of this calculation the following will be assumed:

1. $^3He/^4He$ is 8.5 R_A in the MORB mantle ($^4He/^3He$ = 84,600) and 40 R_A in the OIB mantle ($^4He/^3He$ = 18,000).
2. $^{40}Ar/^{36}Ar$ is 40,000 in the MORB mantle and 8,000 in the OIB mantle (Fig. 14).
3. $^{129}Xe/^{130}Xe$ is 8.2 in the MORB mantle and 7.2 in the OIB mantle (Fig. 16). Corresponding $^{136}Xe/^{130}Xe$ ratios are 2.70 and 2.40, respectively (Fig. 15). This gives $^{136}Xe^*/^{130}Xe = (^{136}Xe/^{130}Xe_M - ^{136}Xe/^{130}Xe_A) = 0.52$ in the MORB mantle and 0.22 in the OIB mantle (Eqn. 14).
4. $^{21}Ne/^{22}Ne_E$ (Eqn. 3) is 0.075 in the MORB mantle and 0.035 in the OIB mantle (Fig. 11).
5. The radiogenic production ratios are $^4He^*/^{21}Ne^* = 2.2\times10^7$, $^4He^*/^{40}Ar^* = 2.5$ and $^4He^*/^{136}Xe^* = 4.5\times10^8$ (which assumes all $^{136}Xe^*$ is derived from fission of ^{238}U).
6. Initial isotope ratios for the Earth are $^3He/^4He$ = 150 R_A ($^4He/^3He_0$ = 4800) and $^{21}Ne/^{22}Ne_S = 0.0328$.

The terrestrial primordial ratios are then computed from:

$$^3He/^{36}Ar=(^4He^*/^{40}Ar^*)(^{40}Ar/^{36}Ar)/\{^4He/^3He - ^4He/^3He_0\}$$

$$^{22}Ne/^{36}Ar=(^4He^*/^{40}Ar^*)(^{40}Ar/^{36}Ar)/\{(^4He^*/^{21}Ne^*)(^{21}Ne/^{22}Ne_E - ^{21}Ne/^{22}Ne_S)\}$$

$$^{130}Xe/^{36}Ar=(^4He^*/^{40}Ar^*)(^{40}Ar/^{36}Ar)/\{(^4He^*/^{136}Xe^*)(^{136}Xe/^{130}Xe_M - ^{136}Xe/^{130}Xe_A)\}$$

The ratios of $^3He/^{36}Ar$ are between 1.2 and 1.5. A meaningful comparison with the atmospheric value (2.3×10^{-7}) is not possible due to the loss of ^3He to space. It is also not possible to use this approach for comparing Kr because isotope differences from atmospheric values have not been reported in oceanic basalts. Values for $^{22}Ne/^{36}Ar$ are 0.10-0.43, which is greater than the atmospheric value (0.053). For $^{130}Xe/^{36}Ar$, the OIB value is 2.0×10^{-4}, while for the popping rock it is 4.3×10^{-4}. These values are ~2 to 3 times the atmospheric $^{130}Xe/^{36}Ar$ ratio (1.13×10^{-4}).

The approach leads to some interesting first-order comparisons, but it is important to emphasize that these abundances are relative ones, and therefore do not constrain the amount of noble gases in different parts of the mantle. The abundances, normalized to solar ratios (Ozima and Podosek 2002) and to $^{36}Ar = 1$, are shown in Figure 23. There are three basic observations. First, the MORB and OIB mantles show relatively flat $^3He/^{22}Ne$. In detail, compared to the solar ratio, the MORB mantle appears to be slightly enriched in $^3He/^{22}Ne$ by about a factor of 3 (consistent with the position of the popping rock in Fig. 19). Second, ^{22}Ne is depleted, relative to ^{36}Ar, by about a factor of 2 to 8 in the atmosphere compared to the mantle. Third, ^{130}Xe is enriched by about a factor of 2 to 4, relative to ^{36}Ar, in the mantle compared to the atmosphere. This might be evidence that there is a small subduction component of atmospheric Xe in the mantle (e.g., Porcelli and Wasserburg, 1995b). Obviously there are considerable uncertainties in any approach such as the one outlined here, and the accuracy of these mantle abundance patterns depends critically on the assumptions about the Ar and Xe isotope compositions and the appropriate radiogenic production ratios.

PRINCIPAL OBSERVATIONS

In attempting to characterize mantle reservoir compositions, any model of the geochemical structure of the Earth's mantle should include or allow for the following basic observations.

1. The range of $^3He/^4He$ in MORBs away from the influence of hotspots or mantle plumes is restricted to 6.5-9.5 R_A, with roughly a normal distribution. Lower (more radiogenic) values usually occur along ridge sections where other geochemical anomalies indicate the presence of compositionally distinct mantle 'blobs' that were entrained into the convective flow beneath the ridge. The higher values in this range of 6.5-9.5 R_A are usually associated with the most trace-element-depleted mantle sources. Fine-scale structure of $^3He/^4He$ along ridges may be related to the manner in which mantle heterogeneity is sampled by secondary convection and melting in the uppermost mantle.
2. $^3He/^4He$ in OIBs ranges to values >40 R_A, supporting the existence of mantle plumes from deep in the Earth. Best model cases are Iceland and Hawaii. Temporal and spatial variations at ocean island hotspots may be weakly associated with variations in plume flux and associated melting processes, but there is no systematic global behavior between plume flux and $^3He/^4He$ signal. Some ocean island hotspots, such as Réunion, may have relatively constant and intermediate $^3He/^4He$ ratios indicating a duration of 10^7-10^8 years. This suggests the possibility of deep mantle reservoirs having variable $^3He/^4He$.
3. The mantle is characterized by elevated ratios of $^{20}Ne/^{22}Ne$ and $^{21}Ne/^{22}Ne$ compared to the atmosphere. Mid-ocean ridge basalts and ocean island basalts show distinct $^{20}Ne/^{22}Ne$-$^{21}Ne/^{22}Ne$ trends that result from differences in the dilution, by primordial Ne, of the nucleogenic ^{21}Ne that is produced in their respective mantle sources. The MORB trend passes through the composition of air and extends to values of $^{20}Ne/^{22}Ne \geq 12.5$ and $^{21}Ne/^{22}Ne \geq 0.07$. OIB trends are much

steeper; in the case of Iceland they pass through the composition of air and extend to values of $^{20}Ne/^{22}Ne \geq 12.5$ and $^{21}Ne/^{22}Ne \leq 0.035$. It seems likely that the whole mantle is characterized by a uniform value of $^{20}Ne/^{22}Ne$, but this has not been proven.

4. MORB and OIB samples show a range of measured $^{40}Ar/^{36}Ar$ that is mostly due to variable proportions of atmospheric and magmatic components. The highest $^{40}Ar/^{36}Ar$ ratio measured in a MORB is ~40,000. The correlation between $^{40}Ar/^{36}Ar$ and $^{20}Ne/^{22}Ne$ for the MAR popping rock, when extrapolated to a solar $^{20}Ne/^{22}Ne = 13.8$, indicates a possible upper limit of 44,000 for $^{40}Ar/^{36}Ar$ in the upper mantle. High $^{3}He/^{4}He$ ocean islands range to moderately high $^{40}Ar/^{36}Ar$ ratios, up to ~8000. This may be the minimum value appropriate for the mantle source of OIBs.

5. $^{129}Xe/^{130}Xe$ anomalies are present in MORBs from all the major ocean basins. Small anomalies also occur in $^{131,132,134,136}Xe/^{130}Xe$ ratios, and these are correlated with the $^{129}Xe/^{130}Xe$ anomalies. The MORB excesses in ^{129}Xe and $^{131,132,134,136}Xe$ are derived from extinct radioactivity of ^{129}I, and fission of ^{238}U and extinct ^{244}Pu. The largest MORB $^{129}Xe/^{130}Xe$ and $^{136}Xe/^{130}Xe$ ratios, and the most precisely determined, are for the popping rock, which range up to 7.73 and 2.57, respectively. The maximum $^{129}Xe/^{130}Xe$ of the MORB mantle may be near 8.2, based on extrapolation of the popping rock Xe-Ne isotope trend to solar $^{20}Ne/^{22}Ne = 13.8$ (Fig. 16). Ocean island basalts and xenoliths show smaller Xe isotope anomalies than MORBs. These small excesses in radiogenic and fissiogenic Xe appear to be correlated, but given the analytical uncertainties this is not firmly established. It is also possible that the OIBs have been contaminated by MORB-type Xe during magma ascent.

6. Coupled He-Ne isotope systematics reveal that the highest values of $^{3}He/^{4}He$ at ocean island localities are accompanied by the lowest values of $^{21}Ne/^{22}Ne_E$, the $^{21}Ne/^{22}Ne$ ratio corrected for air contamination and extrapolated to solar $^{20}Ne/^{22}Ne$. The general $^{3}He/^{4}He$-$^{21}Ne/^{22}Ne_E$ behavior (Fig. 18) suggests that either mixing between OIB and MORB components has occurred, or that the Earth's mantle is characterized by heterogeneity in $^{3}He/^{22}Ne$ ratio that is about a factor of 20. This heterogeneity may derive from fractionation processes associated with melting and degassing, or it may be primordial heterogeneity preserved since planetary accretion. The mean time-integrated $^{3}He/^{22}Ne$ ratio, inferred from coupled He-Ne isotope systematics, is similar for MORBs and OIBs (~9 and ~6, respectively) and appears to be higher than the ratio in the solar wind (~4) (Fig. 17).

7. Relatively recent fractionations dominate the measured ratios of $^{4}He/^{40}Ar^*$, $^{3}He/^{22}Ne_S$, $^{4}He/^{21}Ne^*$ and $^{4}He/^{136}Xe^*$ in MORBs and OIBs. These fractionations are controlled by magma degassing and by partial melting effects. Notable exceptions are deeply erupted basalts from Loihi Seamount and the suite of basalt glasses from Iceland studied by Trieloff et al. (2000), and the Mid-Atlantic Ridge popping rock studied by Moreira et al. (1998). These samples contain noble gases with radiogenic abundance ratios resembling values expected for the mantle. Abundance ratios of the primordial noble gases ($^{3}He/^{36}Ar$, $^{22}Ne/^{36}Ar$ and $^{130}Xe/^{36}Ar$) in the mantle sources of these basalt suites are significantly fractionated from solar ratios. The $^{3}He/^{22}Ne$ ratio is an exception, and is within a factor of three of the solar ratio.

SUMMARY

Variations in the isotope compositions of noble gases are related to processes controlling the distribution of K, U and Th, the major heat producing nuclides in the Earth. Mid-ocean ridge basalts have $^{3}He/^{4}He$ ratios between 3 and 15 R_A, while ocean island basalts have ratios between 3.5 and 43 R_A. The ubiquitous presence of 'excess' ^{3}He in mantle-derived rocks establishes that primordial volatiles are still escaping from the Earth's interior. In addition, $^{3}He/^{4}He$ ratios above 15 R_A are present only at ocean island localities, indicating a lower time-integrated $(U+Th)/^{3}He$ in their mantle source regions. The whole mantle is also characterized by elevated ratios of $^{20}Ne/^{22}Ne$ and $^{21}Ne/^{22}Ne$ compared to the atmosphere. The $^{20}Ne/^{22}Ne$ ratio appears to be relatively uniform throughout the mantle, resembling either solar wind or the solar component trapped in meteorites and the atmosphere of Jupiter. The $^{21}Ne/^{22}Ne$ ratio is variable in the mantle due to nucleogenic production of ^{21}Ne in reservoirs having different $(U+Th)/^{22}Ne$ ratios. This nucleogenic contribution is relatively larger in the MORB mantle source compared to some OIB sources (most notably at Iceland, Hawaii and Réunion), leading to higher $^{21}Ne/^{22}Ne$ in MORBs. The mantle $^{40}Ar/^{36}Ar$ ratio is variable due to variations in $K/^{36}Ar$, with MORBs displaying the highest $^{40}Ar/^{36}Ar$ ratios, up to ~40,000. The upper mantle source of MORBs is therefore characterized by higher radiogenic/primordial noble gas isotope ratios due to its degassed nature and consequent higher parent/daughter ratios (e.g., $(U+Th)/^{3}He$ and $K/^{36}Ar$). The relatively undegassed nature of the mantle source for some ocean islands is also clearly recognized from $^{3}He/^{4}He$, $^{20}Ne/^{22}Ne$-$^{21}Ne/^{22}Ne$ and $^{40}Ar/^{36}Ar$ in oceanic basalts. The contrast between MORB and OIB noble gas isotope compositions is the most fundamental geochemical evidence for some mode of stratification within the Earth's mantle. Ocean island basalts from localities such as Hawaii, Iceland and Réunion have a deeper mantle source than mid-ocean ridge basalts.

The near solar-like Ne isotope compositions, the high $^{40}Ar/^{36}Ar$ ratios, and the non-atmospheric $^{129}Xe/^{130}Xe$ and $^{136}Xe/^{130}Xe$ in oceanic basalts also provide basic clues on the origin and evolution of the atmosphere. The atmosphere appears to have 'formed' within the first 50-70 Ma of Earth's history, probably coincident with the period of terrestrial core formation (Halliday and Lee 1999).

The time-integrated ratio of the primordial nuclides ^{3}He and ^{22}Ne in the mantle may be inferred from coupled He-Ne isotope systematics. This time-integrated ratio, $<^{3}He/^{22}Ne>$, is independent of measured concentrations but rests on assumptions for the initial isotope composition of the solid Earth, usually taken to be solar. MORBs and OIBs show considerable overlap using this approach, and on average have $<^{3}He/^{22}Ne>$ ratios between 6 and 9, seemingly higher than the solar ratio of 4. Other methods for comparing relative abundance ratios in basalts depend on measured noble gas

concentrations, and are subject to more uncertainty from elemental fractionations that occur both in nature and during sample preparation or analysis. Key ratios estimated in this way include $^{3}He/^{22}Ne_{solar}$, $^{4}He/^{21}Ne^{*}$, $^{4}He/^{40}Ar^{*}$ and $^{4}He/^{136}Xe^{*}$ (where the * designates a radiogenic or nucleogenic component after correction for air contamination). Abundance ratios computed in this way may be compared to expected mantle source values, assuming radioactive equilibrium and known values of K/U and Th/U in the mantle source. Differences from the expected mantle values provide information about the style of magma degassing (e.g., bulk vs. fractional) and about crystal/magma partitioning during partial melting.

Much of our knowledge about the noble gas geochemistry of the mantle relies on the analyses of a limited number of samples from three key areas; the popping rock from 14°N on the Mid-Atlantic Ridge, submarine basalt glasses from Loihi Seamount, and subglacial basalt glasses from Iceland. It is amazing in retrospect how much information about the Earth's mantle is contained in the noble gas isotope compositions of these few samples. We should anticipate that much more remains to be learned, as analytical techniques improve and as other key sample localities are discovered.

ACKNOWLEDGMENTS

I thank Don Porcelli for encouraging me to undertake this review, and for his patience in extracting it. The work began during an extended visit to Ken Farley's lab at CalTech, where Pete Burnard graciously shared many ideas with me on noble gas geochemistry and analytical techniques. Discussions with many other people, including Don Anderson, Barry Hanan, Bernard Marty, Manuel Moreira, Don Porcelli and Philippe Sarda were also instrumental in summarizing many of the issues mentioned. John Lupton made helpful comments on several versions of the manuscript. Pete Burnard, Steve Goldstein, Dave Hilton and Don Porcelli provided detailed and constructive reviews. The work was supported by the Marine Geology & Geophysics program of the National Science Foundation.

REFERENCES

Albarède F (1998) Time-dependent models of U-Th-He and K-Ar evolution and the layering of mantle convection. Chem Geol 145:413-429

Alexander EC, Ozima M (1978) Terrestrial Rare Gases. Adv Earth Planet Sci, vol 3. Center for Academic Publications, Japan, Tokyo

Allègre CJ, Turcotte DL (1985) Geodynamic mixing in the mesosphere boundary layer and the origin of oceanic islands. Geophys Res Lett 12:207-210

Allègre CJ, Dupré B, Lewin E (1986) Thorium/uranium ratio of the Earth Chem Geol 56:219-227

Allègre CJ, Hamelin B, Dupré B (1984) Statistical analysis of isotopic ratios in MORB: the mantle blob cluster model and the convective regime of the mantle. Earth Planet Sci Lett 71:71-84

Allègre CJ, Hofmann AW, O'Nions RK (1996) The argon constraints on mantle structure. Geophys Res Lett 23:3555-3557

Allègre CJ, Moreira M, Staudacher T (1995) $^{4}He/^{3}He$ dispersion and mantle convection. Geophys Res Lett 22:2325-2328

Allègre CJ, Staudacher T, Sarda P (1986/87) Rare gas systematics: formation of the atmosphere, evolution and structure of the Earth's mantle. Earth Planet Sci Lett 81:127-150

Allègre CJ, Staudacher T, Sarda P, Kurz M (1983) Constraints on evolution of Earth's mantle from rare gas systematics. Nature 303:762-766

Anderson DL (1993) Helium-3 from the mantle: primordial signal or cosmic dust? Science 261:170-176

Anderson DL (1995) Lithosphere, asthenosphere and perisphere. Rev Geophys 33:125-149

Anderson DL (1998a) The helium paradoxes. Proc Natl Acad Sci 95:4822-4827

Anderson DL (1998b) A model to explain the various paradoxes associated with mantle noble gas geochemistry. Proc Natl Acad Sci 95:9087-9092

Anderson DL (2000a) The statistics of helium isotopes along the global spreading ridge system and the central limit theorem. Geophys Res Lett 27:2401-2404

Anderson DL (2000b) The statistics and distribution of helium in the mantle. Int'l Geol Rev 42:289-311

Anderson DL (2001) A statistical test of the two reservoir model for helium isotopes. Earth Planet Sci Lett 193:77-82

Ballentine CJ, Barfod DN (2000) The origin of air-like noble gases in MORB and OIB. Earth Planet Sci Lett 180:39-48

Ballentine CJ, Porcelli D, Wieler R (2001) Noble gases in mantle plumes. Science 291:2269a

Barfod DN, Ballentine CJ, Halliday AN, Fitton JG (1999) Noble gases in the Cameroon line and the He, Ne and Ar isotopic compositions of high μ (HIMU) mantle. J Geophys Res 104:29509-29527

Barling J, Goldstein SL (1990) Extreme isotope variations in Heard Island lavas and the nature of mantle reservoirs. Nature 348:59-62

Barling J, Goldstein SL, Nicholls IA (1994) Geochemistry of Heard Island (Southern Indian Ocean): characterization of an enriched mantle component and implications for enrichment of the sub-Indian ocean mantle. J Petrol 35:1017-1053

Basu AR, Renne PR, Das Gupta DK, Teichmann F, Poreda RJ (1993) Early and late alkali igneous pulses and a high ^{3}He plume origin for the Deccan flood basalts. Science 261:902-906

Batiza R (1984) Inverse relationship between Sr isotope diversity and rate of oceanic volcanism has implications for mantle heterogenity. Nature 309:440-441

Batiza R, Bernatowicz TJ, Hohenberg CM, Podosek FA (1979) Relations of noble gases to petrogenesis and magmatic evolution of some differentiated volcanic rocks. Contrib Mineral Petrol 69:301-314

Becker TW, Kellogg JB, O'Connell RJ (1999) Thermal constraints on the survival of primitive blobs in the lower mantle. Earth Planet Sci Lett 171:351-365

Benkert J-P, Baur H, Signer P, Wieler R (1993) He, Ne and Ar from the solar wind and solar energetic particles in lunar ilmenites and pyroxenes. J Geophys Res 98:13147-13162

Bernatowicz TJ, Podosek FA (1978) Nuclear components in the atmosphere. *In* Alexander EC, Ozima M (eds) Terrestrial Rare Gases. Center for Academic Publications Japan, Tokyo, p 99-135

Brandon AD, Graham D, Gautason B (2001) ^{187}Os-^{186}Os and He isotope systematics of Iceland picrites. EOS Trans Am Geophys Union 82:F1306

Brandon AD, Norman MD, Walker RJ, Morgan JW (1999) ^{186}Os-^{187}Os systematics of Hawaiian picrites. Earth Planet Sci Lett 174:25-42

Brandon AD, Walker RJ, Morgan JW, Norman MD, Prichard HM (1998) Coupled ^{186}Os and ^{187}Os evidence for core-mantle interaction. Science 280:1570-1573

Breddam K, Kurz MD (2001) Helium isotope signatures of Icelandic alkaline lavas. EOS Trans Am Geophys Union 82:F1315

Breddam K, Kurz MD, Storey M (2000) Mapping out the conduit of the Iceland mantle plume with helium isotopes. Earth Planet Sci Lett 176:45-55

Broadhurst CL, Drake MJ, Hagee BE, Bernatowicz TJ (1990) Solubility and partitioning of Ar in anorthite, diopside, forsterite, spinel, and synthetic basaltic liquids. Geochim Cosmochim Acta 54:299-309

Broadhurst CL, Drake MJ, Hagee BE, Bernatowicz TJ (1992) Solubility and partitioning of Ne, Ar, Kr and Xe in minerals and synthetic basaltic liquids. Geochim Cosmochim Acta 56:709-723

Brooker RA, Wartho J-A, Carroll MR, Kelley SP, Draper DS (1998) Preliminary UVLAMP determinations of argon partition coefficients for olivine and clinopyroxene grown from silicate melts. Chem Geol 147:185-200

Burnard PG (1999a) The bubble-by-bubble volatile evolution of two mid-ocean ridge basalts. Earth Planet Sci Lett 174:199-211

Burnard PG (1999b) Origin of argon-lead isotopic correlation in basalts. Science 286:871a

Burnard PG (2001) Correction for volatile fractionation in ascending magmas: noble gas abundances in primary mantle melts. Geochim Cosmochim Acta 65:2605-2614

Burnard PG, Farley KA, Turner G (1998) Multiple fluid pulses in a Samoan harzburgite. Chem Geol 147:99-114

Burnard PG, Graham DW, Farley KA (2002) Mechanisms of magmatic gas loss along the Southeast Indian Ridge and the Amsterdam-St. Paul Plateau. Earth Planet Sci Lett in press

Burnard PG, Graham DW, Turner G (1997) Vesicle-specific noble gas analyses of "popping rock": Implications for primordial noble gases gases in Earth. Science 276:568-571

Burnard PG, Stuart F, Turner G (1994a) C-He-Ar variations within a dunite nodule as a function of fluid inclusion morphology. Earth Planet Sci Lett 128:243-258

Burnard PG, Stuart FM, Turner G, Oskarsson N (1994b) Air contamination of basaltic magmas: implications for high $^{3}He/^{4}He$ mantle Ar isotopic composition. J Geophys Res 99:17709-17715

Caffee MW, Hudson GB, Veisko C, Huss GR, Alexander ECJ, Chivas AR (1999) Primordial noble gases from Earth's mantle: identification of a primitive volatile component. Science 285:2115-2118

Carroll MR, Draper DS (1994) Noble gases as trace elements in magmatic processes. Chem Geol 117: 37-56

Carroll MR, Stolper EM (1993) Noble gas solubilities in silicate melts and glasses: new experimental results for argon and the relationship between solubility and ionic porosity. Geochim Cosmochim Acta 57:5039-5051

Castillo P, Batiza R (1989) Strontium, neodymium and lead isotope constraints on near-ridge seamount production beneath the South Atlantic. Nature 342:262-265

Chamorro EM, Brooker RA, Wartho JA, Wood BK, Kelley SP, Blundy SP (2002) Ar and K partitioning between clinopyroxene and silicate melt to 8 GPa. Geochim Cosmochim Acta 66:507-519

Chamorro-Pérez E, Gillet P, Jambon A, Badro J, McMillan P (1998) Low argon solubility in silicate melts at high pressure. Nature 393

Chauvel C, Hofmann AW, Vidal P (1992) HIMU-EM: the French Polynesian connection. Earth Planet Sci Lett 110:99-119

Christensen BP, Holm PM, Jambon A, Wilson JR (2001) Helium, argon and lead isotopic composition of volcanics from Santo Antão and Fogo, Cape Verde Islands. Chem Geol 178:127-142

Clarke WB, Jenkins WJ, Top Z (1976) Determination of tritium by mass spectrometric measurement of ^{3}He. Int'l J Appl Rad Isotopes 27:515-522

Coltice N, Ricard Y (1999) Geochemical observations and one layer mantle convection. Earth Planet Sci Lett 174:125-137

Coltice N, Albarède F, Gillet P (2000) ^{40}K-^{40}Ar constraints on recycling continental crust into the mantle. Science 288:845-847

Condomines M, Gronvold K, Hooker PJ, Muehlenbachs K, O'Nions RK, Oskarsson N, Oxburgh ER (1983) Helium, oxygen, strontium and neodymium isotopic relationships in Icelandic volcanics. Earth Planet Sci Lett 66:125-136

Craig H, Lupton JE (1976) Primordial neon, helium, and hydrogen in oceanic basalts. Earth Planet Sci Lett 31:369-385

Craig H, Lupton JE (1981) Helium-3 and mantle volatiles in the ocean and the oceanic crust. *In* Emiliani C (ed) The Oceanic Lithosphere, vol 7. John Wiley & Sons, Inc, New York, p 391-428

Craig H, Clarke WB, Beg MA (1975) Excess ^{3}He in deep water on the East Pacific Rise. Earth Planet Sci Lett 26:125-132

Craig H, Lupton JE, Welhan JA, Poreda R (1978) Helium isotope ratios in Yellowstone and Lassen Park volcanic gases. Geophys Res Lett 5:897-900

Davaille A (1999) Simultaneous generation of hotspots and superswells by convection in a heterogeneous planetary mantle. Nature 402:756-760

Davies GF (1988) Ocean bathymetry and mantle convection 1. Large-scale flow and hotspots. J Geophys Res 93:10467-10480

Davies GF (1999a) Geophysically constrained mantle mass flows and ^{40}Ar budget: a degassed lower mantle? Earth Planet Sci Lett 166:149-162

Davies GF (1999b) Dynamic Earth. Cambridge University Press. Cambridge

Davies GF, Richards MA (1992) Mantle convection. J Geol 100:151-206

Des Marais DJ, Moore JG (1984) Carbon and its isotopes in mid-oceanic basalt glasses. Earth Planet Sci Lett 69:43-57

Desonie DL, Duncan RA, Kurz MD (1991) Helium isotopic composition of isotopically diverse basalts from hotspot volcanic lineaments in French Polynesia. EOS Trans Am Geophys Union 72:536

Detrick RS, Sinton JM, Ito G, Canales JP, Behn M, Blacic T, Cushman B, Dixon JE, Graham DW, Mahoney J (2002) Correlated geophysical, geochemical and volcanological manifestations of plume-ridge interaction along the Galápagos Spreading Center. Geochem Geophys Geosys in press

Dickey JSJ, Frey FA, Hart SR, Watson EB, Thompson G (1977) Geochemistry and petrology of dredged basalts from the Bouvet triple junction, South Atlantic. Geochim Cosmochim Acta 41:1105-1118

Dixon ET, Honda M, McDougall I, Campbell IH, Sigurdsson I (2000) Preservation of near-solar neon isotopic ratios in Icelandic basalts. Earth Planet Sci Lett 180:309-324

Dixon JE, Stolper E, Delaney JR (1988) Infra-red spectroscopic measurements of CO_2 and H_2O in Juan de Fuca Ridge basaltic glasses. Earth Planet Sci Lett 90:87-104

Dosso L, Bougault H, Joron J-L (1993) Geochemical morphology of the North Mid-Atlantic Ridge, 10°-24°N: trace element-isotope complementarity. Earth Planet Sci Lett 120:443-462

Dosso L, Bougault H, Beuzart P, Calvez J-Y, Joron J-L (1988) The geochemical structure of the South-East Indian Ridge. Earth Planet Sci Lett 88:47-59

Dosso L, Hanan BB, Bougault H, Schilling J-G, Joron J-L (1991) Sr-Nd-Pb geochemical morphology between 10° and 17°N on the Mid-Atlantic Ridge: a new MORB isotope signature. Earth Planet Sci Lett 106:29-43

Dosso L, Bougault H, Langmuir C, Bollinger C, Bonnier O, Etoubleau J (1999) The age and distribution of mantle heterogeneity along the Mid-Atlantic Ridge (31-41°N). Earth Planet Sci Lett 170:269-286

Douglass J, Schilling J-G, Fontignie D (1999) Plume-ridge interactions of the Discovery and Shona mantle plumes with the southern Mid-Atlantic Ridge (40°-55°S). J Geophys Res 104:2941-2962

Dupré B, Allégre CJ (1980) Pb-Sr-Nd isotopic correlation and the chemistry of the North Atlantic mantle. Nature 286:17-22

Dupré B, Lambret B, Rousseau D, Allègre CJ (1981) Limitations on the scale of mantle heterogeneities under oceanic ridges. Nature 294:552-554

Dymond J, Hogan L (1978) Factors controlling the noble gas abundance patterns of deep-sea basalts. Earth Planet Sci Lett 38:117-128

Eaby J, Clague DA, Delaney JR (1984) Sr isotopic variations along the Juan de Fuca Ridge. J Geophys Res 89:7883-7890

Edmond JM, Von Damm KL, McDuff RE, Measures CI (1982) Chemistry of hot springs on the East Pacific Rise and their effluent dispersal. Nature 297:187-191

Eiler J, Farley KA, Stolper EM (1998) Correlated He and Pb isotope variations in Hawaiian lavas. Geochim Cosmochim Acta 62:1977-1984

Elliott T, Hawkesworth CJ, Grönvold K (1991) Dynamic melting of the Iceland plume. Nature 351: 201-206

Farley KA (1995) Rapid cycling of subducted sediments into the Samoan mantle plume. Geology 23: 531-534

Farley KA, Craig H (1994) Atmospheric argon contamination of ocean island basalt olivine phenocrysts. Geochim Cosmochim Acta 58:2509-2517

Farley KA, Neroda E (1998) Noble gases in the Earth's mantle. Ann Rev Earth Planet Sci 26:189-218

Farley KA, Poreda RJ (1993) Mantle neon and atmospheric contamination. Earth Planet Sci Lett 114: 325-339

Farley KA, Basu AR, Craig H (1993) He, Sr and Nd isotopic variations in lavas from the Juan Fernandez archipelago. Contrib Mineral Petrol 115:75-87

Farley KA, Love SG, Patterson DB (1997) Atmospheric entry heating and helium retentivity of interplanetary dust particles. Geochim Cosmochim Acta 61:2309-2316

Farley KA, Natland JH, Craig H (1992) Binary mixing of enriched and undegassed (primitive?) mantle components (He, Sr, Nd,Pb) in Samoan lavas. Earth Planet Sci Lett 111:183-199

Farley KA, Poreda RJ, Onstott TC (1994) Noble gases in deformed xenoliths from an ocean island: charcterization of a metasomatic fluid. *In* Matsuda J (ed) Noble Gas Geochemistry and Cosmochemistry. Terra Scientific, Tokyo, p 159-178

Fisher DE (1978) Terrestrial potassium and argon abundances as limits to models of atmospheric evolution. *In* Alexander EC, Ozima M (ed) Terrestrial Rare Gases. Center for Academic Publications Japan, Tokyo, p 173-183

Fisher DE (1994) Mantle and atmospheric-like argon in vesicles of MORB glasses. Earth Planet Sci Lett 123:199-204

Fisher DE (1997) Helium, argon and xenon in crushed and melted MORB. Geochim Cosmochim Acta 14:3003-3012

Fontignie D, Schilling J-G (1996) Mantle heterogeneities beneath the South Atlantic: a Nd-Sr-Pb isotope study along the Mid-Atlantic Ridge (3°S-46°S). Earth Planet Sci Lett 142:209-221

Garcia MO, Rubin KH, Norman MD, Rhodes JM, Graham DW, Muenow DW, Spencer K (1998) Petrology and geochronology of basalt breccia from the 1996 earthquake swarm of Loihi seamount, Hawaii: magmatic history of 1996 eruption. Bull Volc 59:577-592

Georgen JE, Kurz MD, Dick HJB, Lin J (2001) Helium isotope systematics of the western Southwest Indian Ridge: effects of plume influence, spreading rate and source heterogeneity. EOS Trans Am Geophys Union 82:F1169

Goff F, McMurtry GM, Counce D, Simac JA, Roldán-Manzo AR, Hilton DR (2000) Contrasting hydrothermal activity at Sierra Negra and Alcedo volcanoes, Galapagos Archipelago, Ecuador. Bull Volc 62:34-52

Graham DW (1994) Helium isotope variability along mid-ocean ridges: mantle heterogeneity and melt generation effects. Mineral Mag 58A:347-348.

Graham DW, Sarda P (1991) Reply to comment by T. M. Gerlach on "Mid-ocean ridge popping rocks: implications for degassing at ridge crests". Earth Planet Sci Lett 105:568-573

Graham DW, Michael PJ, Hanan BB (1996a) Helium-carbon dioxide relationships in MORB glasses from the Mid-Atlantic Ridge at 33°S. EOS Trans Am Geophys Union 77:F830

Graham DW, Castillo P, Lupton JE, Batiza R (1996b) Correlated helium and strontium isotope ratios in South Atlantic near-ridge seamounts and implications for mantle dynamics. Earth Planet Sci Lett 144:491-503

Graham DW, Christie DM, Harpp KS, Lupton JE (1993) Mantle plume helium in submarine basalts from the Galápagos platform. Science 262:2023-2026

Graham DW, Hoernle KA, Lupton JE, Schmincke H-U (1996c) Helium isotope variations in volcanic rocks from the Canary Islands and Madeira. *In* Bohrson WA, Davidson J, Wolff JA (eds) Shallow Level Processes in Ocean Island Magmatism: Distinguishing Mantle and Crustal Signatures, Chapman Conference, Puerto de la Cruz, Tenerife. American Geophys Union, p 13-14

Graham DW, Humphris SE, Jenkins WJ, Kurz MD (1992a) Helium isotope geochemistry of some volcanic rocks from Saint Helena. Earth Planet Sci Lett 110:121-131

Graham DW, Johnson KTM, Priebe LD, Lupton JE (1999) Hotspot-ridge interaction along the Southeast Indian Ridge near Amsterdam and St. Paul Islands: helium isotope evidence. Earth Planet Sci Lett 167:297-310

Graham DW, Lupton JE, Albarède F, Condomines M (1990) Extreme temporal homogeneity of helium isotopes at Piton de la Fournaise, Réunion Island. Nature 347:545-548

Graham DW, Lupton JE, Spera FJ, Christie DM (2001) Upper mantle dynamics revealed by helium isotope variations along the Southeast Indian Ridge. Nature 409:701-703

Graham DW, Jenkins WJ, Schilling J-G, Thompson G, Kurz MD, Humphris SE (1992b) Helium isotope geochemistry of mid-ocean ridge basalts from the South Atlantic. Earth Planet Sci Lett 110:133-147

Graham DW, Larsen LM, Hanan BB, Storey M, Pedersen AK, Lupton JE (1998) Helium isotope composition of the early Iceland mantle plume inferred from the Tertiary picrites of West Greenland. Earth Planet Sci Lett 160:241-255

Graham DW, Zindler A, Kurz MD, Jenkins WJ, Batiza R, Staudigel H (1988) He, Pb, Sr and Nd isotope constraints on magma genesis and mantle heterogeneity beneath young Pacific seamounts. Contrib Mineral Petrol 99:446-463

Gurnis M, Davies GF (1986) The effect of depth-dependent viscosity on convective mixing in the mantle and the possible survival of primitive mantle. Geophys Res Lett 13:541-544

Halliday AN, Lee D-C (1999) Tungsten isotopes and the early development of the Earth and Moon. Geochim Cosmochim Acta 63:4157-4179

Halliday AN, Davidson JP, Holden P, DeWolf C, Lee D-C, Fitton JG (1990) Trace-element fractionation in plumes and the origin of HIMU mantle beneath the Cameroon line. Nature 347:523-528

Hamano Y, Ozima M (1978) Earth-atmosphere evolution model based on Ar isotopic data. *In* Alexander EC, Ozima M (eds) Terrestrial Rare Gases. Center for Academic Publications Japan, Tokyo, p 155-171

Hamelin B, Dupré B, Allègre C-J (1984) Lead-strontium isotopic variations along the East Pacific Rise and the Mid-Atlantic Ridge: a comparative study. Earth Planet Sci Lett 67:340-350

Hanan BB, Graham DW (1996) Lead and helium isotope evidence from oceanic basalts for a common deep source of mantle plumes. Science 272:991-995

Hanan BB, Schilling J-G (1997) The dynamic evolution of the Iceland mantle plume: the lead isotope perspective. Earth Planet Sci Lett 151:43-60

Hanan BB, Graham DW, Michael PJ (1994) Highly correlated lead, strontium and helium isotopes in Mid-Atlantic Ridge basalts from a dynamically evolving spreading centre at 31-34°S. Mineral Mag 58A:370-371

Hanan BB, Kingsley RH, Schilling J-G (1986) Pb isotope evidence in the South Atlantic for migrating ridge-hotspot interactions. Nature 322:137-144

Hanyu T, Kaneoka I (1997) The uniform and low $^{3}He/^{4}He$ ratios of HIMU basalts as evidence for their origin as recycled materials. Nature 390:273-276

Hanyu T, Kaneoka I, Nagao K (1999) Noble gas study of HIMU and EM ocean island basalts in the Polynesian region. Geochim Cosmochim Acta 63:1181-1201

Hanyu T, Dunai TJ, Davies GR, Kaneoka I, Nohda S, Uto K (2001) Noble gas study of the Reunion hotspot: evidence for distinct less-degassed mantle sources. Earth Planet Sci Lett 193:83-98

Harpp KS, White WM (2001) Tracing a mantle plume: isotopic and trace element variations of Galápagos seamounts. Geochem Geophys Geosys Paper 2000GC000137

Harrison D, Burnard P, Turner G (1999) Noble gas behaviour and composition in the mantle: constraints from the Iceland plume. Earth Planet Sci Lett 171:199-207

Harrison D, Burnard P, Trieloff M, Turner G (2002) Resolving atmospheric contaminants in mantle noble gas analyses. submitted

Hart R, Dymond J, Hogan L (1979) Preferential formation of the atmosphere-sialic crust system from the upper mantle. Nature 278:156-159

Hart SR, Schilling J-G, Powell JL (1973) Basalts from Iceland and along the Reykjanes Ridge: Sr isotope geochemistry. Nature 246:104-107

Hart SR, Hauri EH, Oschmann LA, Whitehead JA (1992) Mantle plumes and entrainment: isotopic evidence. Science 256:517-520

Hartmann WK (1984) Moon origin: the impact-trigger hypothesis. *In* Hartmann WK, Phillips RJ, Taylor GJ (eds) Origin of the Moon. Lunar and Planetary Institute, Houston, p 579-608

Hauri EH, Whitehead JA, Hart SR (1994) Fluid dynamic and geochemical aspects of entrainment in mantle plumes. J Geophys Res 99:24275-24300

Hegner E, Tatsumoto M (1989) Pb, Sr and Nd isotopes in seamount basalts from the Juan de Fuca Ridge and Kodiak-Bowie seamount chain, northeast Pacific. J Geophys Res 94:17839-17846

Hémond C, Arndt NT, Lichtenstein U, Hofmann AW (1993) The heterogeneous Iceland plume: Nd-Sr-O isotopes and trace element constraints. J Geophys Res 98:15833-15850

Hilton DL, Hammerschmidt K, Loock G, Friedrichsen H (1993) Helium and argon isotope systematics of the central Lau Basin and Valu Fa Ridge: evidence of crust/mantle interactions in a back-arc basin. Geochim Cosmochim Acta 57:2819-2841

Hilton DR, Barling J, Wheller GE (1995) Effect of shallow-level contamination on the helium isotope systematics of ocean-island lavas. Nature 373:330-333

Hilton DR, Macpherson CG, Elliott TR (2000a) Helium isotope ratios in mafic phenocrysts and geothermal fluids from La Palma, the Canary Islands (Spain): implications for HIMU mantle sources. Geochim Cosmochim Acta 64:2119-2132

Hilton DR, McMurtry GM, Goff F (1998a) Large variations in vent fluid $CO_2/^3He$ ratios signal rapid chnages in magma chemistry at Loihi Seamount, Hawaii. Nature 396:359-362

Hilton DR, McMurtry GM, Kreulen R (1997) Evidence for extensive degassing of the Hawaiian mantle plume from helium-carbon relationships at Kilauea volcano. Geophys Res Lett 24:3065-3068

Hilton DR, Gronvold K, Macpherson CG, Castillo PR (1999) Extreme $^3He/^4He$ ratios in northwest Iceland: constraining the common component in mantle plumes. Earth Planet Sci Lett 173:53-60

Hilton DR, Grönvold K, O'Nions RK, Oxburgh R (1990) Regional distribution of ^3He anomalies in the Icelandic crust. Chem Geol 88:53-67

Hilton DR, Gronvold K, Sveinbjornsdottir AE, Hammerschmidt K (1998b) Helium isotope evidence for off-axis degassing of the Icelandic hotspot. Chem Geol 149:173-187

Hilton DR, Thirlwall MF, Taylor RN, Murton BJ, Nichols A (2000b) Controls on magmatic degassing along the Reykjanes Ridge with implications for the helium paradox. Earth Planet Sci Lett 183:43-50

Hirschmann MM, Stolper EM (1996) A possible role for garnet pyroxenite in the origin of the "garnet signature" in MORB. Contrib Mineral Petrol 124:185-208

Hiyagon H (1994a) Retention of solar helium and neon in IDPs in deep sea sediment. Science 263: 1257-1259

Hiyagon H (1994b) Constraints on rare gas partition coefficients from analysis of olivine-glass from a picritic mid-ocean ridge basalt-Comments. Chem Geol 112:119-122

Hiyagon H, Ozima M (1982) Noble gas distribution between basalt melt and crystals. Earth Planet Sci Lett 58:255-264

Hiyagon H, Ozima M (1986) Partition of noble gases between olivine and basalt melt. Geochim Cosmochim Acta 50:2045-2057

Hiyagon H, Ozima M, Marty B, Zashu S, Sakai H (1992) Noble gases in submarine glasses from mid-ocean ridges and Loihi seamount: constraints on the early history of the Earth. Geochim Cosmochim Acta 56:1301-1316

Hofmann AW (1997) Mantle geochemistry: the message from oceanic volcanism. Nature 385:219-229

Hofmann AW, White WM (1982) Mantle plumes from ancient oceanic crust. Earth Planet Sci Lett 57: 421-436

Hofmann AW, Jochum KP, Seufert M, White WM (1986) Nb and Pb in oceanic basalts: new constraints on mantle evolution. Earth Planet Sci Lett 79:33-45

Holness MB, Richter FM (1989) Possible effects of spreading rate on MORB isotopic and rare earth composition arising from melting of a heterogeneous source. J Geol 97:247-260

Honda M, McDougall I (1998) Primordial helium and neon in the Earth-a speculation on early degassing. Geophys Res Lett 25:1951-1954

Honda M, Patterson DB (1999) Systematic elemental fractionation of mantle-derived helium, neon, and argon in mid-oceanic ridge glasses. Geochim Cosmochim Acta 63:2863-2874

Honda M, McDougall I, Patterson D (1993a) Solar noble gases in the Earth: the systematics of helium-neon isotopes in mantle derived samples. Lithos 30:257-265

Honda M, Reynolds J, Roedder E, Epstein S (1987) Noble gases in diamonds: occurrences of solar like helium and neon. J Geophys Res 92:12507-12521

Honda M, McDougall I, Patterson DB, Doulgeris A, Clague DA (1991) Possible solar noble-gas component in Hawaiian basalts. Nature 349:149-151

Honda M, McDougall I, Patterson DB, Doulgeris A, Clague DA (1993b) Noble gases in submarine pillow basalt glasses from Loihi and Kilauea, Hawaii: a solar component in the Earth. Geochim Cosmochim Acta 57:859-874

Jambon W, Weber HW, Braun O (1986) Solubility of He, Ne, Ar, Kr and Xe in a basalt melt in the range 1250-1600°C. Geochemical Implications. Geochim Cosmochim Acta 50:401-408

Javoy M, Pineau F (1991) The volatiles record of a "popping" rock from the Mid-Altantic ridge at 14°N: chemical and isotopic composition of gas trapped in the vesicles. Earth Planet Sci Lett 107:598-611

Jenkins WJ, Edmond JM, Corliss JB (1978) Excess ^3He and ^4He in Galapagos submarine hydrothermal waters. Nature 272:156-158

Jochum KP, Hofmann AW, Ito E, Seufert HM, White WM (1983) K, U and Th in mid-ocean ridge basalt glasses and heat production, K/U and K/Rb in the mantle. Nature 306:431-435

Kaneoka I (1983) Noble gas constraints on the layered structure of the mantle. Nature 302:698-700

Kaneoka I (1987) Constraints on the characteristics of magma sources for Hawaiian volcanoes based on noble gas systematics. *In* Decker RW, Wright TL, Stauffer PH (eds) Volcanism in Hawaii, US Geol Survey Prof Paper 1350. U S Government Printing Office, Washington, p 745-757

Kaneoka I, Takaoka N (1978) Excess ^{129}Xe and high $^3He/^4He$ ratios in olivine phenocrysts of Kapuho lava and xenolithic dunites from Hawaii. Earth Planet Sci Lett 39:382-386

Kaneoka I, Takaoka N (1980) Rare gas isotopes in Hawaiian ultramafic nodules and volcanic rocks : constraints on genetic relationships. Science 208:1366-1368

Kaneoka I, Takaoka N (1985) Noble-gas state in the Earth's interior-some constraints on the present state. Chem Geol (Isotope Geosci) 52:75-95

Kaneoka I, Takaoka N (1991) Evolution of the lithosphere and its interaction with the underlying mantle as inferred from noble gas isotopes. Austraian J Earth Sci 38:559-567

Kaneoka I, Takaoka N, Clague DA (1983) Noble gas systematics for coexisting glass and olivine crystals in basalts and dunite xenoliths from Loihi Seamount. Earth Planet Sci Lett 66:427-437

Kaneoka I, Takaoka N, Upton BGJ (1986) Noble gas systematics in basalts and a dunite nodule from Réunion and Grand Comore islands, Indian Ocean. Chem Geol (Isotope Geosci) 59:35-42

Keevil NB (1940) Interatomic forces and helium in rocks. Proc Am Acad Arts Sci 73:311-359

Kellogg LH (1992) Mixing in the mantle. Ann Rev Earth Planet Sci 20:365-388

Kellogg LH, Wasserburg GJ (1990) The role of plumes in mantle helium fluxes. Earth Planet Sci Lett 99:276-289

Kellogg LH, Hager B, van der Hilst R (1999) Compositional stratification in the deep mantle. Science 283:1881-1884

Kingsley RH, Schilling J-G (1995) Carbon in mid-Atlantic ridge basalt glasses from 28°N to 63°N: Evidence for a carbon-enriched Azores mantle plume. Earth Planet Sci Lett 129:31-53

Kirstein LA, Timmerman MJ (2000) Evidence of the proto-Iceland plume in northwestern Ireland at 42 Ma from helium isotopes. J Geol Soc Lond 157:923-927

Klein EM, Karsten J (1995) Ocean-ridge basalts with convergent margin geochemical affinities from the Chile Ridge. Nature 374:52-57

Klein EM, Langmuir CH (1987) Global correlations of ocean ridge basalt chemistry with axial depth and crustal thickness. J Geophys Res 92: 8089-8115

Krylov A, Mamyrin BA, Khabarin LA, Mazina TI, Silin YI (1974) Helium isotopes in ocean floor bedrock. Geochem Int'l 11:839-844

Kumagai H, Kaneoka I (1998) Variations in noble gas abundances and isotope ratios in a single MORB pillow. Geohys Res Lett 25:3891-3894

Kunz J (1999) Is there solar argon in the Earth's mantle? Nature 399:649-650

Kunz J, Staudacher T, Allègre CJ (1998) Plutonium-fission xenon found in Earth's mantle. Science 280:877-880

Kurz MD (1982) Helium isotopic geochemistry of oceanic volcanic rocks: implications for mantle heterogeneity and degassing. PhD dissertation MIT/WHOI

Kurz MD (1986) *In situ* production of terrestrial cosmogenic helium and some applications to geochronology. Geochim Cosmochim Acta 50:2855-2862

Kurz MD (1993) Mantle heterogeneity beneath oceanic islands: some inferences from isotopes. Phil Trans R Soc Lond A 342:91-103

Kurz MD, Geist D (1999) Dynamics of the Galapagos hotspot from helium isotope geochemistry. Geochim Cosmochim Acta 63:4139-4156

Kurz MD, Jenkins WJ (1981) The distribution of helium in oceanic basalt glasses. Earth Planet Sci Lett 53:41-54

Kurz MD, Kammer DP (1991) Isotopic evolution of Mauna Loa volcano. Earth Planet Sci Lett 103: 257-269
Kurz MD, Jenkins WJ, Hart SR (1982a) Helium isotopic systematics of oceanic islands and mantle heterogeneity. Nature 297:43-46
Kurz MD, le Roex AP, Dick HJB (1998) Isotope geochemistry of the oceanic mantle near the Bouvet triple junction. Geochim Cosmochim Acta 62:841-852
Kurz MD, Meyer PS, Sigurdsson H (1985) Helium isotopic systematics within the neovolcanic zones of Iceland. Earth Planet Sci Lett 74:291-305
Kurz MD, Garcia MO, Frey FA, O'Brien PA (1987) Temporal helium isotopic variations within Hawaiian volcanoes: basalts from Mauna Loa and Haleakala. Geochim Cosmochim Acta 51:2905-2914
Kurz MD, Jenkins WJ, Hart SR, Clague D (1983) Helium isotopic variations in the volcanic rocks from Loihi Seamount and the island of Hawaii. Earth Planet Sci Lett 66:388-406
Kurz MD, Jenkins WJ, Schilling J-G, Hart SR (1982b) Helium isotopic variations in the mantle beneath the central North Atlantic Ocean. Earth Planet Sci Lett 58:1-14
Kurz MD, Kammer DP, Gulessarian A, Moore RB (1990) Helium isotopes in dated alkali basalts from Sao Miguel, Azores. EOS Trans Am Geophys Union 71:657
Kurz MD, Kenna TC, Lassiter JK, DePaolo DJ (1996) Helium isotopic evolution of Mauna Kea Volcano: first results from the 1-km drill core. J Geophys Res 101:11781-11792
Kyser TK, Rison W (1982) Systematics of rare gas isotopes in basic lavas and ultramafic xenoliths. J Geophys Res 87:5611-5630
Lassiter JC, DePaolo DJ, Tatsumoto M (1996) Isotopic evolution of Mauna Kea volcano: results from the initial phase of the Hawaii Scientific Drilling Project. J Geophys Res 101:11769-11780
le Roex AP, Dick HJB, Gulen L, Reid AM, Erlank AJ (1987) Local and regional hetrogeneity in MORB from the Mid-Atlantic Ridge between 54.5°S and 51°S: evidence for geochemical enrichment. Geochim Cosmochim Acta 51:541-555
Lewis RS (1975) Rare gases in separated whitlockite from the St. Severin chondrite: xenon and krypton from fission of extinct ^{244}Pu. Geochim Cosmochim Acta 39:417-432
Leya I, Wieler R (1999) Nucleogenic production of Ne isotopes in the Earth's crust and upper mantle induced by alpha particles from the decay of U and Th. J Geophys Res 104:15439-15450
Lin WJ, Manuel OK (1987) Xenon decay products of extinct radionuclides in the Navajo, New Mexico well gas. Geochem J 21:197-207
Lupton JE (1983) Terrestrial inert gases: isotope tracer studies and clues to primordial components in the mantle. Ann Rev Earth Planet Sci 11:371-414
Lupton JE, Craig H (1975) Excess ^{3}He in oceanic basalts: evidence for terrestrial primordial helium. Earth Planet Sci Lett 26:133-139
Lupton JE, Baker ET, Massoth GJ (1989) Variable ^{3}He/heat ratios in submarine hydrothermal systems: evidence from two plumes over the Juan de Fuca Ridge. Nature 337:161-164
Lupton JE, Graham DW, Delaney JR, Johnson HP (1993) Helium isotope variations in Juan de Fuca Ridge basalts. Geophys Res Lett 20:1851-1854
Lux G (1987) The behavior of noble gases in silicate liquids: solution, diffusion, bubbles and surface effects, with applications to natural samples. Geochim Cosmochim Acta 51:1549-1560
Machado N, Ludden JN, Brooks C, Thompson G (1982) Fine-scale isotopic heterogeneity in the sub-Atlantic mantle. Nature 295:226-228
Mahaffy PR, Niemann HB, Alpert A, Atreya SK, Demick J, Donahue TM, Harpold DN, Owen TC (2000) Noble gas abundance and isotope ratios in the atmosphere of Jupiter from the Galileo probe mass spectrometer. J Geophys Res 105:15061-15071
Mahoney JJ, Graham DW, Christie DM, Johnson KTM, Hall LS, VonderHaar DL (2002) Between a hot spot and cold spot: asthenospheric flow and geochemical evolution in the Southeast Indian Ridge mantle, 86°-118°E. J Petrol in press
Mahoney JJ, Sinton JM, Kurz MD, Macdougall JD, Spencer KJ, Lugmair GW (1994) Isotope and trace element characteristics of a super-fast spreading ridge: East Pacific Rise, 13-23°S. Earth Planet Sci Lett 121:173-193
Mahoney JJ, Natland JH, White WM, Poreda R, Bloomer SH, Fisher RL, Baxter AN (1989) Isotopic and geochemical provinces of the western Indian Ocean spreading centers. J Geophys Res 94:4033-4052
Mamyrin BA, Tolstikhin IN (1984) Helium Isotopes in Nature. Elsevier. Amsterdam
Mamyrin BA, Anufriev GS, Kamenskii IL, Tolstikhin IN (1970) Determination of the isotopic composition of atmospheric helium. Geochem Int'l 7:498-505
Manga M (1996) Mixing of heterogeneities in the mantle: effect of viscosity differences. Geophys Res Lett 23:403-406
Marty B (1989) Neon and xenon isotopes in MORB: implications for the earth-atmosphere evolution. Earth Planet Sci Lett 94:45-56
Marty B (1995) Nitrogen content of the mantle inferred from N_2-Ar correlation in oceanic basalts. Nature 377:326-329
Marty B, Humbert F (1997) Nitrogen and argon isotopes in oceanic basalts. Earth Planet Sci Lett 152: 101-112
Marty B, Jambon A (1987) C/^{3}He in volatile fluxes from the solid Earth: implications for carbon geodynamics. Earth Planet Sci Lett 83:16-26
Marty B, Lussiez P (1993) Constraints on rare gas partition coefficients from analysis of olivine-glass from a picritic mid-ocean ridge basalt. Chem Geol 106:1-7
Marty B, Lussiez P (1994) Constraints on rare gas partition coefficients from analysis of olivine-glass from a picritic mid-ocean ridge basalt -Reply. Chem Geol 112:122-127
Marty B, Ozima M (1986) Noble gas distribution in oceanic basalt glasses. Geochim Cosmochim Acta 50:1093-1098
Marty B, Zimmerman L (1999) Volatiles (He, C, N, Ar) in mid-ocean ridge basalts: assessment of shallow-level fractionation and characterization of source composition. Geochim Cosmochim Acta 63:3619-3633
Marty B, Pik R, Yirgu G (1996) Helium isotopic variations in Ethiopian plume lavas: nature of magmatic sources and limit on lower mantle contribution. Earth Planet Sci Lett 144:223-237
Marty B, Upton BGJ, Ellam RM (1998) Helium isotopes in early Tertiary basalts, northeast Greenland: evidence for 58 Ma plume activity in the North Atlantic-Iceland volcanic province. Geology 26: 407-410
Marty B, Meynier V, Nicolini E, Greisshaber E, Toutain JP (1993a) Geochemistry of gas emanations: a case study of the Réunion hot spot, Indian Ocean. Appl Geochem 8:141-152
Marty B, Appora I, Barrat J-A, Deniel C, Vellutini P, Vidal P (1993b) He, Ar, Sr, Nd and Pb isotopes in volcanic rocks from Afar: evidence for a primitive mantle component and constraints on magmatic sources. Geochem J 27:223-232
Marty B, Gunnlaugsson E, Jambon A, Oskarsson N, Ozima M, Pineau F, Torssander P (1991) Gas geochemistry of geothermal fluids, the Hengill area, southwest rift zone of Iceland. Chem Geol 91: 207-225
Matsuda J (1994) Noble Gas Geochemistry and Cosmochemistry. Terra Scientific Publishing Co, Tokyo
McDougall I, Honda M (1998) Primordial solar noble-gas component in the Earth: consequences for the origin and evolution of the Earth and its atmosphere. *In* Jackson I (ed) The Earth's mantle: composition, structure and evolution. Cambridge University Press, Cambridge, p 159-187
McKenzie D, O'Nions RK (1995) The source regions of ocean island basalts. J Petrol 36:133-159
Mertz DF, Haase KM (1997) The radiogenic isotope composition of the high-latitude North Atlantic mantle. Geology 25:411-414
Mertz DF, Devey CW, Todt W, Stoffers P, Hofmann AW (1991) Sr-Nd-Pb isotope evidence against plume-asthenosphere mixing north of Iceland. Earth Planet Sci Lett 107:243-255
Michael PJ, Cornell WC (1998) Influence of spreading rate and magma supply on crystallization and assimilation beneath mid-ocean ridges: evidence from chlorine and major element chemistry of mid-ocean ridge basalts. J Geophys Res 103:18325-18356
Michael PJ, Forsyth DW, Blackman DK, Fox PJ, Hanan BB, Harding AJ, Macdonald KC, Neumann GA, Orcutt JA, Tolstoy M, Weiland CM (1994) Mantle control of a dynamically evolving spreading center: Mid-Atlantic Ridge 31-34°S. Earth Planet Sci Lett 121:451-468

Mizuno H, Nakazawa K, Hayashi C (1980) Dissolution of the primordial rare gases into the molten Earth's material. Earth Planet Sci Lett 50:202-210

Moreira M, Allègre C-J (2002) Rare gas systematics on Mid-Atlantic Ridge (37-40°N). Earth Planet Sci Lett 198:401-416.

Moreira M, Allègre CJ (1998) Helium-neon systematics and the structure of the mantle. Chem Geol 147:53-59

Moreira M, Kurz MD (2001) Subducted oceanic lithosphere and the origin of the 'high □' basalt helium isotopic signature. Earth Planet Sci Lett 189:49-57

Moreira M, Sarda P (2000) Noble gas constraints on degassing processes. Earth Planet Sci Lett 176: 375-386

Moreira M, Kunz J, Allègre C (1998) Rare gas systematics in popping rock: isotopic and elemental compositions in the upper mantle. Science 279:1178-1181

Moreira M, Valbracht PJ, Staudacher T, Allègre CJ (1996) Rare gas systematics in Red Sea ridge basalts. Geophys Res Lett 23:2453-2456

Moreira M, Doucelance R, Kurz MD, Dupré B, Allègre CJ (1999) Helium and lead isotope geochemistry of the Azores Archipelago. Earth Planet Sci Lett 169:489-205

Moreira M, Gautheron C, Breddam K, Curtice J, Kurz MD (2001) Solar neon in the Icelandic mantle: new evidence for an undegassed lower mantle. Earth Planet Sci Lett 185:15-23

Moreira M, Staudacher T, Sarda P, Schilling J-G, Allègre CJ (1995) A primitive plume neon component in MORB: the Shona ridge anomaly, South Atlantic (51-52°S). Earth Planet Sci Lett 133:367-377

Morgan WJ (1971) Convection plumes in the lower mantle. Nature 230:42-43

Morrison P, Pine J (1955) Radiogenic origin of the helium isotopes in rock. Annals NY Acad Sci 62:71-92

Mukhopadhyay S, Farley K, Bogue S (1996) Loihi-like $^{3}He/^{4}He$ ratios in shield and caldera-filling lavas from Kauai. EOS Trans Am Geophys Union 77:F811

Newsom HE, Taylor SR (1989) Geochemical implications of the formation of the moon by a single giant impact. Nature 338:29-34

Nicolaysen KE, Johnson KTM, Graham DW, Mahoney JJ, Frey FA (2002) Pb, Sr and Nd isotopes in Southeast Indian Ridge MORB near the Amsterdam and St. Paul hotspots. in prep.

Niedermann S, Bach W (1998) Anomalously nucleogenic neon in North Chile Ridge basalt glasses, suggesting a previously degassed mantle source. Earth Planet Sci Lett 160:447-462

Niedermann S, Bach W, Erzinger J (1997) Noble gas evidence for a lower mantle component in MORBs from the southern East Pacific Rise: decoupling of helium and neon isotope systematics. Geochim Cosmochim Acta 61:2697-2715

Nuccio PM, Paonita A (2000) Investigation of the noble gas solubility in H_2O-CO_2 bearing silicate liquids at moderate pressure II: the extended ionic porosity (EIP) model. Earth Planet Sci Lett 183:499-512

O'Nions RK (1987) Relationships between chemical and convective layering in the Earth. J Geol Soc Lond 144:259-274

O'Nions RK, McKenzie D (1993) Estimates of mantle thorium/uranium ratios from Th, U and Pb isotopic abundances in basaltic melts. Phil Trans R Soc Lond A342:65-74

O'Nions RK, Oxburgh ER (1983) Heat and helium in the Earth. Nature 306:429-431

O'Nions RK, Tolstikhin IN (1994) Behaviour and residence times of lithophile and rare gas tracers in the upper mantle. Earth Planet Sci Lett 124:131-138

O'Nions RK, Tolstikhin IN (1996) Limits on the mass flux between lower and upper mantle and stability of layering. Earth Planet Sci Lett 139:213-222

O'Nions RK, Evensen NM, Hamilton PJ (1979) Geochemical modeling of mantle differentiation and crustal growth. J Geophys Res 84:6091-6101

O'Nions RK, Pankhurst PJ, Grönvold K (1976) Nature and development of basalt magma sources beneath Iceland and the Reykjanes Ridge. J Petrol 17:315-338

Ozima M, Podosek FA (1999) Formation age of the Earth from $^{129}I/^{127}I$ and $^{244}Pu/^{238}U$ systematics and the missing Xe. J Geophys Res 104:25493-25499

Ozima M, Podosek FA (2002) Noble Gas Geochemistry. Cambridge University Press. Cambridge, UK

Ozima M, Zashu S (1983) Noble gases in submarine pillow volcanic glasses. Earth Planet Sci Lett 62: 24-40

Ozima M, Zashu S (1988) Solar-type Ne in Zaire cubic diamonds. Geochim Cosmochim Acta 52:19-25

Ozima M, Podosek FA, Igarashi G (1985) Terrestrial xenon isotope constraints on the early history of the Earth. Nature 315:471-474

Paonita A, Gigli G, Gozzi D, Nuccio PM, Trigila R (2000) Investigation of the He solubility in H_2O - CO_2 bearing silicate liquids at moderate pressure: a new experimental method. Earth Planet Sci Lett 181:595-604

Patterson DB, Honda M, Mcdougall I (1990) Atmospheric contamination: a possible source for heavy noble gases in basalts from Loihi seamount, Hawaii. Geophys Res Lett 17:705-708

Pepin RO (1997) Evolution of Earth's noble gases: consequences of assuming hydrodynamic loss driven by giant impact. Icarus 126:148-156

Pepin RO (1998) Isotopic evidence for a solar argon component in the Earth's mantle. Nature 394:664-667

Pepin RO, Porcelli D (2002) Origin of noble gases in the terrestrial planets. *In* Porcelli D, Ballentine CJ, Wieler R (eds) Noble gases in geochemistry and cosmochemistry, Rev Mineral Geochem (this volume)

Perez NM, Nakai S, Wakita H, Sano Y, Williams SN (1994) $^{3}He/^{4}He$ isotopic ratios in volcanic-hydrothermal discharges from the Canary Islands, Spain: implications on the origin of the volcanic activity. Mineral Mag 58:709-710

Pineau F, Javoy M (1994) Strong degassing at ridge crests: the behaviour of dissolved carbon and water in basalt glasses at 14°N, Mid-Atlantic Ridge. Earth Planet Sci Lett 123:179-198

Podosek FA, Ozima M (2000) The xenon age of the Earth. *In* Canup RM, Righter K (eds) Origin of the Earth and Moon. The University of Arizona Press, Tucson, p 63-72

Porcelli D, Ballentine CJ (2002) Models for the distribution of terrestrial noble gases and the evolution of the atmosphere. *In* Porcelli D, Ballentine CJ, Wieler R (eds) Noble gases in geochemistry and cosmochemistry, Rev Mineral Geochem (this volume)

Porcelli D, Halliday AN (2001) The core as a possible source of mantle helium. Earth Planet Sci Lett 192:45-56

Porcelli D, Pepin RO (2000) Rare gas constraints on early Earth history. *In* Canup RM, Righter K (eds) Origin of the Earth and Moon. The University of Arizona Press, Tucson, p 435-458

Porcelli D, Wasserburg GJ (1995a) Mass transfer of helium, neon, argon, and xenon through a steady-state upper mantle. Geochim Cosmochim Acta 59:4921-4937

Porcelli D, Wasserburg GJ (1995b) Mass transfer of xenon through a steady-state upper mantle. Geochim Cosmochim Acta 59:1991-2007

Porcelli D, Ballentine CJ, Wieler R (2002) General Introduction. *In* Porcelli D, Ballentine CJ, Wieler R (eds) Noble gases in geochemistry and cosmochemistry, Rev Mineral Geochem (this volume)

Poreda R, Radicati di Brozolo F (1984) Neon isotope variations in Mid-Atlantic Ridge basalts. Earth Planet Sci Lett 69:277-289

Poreda RJ, Farley KA (1992) Rare gases in Samoan xenoliths. Earth Planet Sci Lett 113:129-144

Poreda RJ, Schilling J-G, Craig H (1986) Helium and hydrogen isotopes in ocean-ridge basalts north and south of Iceland. Earth Planet Sci Lett 78:1-17

Poreda RJ, Schilling J-G, Craig H (1993) Helium isotope ratios in Easter Microplate basalts. Earth Planet Sci Lett 119:319-329

Poreda RJ, Craig H, Arnorsson S, Welhan JA (1992) Helium isotopes in Icelandic geothermal systems: I. ^{3}He, gas chemistry and ^{13}C relations. Geochim Cosmochim Acta 56:4221-4228

Richter FM, Parsons B (1973) On the interaction of two scales of convection in the mantle. J Geophys Res 80:2529-2541

Ringwood AE (1982) Phase transformations and differentiation in subducted lithosphere: implications for mantle dynamics, basalt petrogenesis, and crustal evolution. J Geol 90:611-643

Rison W, Craig H (1983) Helium isotopes and mantle volatiles in Loihi Seamount and Hawaiian Island basalts and xenoliths. Earth Planet Sci Lett 66:407-426

Rison W, Craig H (1984) Helium isotope variations along the Galapagos Spreading Center. EOS Trans Am Geophys Union 65:1139-1140
Ritsema J, van Heijst HJ, Woodhouse JH (1999) Complex shear wave velocity structure imaged beneath Africa and Iceland. Science 286:1925-1928
Roden MF, Trull T, Hart SR, Frey FA (1994) New He, Nd, Pb and Sr isotopic constraints on the constitution of the Hawaiian plume: results from Koolau Volcano, Oahu, Hawaii, USA. Geochim Cosmochim Acta 58:1431-1440
Sarda P, Graham D (1990) Mid-ocean ridge popping rocks: implications for degassing at ridge crests. Earth Planet Sci Lett 97:268-289
Sarda P, Moreira M (2002) Vesiculation and vesicle loss in mid-ocean ridge basalt glasses: He, Ne, Ar elemental fractionation and pressure influence. Geochim Cosmochim Acta 66:1449-1458
Sarda P, Moreira M, Staudacher T (1999a) Argon-lead isotopic correlation in Mid-Atlantic Ridge basalts. Science 283:666-668
Sarda P, Moreira M, Staudacher T (1999b) Response: Origin of argon-lead isotopic correlation in basalts. Science 286:871a
Sarda P, Staudacher T, Allègre CJ (1985) $^{40}Ar/^{36}Ar$ in MORB glasses: constraints on atmosphere and mantle evolution. Earth Planet Sci Lett 72:357-375
Sarda P, Staudacher T, Allègre CJ (1988) Neon isotopes in submarine basalts. Earth Planet Sci Lett 91: 73-88
Sarda P, Moreira M, Staudacher T, Schilling J-G, Allègre CJ (2000) Rare gas systematics on the southernmost Mid-Atlantic Ridge: constraints on the lower mantle and the Dupal source. J Geophys Res 105:5973-5996
Scarsi P (2000) Fractional extraction of helium by crushing of olivine and clinopyroxene phenocrysts: effects on the $^{3}He/^{4}He$ measured ratio. Geochim Cosmochim Acta 64:3751-3762
Scarsi P, Craig H (1996) Helium isotope ratios in Ethiopian Rift basalts. Earth Planet Sci Lett 144: 505-516
Schilling J-G (1973) Iceland mantle plume: Geochemical evidence along Reykjanes Ridge. Nature 242: 565-571
Schilling J-G, Kingsley RH, Devine JD (1982) Galapagos hot spot-spreading center system 1. spatial petrological and geochemical variations (83°W-101°W). J Geophys Res 87:5593-5610
Schilling J-G, Thompson G, Kingsley RH, Humphris SE (1985) Hotspot-migrating ridge interaction in the South Atlantic: geochemical evidence. Nature 313:187-191
Schilling J-G, Hanan BB, McCully B, Kingsley RH, Fontignie D (1994) Influence of the Sierra Leone mantle plume on the equatorial Mid-Atlantic Ridge: a Nd-Sr-Pb isotopic study. J Geophys Res 99:12005-12028
Schilling J-G, Kingsley R, Fontignie D, Poreda R, Xue S (1998) Dispersion of the Jan Mayen and Iceland mantle plumes in the Arctic: a He-Pb-Nd-Sr isotope tracer study of basalts from the Kolbeinsey, Mohns and Knipovich Ridges. J Geophys Res 104:10543-10569
Schmidt BC, Keppler H (2002) Experimental evidence for high noble gas solubilities in silicate melts under mantle pressures. Earth Planet Sci Lett 195:277-290
Schubert G, Turcotte DL, Olson P (2001) Mantle Convection in the Earth and Planets. Cambridge University Press, Cambridge, UK
Sempéré J-C, Cochran JR, Team SS (1997) The Southeast Indian Ridge between 88°E and 118°E: variations in crustal accretion at constant spreading rate. J Geophys Res 102:15489-15505
Shaw AM, Hilton DR, Macpherson CG, Sinton JM (2001) Nucleogenic neon in high $^{3}He/^{4}He$ lavas from the Manus back-arc basin: a new perspective on He-Ne decoupling. Earth Planet Sci Lett 194:53-66
Shibata T, Takahashi E, Matsuda J-I (1998) Solubility of neon, argon, krypton, and xenon in binary and ternary silicate systems: a new view on noble gas solubility. Geochim Cosmochim Acta 62:1241-1253
Shirey SB, Bender JF, Langmuir CH (1987) Three-component isotopic heterogeneity near the Oceanographer transform, Mid-Atlantic Ridge. Nature 325:217-223
Sleep NH (1979) Thermal history and degassing of the Earth: some simple calculations. J Geol 87:671-686
Sleep NH (1990) Hotspots and mantle plumes: some phenomenology. J Geophys Res 95:6715-6736
Small C (1995) Observations of ridge-hotspot interactions in the Southern Ocean. J Geophys Res 100:17931-17946
Small C, Cochran JR, Sempéré J-C, Christie DM (1999) The structure and segmentation of the Southeast Indian Ridge. Mar Geol 161:1-12
Staudacher T (1987) Upper mantle origin for Harding County well gases. Nature 325:605-607
Staudacher T, Allègre CJ (1982) Terrestrial xenology. Earth Planet Sci Lett 60:389-406
Staudacher T, Allègre CJ (1988) Recycling of oceanic crust and sediments: The noble gas subduction barrier. Earth Planet Sci Lett 89:173-183
Staudacher T, Allègre CJ (1989) Noble gases in glass samples from Tahiti: Teahitia, Rocard and Mehetia. Earth Planet Sci Lett 93:210-222
Staudacher T, Kurz MR, Allègre CJ (1986) New noble-gas data on glass samples from Loihi seamount and Hualalai and on dunite samples from Loihi and Réunion Island. Chem Geol 56:193-205
Staudacher T, Sarda P, Allègre CJ (1990) Noble gas systematics of Réunion Island. Chem Geol 89:1-17
Staudacher T, Sarda P, Richardson SH, Allègre CJ, Sagna I, Dmitriev LV (1989) Noble gases in basalt glasses from a Mid-Atlantic Ridge topographic high at 14°N: Geodynamic consequences. Earth Planet Sci Lett 96:119-133
Steinberger B, O'Connell RJ (1998) Advection of plumes in mantle flow: implications for hotspot motion, mantle viscosity and plume distribution. Geophys J Int'l 132:412-434
Stolper EM, Holloway JR (1988) Experimental determination of the solubility of carbon dioxide in molten basalt at low pressure. Earth Planet Sci Lett 87:397-408
Stuart FM, Ellam RM, J. HP, Fitton JG, Bell BR (2000) Constraints on mantle plumes from the helium isotope composition of basalts from the British Tertiary Igneous Province. Earth Planet Sci Lett 177:273-285
Sturm ME, Klein E, M., Graham DW, Karsten J (1999) Age constraints on crustal recycling to the mantle beneath the southern Chile Ridge: He-Pb-Sr-Nd isotope systematics. J Geophys Res 104:5097-5114
Sun S-S, Jahn BM (1975) Lead and strontium isotopes in post-glacial basalts from Iceland. Nature 255:527
Sun S-S, Tatsumoto M, Schilling J-G (1975) Mantle plume mixing along the Reykjanes Ridge axis: Lead isotopic evidence. Science 190:143-147
Swindle TD, Caffee MW, Hohenberg CM, Taylor SR (1984) I-Pu-Xe dating and the relative ages of the Earth and Moon. *In* Hartmann WK, Phillips RJ, Taylor GJ (eds) Origin of the Moon. Lunar and Planetary Institute, Houston, p 331-357
Tackley PJ (1998) Three-dimensional simulations of mantle convection with a thermo-chemical basal boundary layer: D" ? *In* Gurnis M, Wysession ME, Knittle E, Buffett BA (eds) The Core-Mantle Boundary Region, 28. American Geophysical Union, Washington, DC, p 231-253
Tatsumoto M, Unruh DM, Stille P, Fujimaki H (1984) Pb, Sr and Nd isotopes in oceanic island basalts. *In* Proc 27th Int'l Geol Congr 2, Geochemistry and Cosmochemistry, p 485-501
Taylor RN, Thirlwall MF, Murton BJ, Hilton DR, Gee MAM (1997) Isotopic constraints on the influence of the Icelandic plume. Earth Planet Sci Lett 148:E1-E8
Thompson L (1980) ^{129}Xe on the outgassing of the atmosphere. J Geophys Res 85:4374-4378
Tolstikhin IN, Marty B (1998) The evolution of terrestrial volatiles: a view from helium, neon, argon and nitrogen isotope modeling. Chem Geol 147:27-52
Trieloff M, Kunz J, Clague DA, Harrison D, Allègre CJ (2000) The nature of pristine noble gases in mantle plumes. Science 288:1036-1038
Trull TW (1994) Influx and age constraints on the recycled cosmic dust explanation for high $^{3}He/^{4}He$ ratios at hotspot volcanos. *In* Matsuda J (ed) Noble Gas Geochemistry and Cosmochemistry. Terra Scientific, Tokyo, p 77-88
Trull TW, Nadeau S, Pineau F, Polvé M, Javoy M (1993) C-He systematics in hotspot xenoliths: implications for mantle carbon contents and carbon recycling. Earth Planet Sci Lett 118:43-64
Turcotte DL, Schubert G (1988) Tectonic implications of radiogenic noble gases in planetary atmospheres. Icarus 74:36-46

Turekian KK (1959) The terrestrial economy of helium and argon. Geochim Cosmochim Acta 17:37f
Turner G (1989) The outgassing history of the Earth's atmosphere. J Geol Soc 146:147-154
Valbracht PJ, Staudacher TJ, Malahoff A, Allègre CJ (1997) Noble gas systematics of deep rift zone glasses from Loihi Seamount, Hawaii. Earth Planet Sci Lett 150:399-411
Valbracht PJ, Honda M, Staudigel H, McDougall I, Trost AP (1994) Noble gas partitioning in natural samples: results from coexisting glass and olivine phenocrysts in four Hawaiian submarine basalts. *In* Matsuda J (ed) Noble Gas Geochemistry and Cosmochemistry. Terra Scientific, Tokyo, p 373-381
Valbracht PJ, Honda M, Matsumoto T, Mattielli N, McDougall I, Ragettli R, Weis D (1996) Helium, neon and argon isotope systematics in Kerguelen ultramafic xenoliths: implications for mantle source signatures. Earth Planet Sci Lett 138:29-38
van der Hilst R, Kárason H (1999) Compositional heterogeneity on the bottom 1000 kilometers of Earth's mantle: toward a hybrid convection model. Science 283:1885-1888
van der Hilst RD, Widiyantoro S, Engdahl ER (1997) Evidence for deep mantle circulation from global tomography. Nature 386:578-584
van Keken PE, Ballentine CJ (1998) Whole-mantle versus layered mantle convection and the role of a high-viscosity lower mantle in terrestrial volatile evolution. Earth Planet Sci Lett 156:19-32
van Keken PE, Ballentine CJ (1999) Dynamical models of mantle volatile evolution and the role of phase transitions and temperature-dependent rheology. J Geophys Res 104:7137-7151
van Keken PE, Ballentine CJ, Porcelli D (2001) A dynamical investigation of the heat and helium imbalance. Earth Planet Sci Lett 188:421-434
Vance D, Stone JOH, O'Nions RK (1989) He, Sr, and Nd isotopes in xenoliths from Hawaii and other oceanic islands. Earth Planet Sci Lett 96:147-160
Verma SP, Schilling J-G (1982) Galapagos hot spot-spreading center system 2. $^{87}Sr/^{86}Sr$ and large ion lithophile element variations (85°W-101°W). J Geophys Res 87:10838-10856
Walker RJ, Morgan JW, Horan MF (1995) Osmium-187 enrichment in some plumes: Evidence for core-mantle interaction ? Science 269:819-822
Weaver BL (1991) Trace element evidence for the origin of ocean-island basalts. Geology 19:123-126
Wetherill GW (1954) Variations in the isotopic abundances of neon and argon extracted from radioactive minerals. Phys Rev 96:679-683
Wetherill GW (1975) Radiometric chronology of the early solar system. Ann Rev Nucl Sci 25:283-328
White WM (1985) Sources of oceanic basalts: radiogenic isotopic evidence. Geology 13:115-118
White WM, Schilling J-G (1978) The nature and origin of geochemical variation in Mid-Atlantic Ridge basalts from the central North Atlantic. Geochim Cosmochim Acta 42:1501-1516
White WM, McBirney AR, Duncan AR (1993) Petrology and geochemistry of the Galápagos islands: portrait of a pathological mantle plume. J Geophys Res 98:19533-19563
White WM, Schilling J-G, Hart SR (1976) Strontium isotope geochemistry of the central North Atlantic: evidence for the Azores mantle plume. Nature 263:659-
Yatsevich I, Honda M (1997) Production of nucleogenic neon in the Earth from natural radioactive decay. J Geophys Res 102:10291-10298
Zindler A, Hart SR (1986a) Helium: problematic primordial signals. Earth Planet Sci Lett 79:1-8
Zindler A, Hart SR (1986b) Chemical geodynamics. Ann Rev Earth Planet Sci 14:493-571
Zindler A, Jagoutz E, Goldstein SL (1982) Nd, Sr and Pb isotope systematics in a three-component mantle: a new perspective. Nature 298:519-523
Zindler A, Hart SR, Frey FA, Jakobsson SP (1979) Nd and Sr isotope ratios and rare earth element abundances in Reykjanes Peninsula basalts: Evidence for mantle heterogeneity beneath Iceland. Earth Planet Sci Lett 45:249-262

Table 1. Some important production pathways for noble gas isotopes.

Isotope ratio	***Process***	***Half-Life (Ma)***	***Energy Released (MeV/atom)***
LONG-LIVED RADIOACTIVITY			
	^{238}U ----> $^{206}Pb+8\ ^{4}He+6\beta^-$	4,468	47.4
$^{3}He/^{4}He$	^{235}U ----> $^{207}Pb+7\ ^{4}He+4\beta^-$	704	45.2
	^{232}Th----> $^{208}Pb+6\ ^{4}He+4\beta^-$	14,010	39.8
$^{40}Ar/^{36}Ar$	^{40}K--^{ec}-> 0.105 ^{40}Ar	1,250	0.71
$^{136,134}Xe/^{130}Xe$	^{238}U Fission	4,468	
EXTINCT RADIOACTIVITY			
$^{129}Xe/^{130}Xe$	^{129}I ----> $^{129}Xe+\beta^-$	16	
$^{136,134}Xe/^{130}Xe$	^{244}Pu Fission	82	
NUCLEOGENIC REACTIONS FROM U AND TH DECAY			
$^{21}Ne/^{22}Ne$	$^{18}O(\alpha,n)$ ---> ^{21}Ne		
	$^{24}Mg(n,\alpha)$ ---> ^{21}Ne		

Table 2. Helium isotopes in MORB glasses.

Location	*n*	*Median*	*Mean*	*Standard deviation*	*Skewness*
Atlantic	236	8.08	9.58	2.94	1.10
Pacific	245	8.14	8.13	0.98	0.04
Indian	177	8.24	8.49	1.62	1.73
All	658	8.11	8.75	2.14	1.92

Figure Captions

Figure 1. Location map of ocean ridge basalt glasses analyzed for $^{3}He/^{4}He$. Only submarine samples are included; the total number of sampling localities is 658. Data sources are Kurz (1982), Kurz and Jenkins (1981), Kurz et al. (1982b, 1998), Ozima and Zashu (1983), Rison and Craig (1984), Poreda et al. (1986, 1993), Graham et al. (1988, 1992b, 1996a,b, 1999, 2001 and unpublished data) Staudacher et al. (1989), Mahoney et al (1989, 1994), Hiyagon et al. (1992), Marty et al. (1993b) Lupton et al. (1993), Moreira et al. (1995, 1996), Taylor et al. (1997), Niedermann et al. (1997), Niedermann and Bach (1998), Schilling et al. (1998), Sturm et al. (1999), Sarda et al. (2000), Hilton et al. (2000b).

Figure 2. Histogram of MORB $^{3}He/^{4}He$ by ocean basin. For the few cases where several analyses have been performed at one sampling locality, only one sample was included as an attempt to avoid over sampling of unusually high or low $^{3}He/^{4}He$ localities. Data sources are given in the caption to Figure 1.

Figure 3. Variations in $^{3}He/^{4}He$, $^{206}Pb/^{204}Pb$ and $^{87}Sr/^{86}Sr$ along the axis of the Mid-Atlantic Ridge. Data sources are: MORB $^{3}He/^{4}He$ - Kurz et al. (1982b, 1998), Poreda et al. (1986), Graham et al. (1992b, 1996a,b and unpublished data), Staudacher et al. (1989), Moreira et al. (1995), Taylor et al. (1997), Schilling et al. (1998), Sarda et al. (2000), Hilton et al. (2000b). Iceland $^{3}He/^{4}He$ - Condomines et al. (1983), Kurz et al. (1985), Dixon et al. (2000), Breddam et al. (2000), Moreira et al. (2001). Additional MORB Sr and Pb isotopes - Hart et al. (1973), Sun et al. (1975), White et al. (1976), Dickey et al. (1977), White and Schilling (1978), Dupré and Allègre (1980), Dupré et al. (1981), Machado et al. (1982), Hamelin et al. (1984), le Roex et al. (1987), Dosso et al. (1991, 1993, 1999), Hanan et al. (1986, 1994), Castillo and Batiza (1989), Mertz et al. (1991), Shirey et al. (1987), Schilling et al. (1994, 1998), Fontignie and Schilling (1996), Mertz and Haase (1997), Kurz et al. (1998), Douglass et al. (1999). Iceland Sr and Pb - Sun and Jahn (1975), O'Nions et al. (1976), Zindler et al. (1979), Elliott et al. (1991), Hémond et al. (1993), Hanan and Schilling (1997).

Figure 4. $^{3}He/^{4}He$, Fe8, $^{87}Sr/^{86}Sr$ and ridge axis water depth vs. distance along the Southeast Indian Ridge between the Rodrigues Triple Junction and the Australian-Antarctic Discordance. Data are from Graham et al. (1999, 2001), Dosso et al. (1988), Mahoney et al. (2002), and Nicolaysen et al. (2002). The line shown for Fe8 is the 5 point running mean. Triangles represent lavas from seamounts and off-axis lava fields. The Amsterdam-St. Paul Plateau and AAD regions are depicted as shaded bands. Dashed lines and roman numerals delineate the regional tectonic segmentation from satellite gravity analysis of Small et al. (1999). Some of the geochemical structure roughly coincides with this tectonic segmentation.

Figure 5. $^{3}He/^{4}He$ vs. **A.** buoyancy flux, **B.** lithosphere age and **C.** plate speed. Points show the highest $^{3}He/^{4}He$ ratios at each island with dashed lines extending to the lowest values. Only crushing analyses are used to avoid post-eruptive addition of cosmogenic ^{3}He and radiogenic ^{4}He. Buoyancy flux is taken directly from Davies (1988) or calculated from Sleep (1990) assuming an excess plume temperature of 200°C. He data are from Kurz et al. (1982a, 1983) for Gough, Tristan da Cunha and Hawaii; Hilton et al. (1995) for Heard; Condomines et al. (1983), Kurz et al. (1985), Hilton et al. (1998b, 1999), Dixon et al. (2000), Breddam et al. (2000), Moreira et al. (2001) and Breddam and Kurz (2001) for Iceland; Kaneoka et al. (1986), Graham et al. (1990), Staudacher et al. (1990) and Marty et al. (1993a) for Réunion; Farley et al. (1992, 1993) for Samoa and Juan Fernandez; Hanyu et al. (1999) and Scarsi (2000) for Cook-Australs; Staudacher et al. (1989) and Scarsi (2000) for Societies; Graham et al. (1993) and Kurz and Geist (1999) for Galápagos; Graham et al. (1992a) for St. Helena; Poreda et al. (1993) for Easter; Kurz et al. (1998) for Bouvet; Christensen et al. (2001) for Cape Verde Islands; Graham et al. (1999) for Amsterdam/St. Paul; Moreira et al. (1999) for Azores; Hilton et al. (2000a) and Graham et al. (1996c) for Canary Islands; Desonie et al. (1991) for the Marquesas. For Easter and Amsterdam/St. Paul, the data are for values measured at the nearby spreading center because island data are not yet available. Two continental plumes (Y-Yellowstone and Afar/Ethiopia) are shown for comparison; data for Afar are from Marty et al. (1996) and Scarsi and Craig (1996) and for Yellowstone from Craig et al. (1978).

Figure 6. Map of the range of $^{3}He/^{4}He$ ratios for phenocrysts and xenoliths from historical and Quaternary lavas of the Canary Islands. Data are from Vance et al. (1989), Graham et al. (1996c) and Hilton et al. (2000a). $^{3}He/^{4}He$ ratios are systematically higher in young lavas from the western islands of La Palma and Hierro compared to the eastern islands. Pliocene lavas from La Palma extend to even higher values (8.9 R_A; Graham et al., 1996c, Hilton et al. 2000a). No Quaternary lavas are present on Gomera, but Pliocene lavas there show the full range seen in the Canary Island volcanic rocks (5.5-8.6 R_A; n = 4, Graham et al. 1996c).

Figure 7. Map of $^{3}He/^{4}He$ ratios in young lavas and fumaroles from the Galápagos Archipelago. Data are from Graham et al. (1993), Kurz and Geist (1999) and Goff et al. (2000). There is a systematic spatial variation in $^{3}He/^{4}He$ similar to the variations for other isotopic systems in the region (e.g., White et al. 1993; Harpp and White 2001). The highest $^{3}He/^{4}He$ ratios occur at the western islands of Fernandina and Isabela, while MORB-like values are found to the east near the center of the archipelago.

Figure 8. $^{3}He/^{4}He$ and $\square_{Nd}$ in basaltic lavas from Mauna Kea sampled by the Hawaii Scientific Drilling Project (HSDP). Data are from Kurz et al. (1996) and Lassiter et al. (1996). There is a covariation in He and Nd isotopes during the end of the tholeiitic shield-building stage in lavas from Mauna Kea. The temporal trend is similar to that for dated lavas from Mauna Loa (Kurz et al. 1987; Kurz and Kammer 1991), in which MORB-like compositions dominate at the very end of the shield-building stage.

Figure 9. Stratigraphic section of the variations in $^{3}He/^{4}He$, $^{87}Sr/^{86}Sr$, $^{143}Nd/^{144}Nd$ and $^{206}Pb/^{204}Pb$ at Masefau Bay, island of Tutuila (Farley et al. 1992). The data are for the alkalic basalt shield-building stage which is characteristic of the Samoan Islands.

Figure 10. He-Sr, Nd, Pb isotopic relations for mid-ocean ridge and ocean island basalts (after Graham et al. 1998 and references therein). The fields shown encompass paired analyses of the same samples in all cases, except that where boxes are shown they encompass the range of values at those localities. The $^{208}Pb^*/^{206}Pb^*$ is the isotopic ratio corrected for primordial Pb, and is related to the time-integrated Th/U ratio, designated $\square_{Pb}$ (Allègre et al. 1986). Selardalur, in northwest Iceland, is currently the locality having the highest measured $^{3}He/^{4}He$ ratio in a lava for which Sr, Nd and Pb isotope data are also available (Hilton et al. 1999).

Figure 11. The Ne three-isotope diagram ($^{20}Ne/^{22}Ne$ vs. $^{21}Ne/^{22}Ne$). Data sources are MORB - Sarda et al. (1988, 2000), Hiyagon et al. (1992), Moreira et al. (1995, 1996, 1998), Moreira and Allègre (2002), Niedermann et al. (1997), Niedermann and Bach (1998), Shaw et al. (2001); OIB- Sarda et al. (1988), Poreda and Farley (1992), Staudacher et al. (1990), Hiyagon et al. (1992), Honda et al. (1991, 1993), Valbracht et al. (1996, 1997), Dixon et al. (2000), Barfod et al. (1999), Trieloff et al. (2000), Moreira et al. (2001) and Hanyu et al. (2001). Other MORBs and OIBs are omitted for clarity. Plotted points include individual analysis steps (crushing or heating), but only when the measured $^{20}Ne/^{22}Ne$ was >2-sigma above the air ratio. Darker symbols for the southern MAR data set crudely form a vector between the MORB line and solar compositions; these are lavas from the Shona and Discovery hotspot-influenced sections of the ridge, where $^{3}He/^{4}He$ ratios range up to 15 R_A (Moreira et al. 1995; Sarda et al. 2000); see text for further discussion. Dashed lines depict mixing between air and mantle Ne for Iceland, Loihi, Réunion, Kerguelen and MORB (MAR popping rock), drawn through the highest $^{20}Ne/^{22}Ne$ or the most precisely determined compositions for each locality. The extrapolated $^{21}Ne/^{22}Ne$ ratio, corresponding to solar $^{20}Ne/^{22}Ne$ at each locality, is 0.035 for Iceland, 0.039 for Loihi, 0.043 for Réunion, 0.053 for Kerguelen and 0.075 for MORB.

Figure 12. Schematic illustration for determining $^{21}Ne/^{22}Ne_E$, the extrapolated $^{21}Ne/^{22}Ne$ ratio of the mantle. S, A, M and E correspond to solar, air, measured and extrapolated values.

Figure 13. $^{3}He/^{4}He$ vs. $^{40}Ar/^{36}Ar$. Plotted points include individual analysis steps (crushing or heating), but only when the measured $^{40}Ar/^{36}Ar$ was >2-sigma above the air ratio. Data sources are given in the caption to Figure 11.

Figure 14. $^{40}Ar/^{36}Ar$ vs. $^{20}Ne/^{22}Ne$. Data sources are given in the caption to Figure 11. Plotted points include individual analysis steps (crushing or heating), but only when the measured Ne and Ar isotope ratios were >2-sigma above the air ratio.

Figure 15. $^{136}Xe/^{130}Xe$ vs. $^{129}Xe/^{130}Xe$. Data sources are Staudacher and Allègre (1982), Staudacher et al. (1989), Marty (1989), Hiyagon et al. (1992), Poreda and Farley (1992), Moreira et al. (1998), Kunz et al. (1998), Trieloff et al. (2000), Sarda et al. (2000). The lines show trends produced by decay of the indicated parental nuclides. Plotted points include individual analysis steps (crushing or heating), but only when both measured Xe isotope ratios were >2-sigma above the air values, and when 2-sigma errors were <10%. A proportion of 32% for fissiogenic ^{136}Xe that is ^{244}Pu-derived, as suggested by Kunz et al. (1998), is illustrated.

Figure 16. $^{129}Xe/^{130}Xe$ vs. $^{20}Ne/^{22}Ne$. Data sources are Hiyagon et al. (1992), Poreda and Farley (1992), Moreira et al. (1998), Kunz et al. (1998), Trieloff et al. (2000), Sarda et al. (1988, 2000). Plotted points include individual analysis steps (crushing or heating), but only when measured ratios were >2-sigma above the air values, and when 2-sigma error for $^{129}Xe/^{130}Xe$ <10%.

Figure 17. Histogram of $<^{3}He/^{22}Ne>$ for MORBs and OIBs inferred from the He-Ne isotope systematics. Data sources are given in the caption to Figure 11.

Figure 18. $^{4}He/^{3}He$ vs. $^{21}Ne/^{22}Ne_E$. Data sources are given in the caption to Figure 11. Two hypothetical mixing curves are shown by the dashed lines, for values of r = 1 and r = 10, where $r = [^{3}He/^{22}Ne]_{MORB}/[^{3}He/^{22}Ne]_{OIB}$. The OIB end-member has $^{3}He/^{4}He = 35\ R_A$ and $^{21}Ne/^{22}Ne_E = 0.035$, and the MORB end-member has $^{3}He/^{4}He = 8.5\ R_A$ and $^{21}Ne/^{22}Ne_E = 0.075$ for this illustration. Closed system evolution lines from solar He and Ne isotope compositions are also illustrated, for $^{3}He/^{22}Ne$ ratios of 1, 10, 20 and 50.

Figure 19. $^{3}He/^{22}Ne_S$ vs. $^{4}He/^{21}Ne^*$. Data sources are given in the caption to Figure 11. In figures 19-22, individual analyses carried out by stepwise crushing are plotted, but for incremental heating analyses only the total gas contents are shown in order to avoid possible inter-elemental fractionation during heating. The box shows theoretical values for the mantle. The mantle production ratio for $^{4}He^*/^{21}Ne^* = 2.2\square10^{7}$ (Yatsevich and Honda 1997). The range of $^{3}He/^{22}Ne_S$ shown by the box is between 4, the value for modern solar wind, and 9, the mean value for the time-integrated $^{3}He/^{22}Ne$ ratio of the upper mantle (Fig. 17).

Figure 20. $^{4}He/^{40}Ar^*$ vs. $^{4}He/^{21}Ne^*$. Data sources are given in the caption to Figure 11. The box shows the range of mantle production ratios for $^{4}He^*/^{40}Ar^* = 1.6\text{-}4.2$, and $^{4}He^*/^{21}Ne^* = 2.2\square10^{7}$ for reference. Two degassing lines are illustrated, one for open-system Rayleigh degassing, and one for closed-system, bulk degassing. The Rayleigh curve shows the trajectory for a residual magma which underwent open system gas loss, given by $R/R_0 = f^{(1-\square)}$, where R is the He/Ne or He/Ar ratio in the magma, R_0 is the initial ratio, f is the fraction of He remaining, and $\square$ is the solubility ratio S_{He}/S_{Ne} or S_{He}/S_{Ar}, where S is noble gas solubility. For basaltic melts, $S_{He}/S_{Ne} = 2$ and $S_{He}/S_{Ar} = 10$ (Jambon et al. 1986; Lux 1987). Closed-system degassing occurs when bulk loss of bubbles follows equilibrium vesiculation, and is shown by the curves labeled melt and vesicles. The melt curve corresponds to the residual magma and the vesicle curve shows the range of values in the exsolved gas phase when vesicularity is >0.01 % by volume.

Figure 21. $^{4}He/^{40}Ar^*$ vs. $^{3}He/^{22}Ne_S$. Data sources are given in the caption to Figure 11. The box shows the range of $^{4}He^*/^{40}Ar^* = 1.6\text{-}4.2$ and $^{3}He/^{22}Ne_S = 4\text{-}9$ for reference. The two degassing curves are described in the caption to Figure 20.

Figure 22. $^{4}He/^{136}Xe^*$ vs. $^{4}He/^{21}Ne^*$. Data sources are given in the caption to Figure 11. The box shows mantle production ratios for $^{4}He^*/^{136}Xe^* = 4.5\square10^{8}$ and $^{4}He^*/^{21}Ne^* = 2.2\square10^{7}$ for reference.

Figure 23. Abundance pattern of primordial noble gases in model MORB and OIB mantle sources, calculated as outlined in the text. The ratios are normalized to the solar pattern and to $^{36}Ar = 1$. The pattern for the atmosphere is shown for comparison.

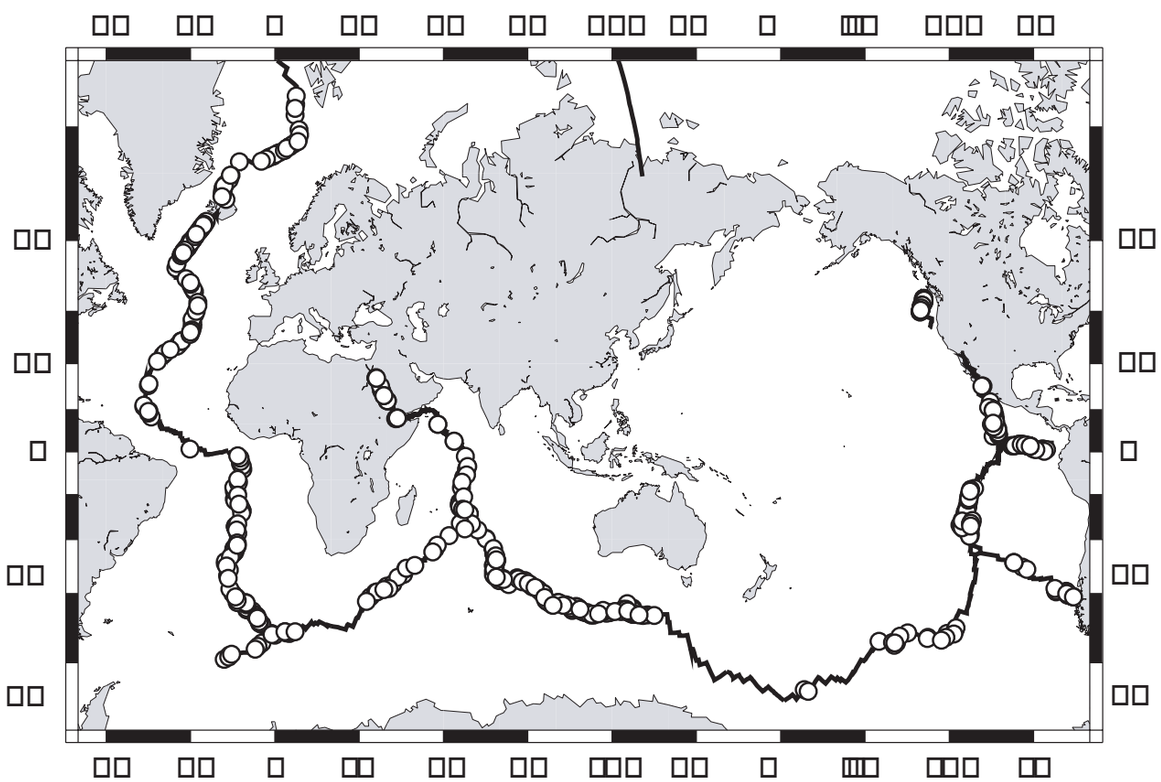

Figure 1

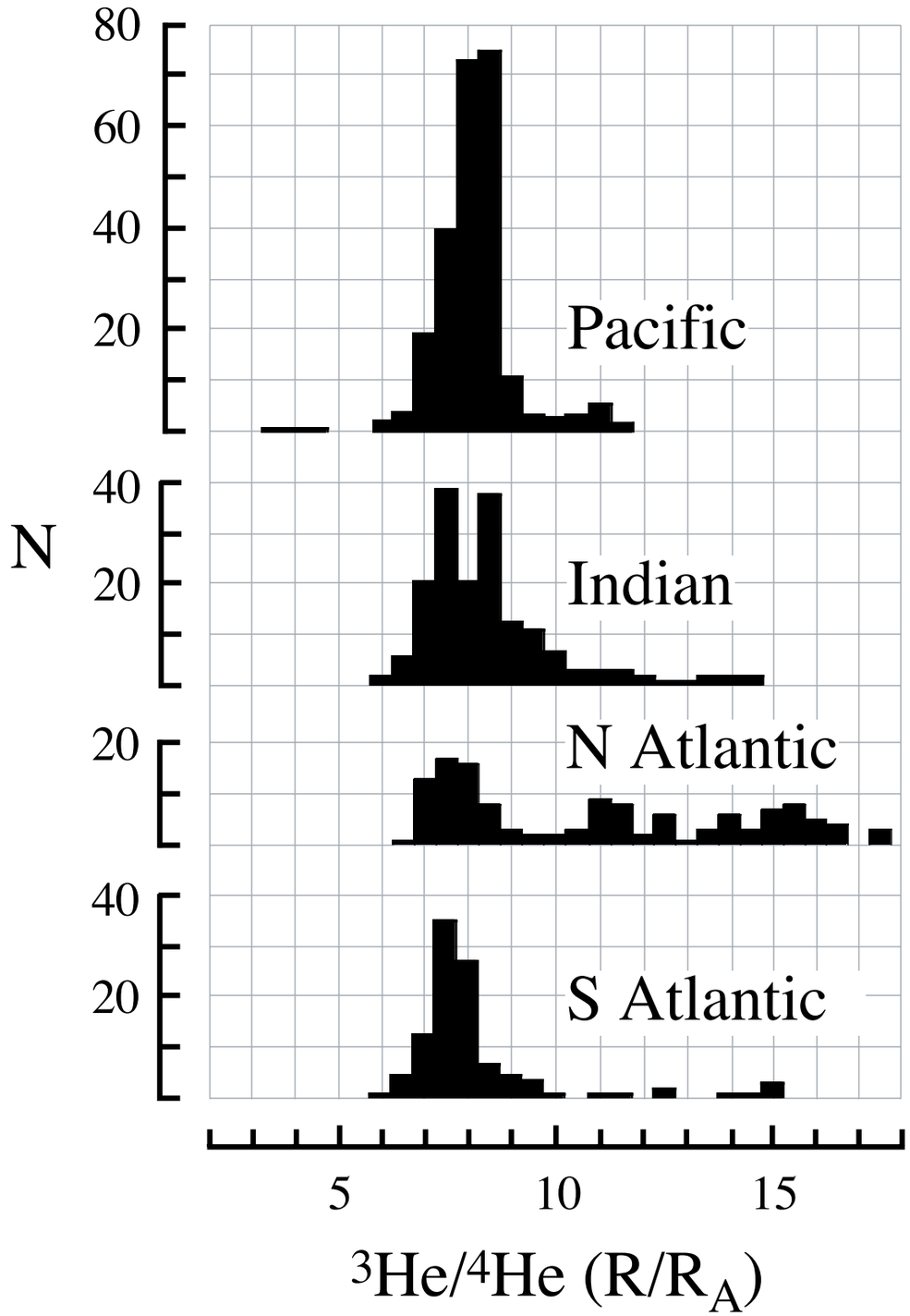

Figure 2

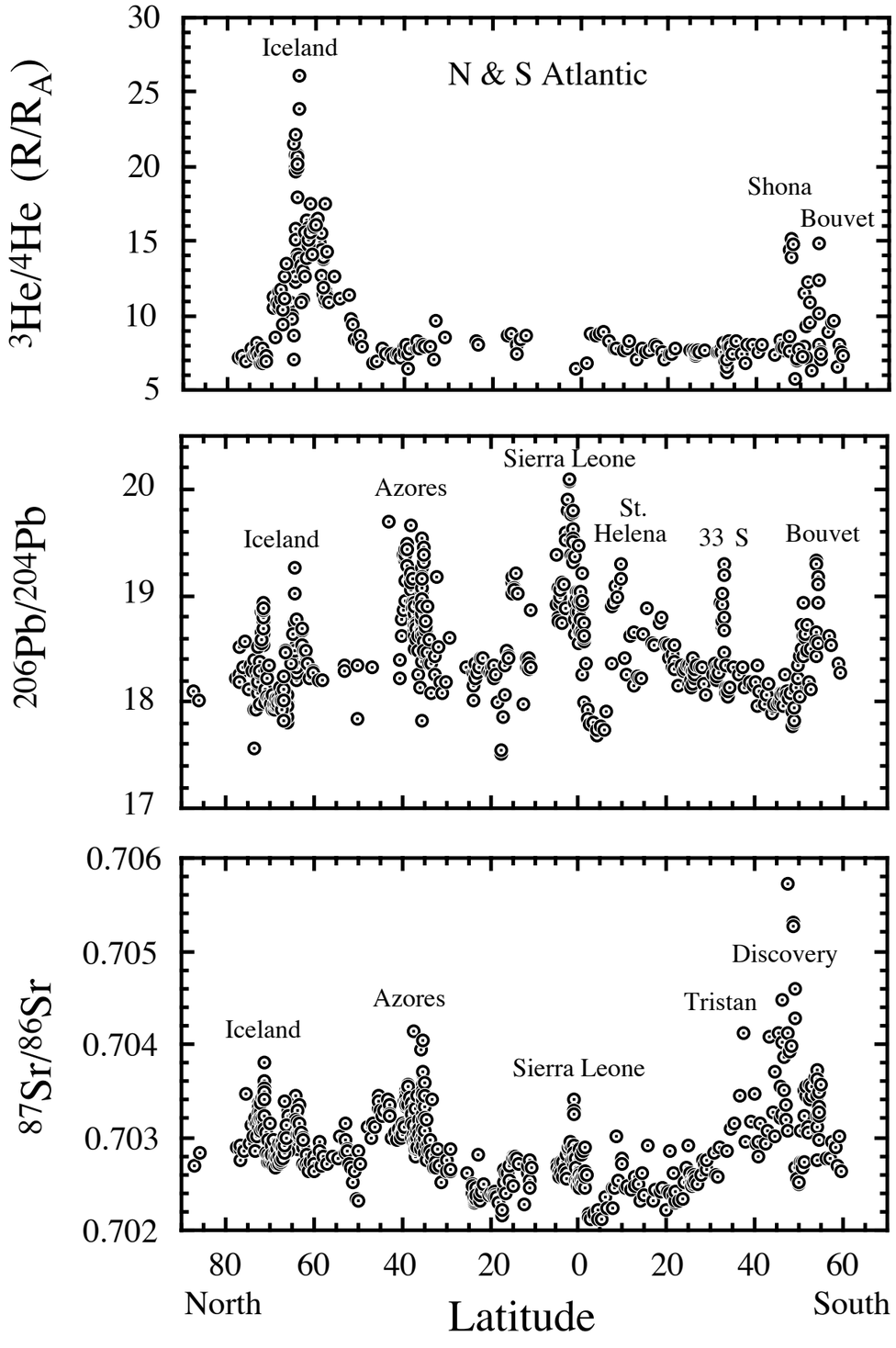

Figure 3

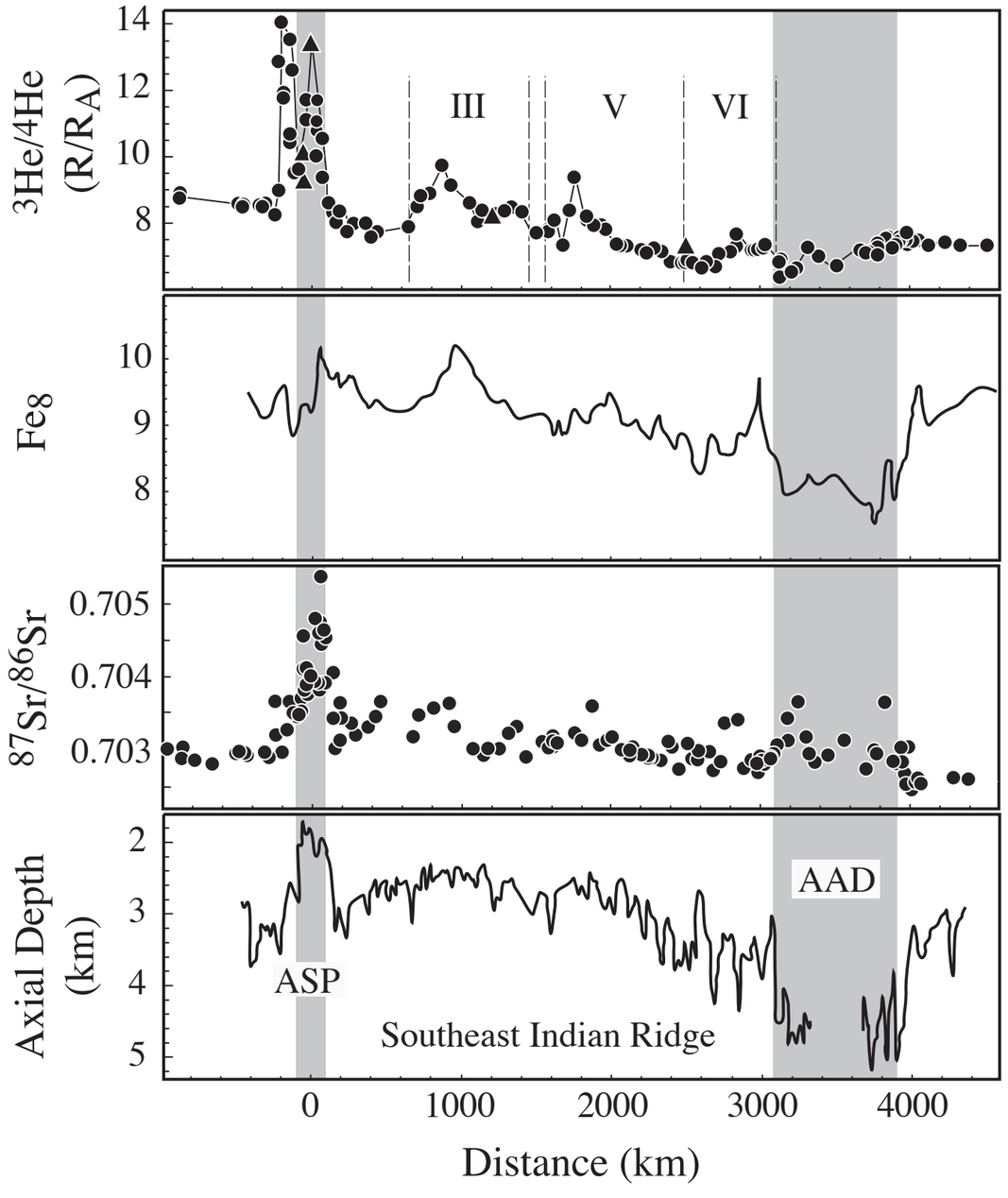

Figure 4

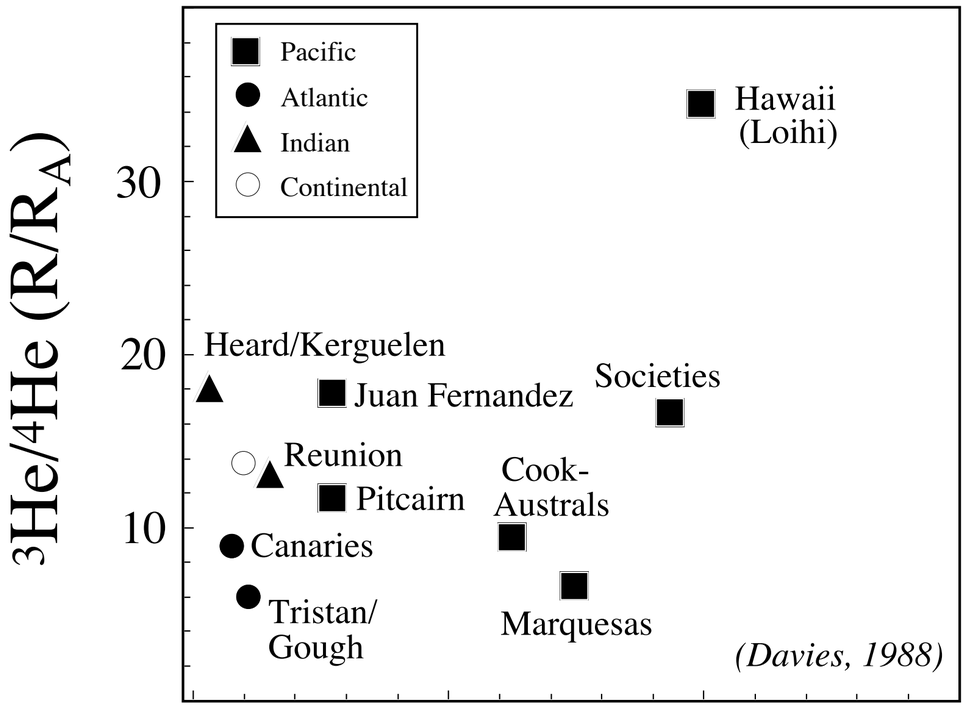
Pacific
Atlantic
Indian
Continental
Hawaii (Loihi)
Heard/Kerguelen
Juan Fernandez
Societies
Reunion
Pitcairn
Cook-Australs
Canaries
Tristan/ Gough
Marquesas
(Davies, 1988)
3He/4He (R/RA)
30
20
10

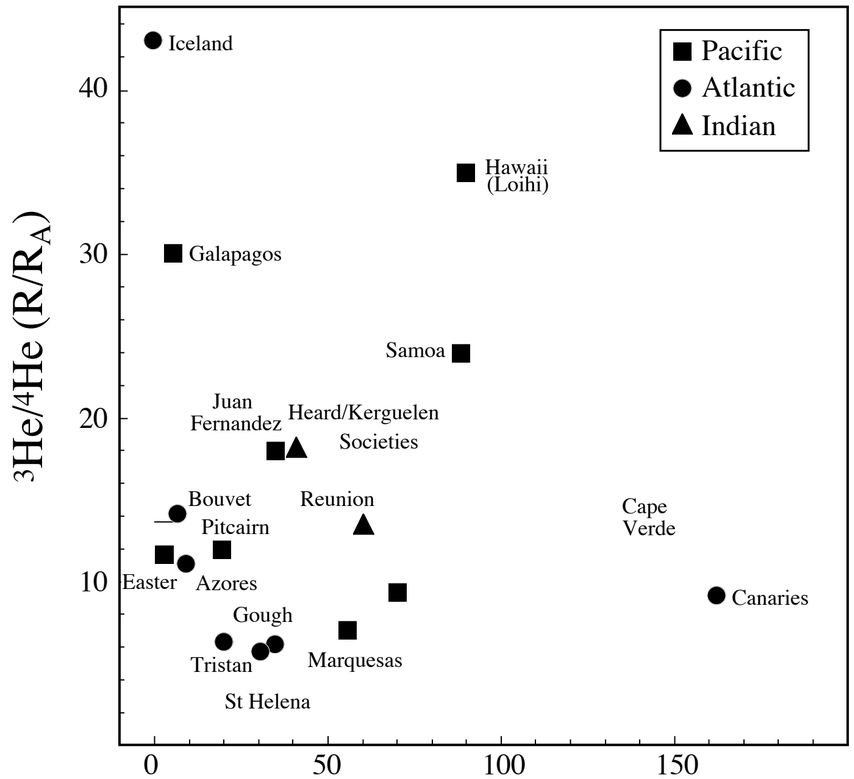
Iceland
Pacific
Atlantic
Indian
Hawaii (Loihi)
Galapagos
Samoa
Juan Fernandez
Heard/Kerguelen
Societies
Bouvet
Reunion
Pitcairn
Cape Verde
Easter
Azores
Canaries
Gough
Tristan
Marquesas
St Helena
3He/4He (R/RA)
40
30
20
10
0
50
100
150
Lithosphere Age (Ma)

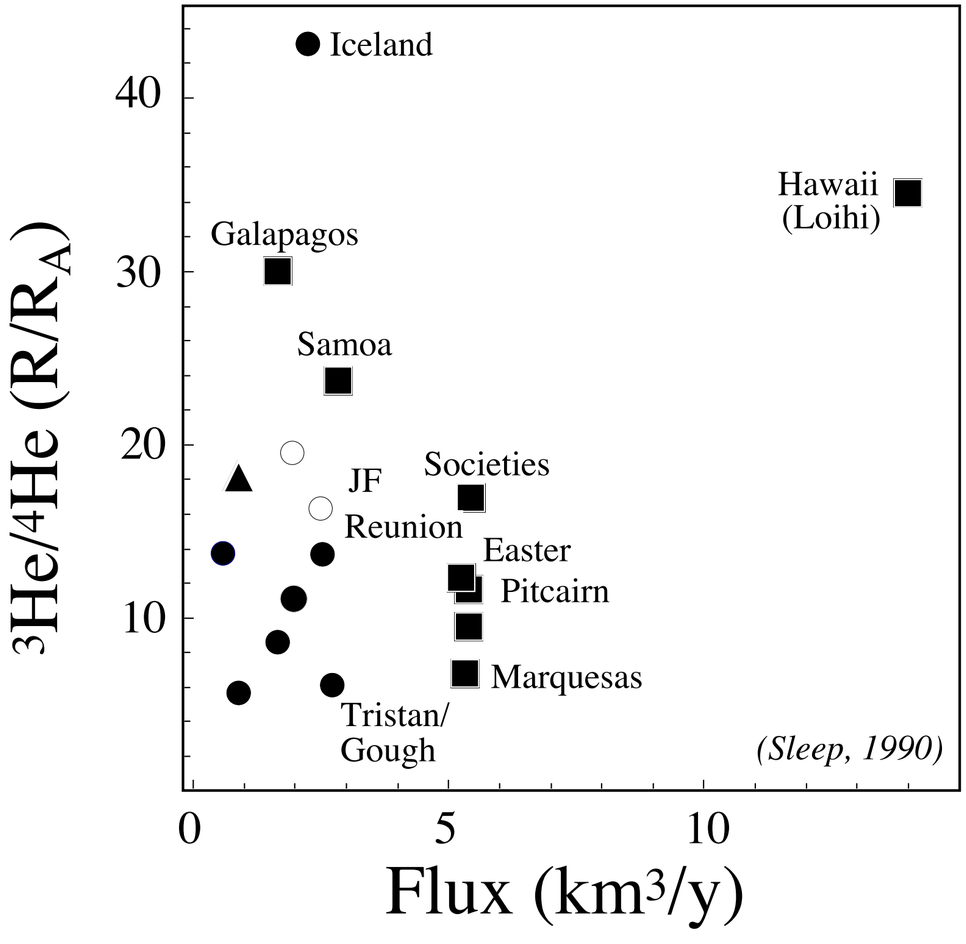
Iceland
Hawaii (Loihi)
Galapagos
Samoa
JF
Societies
Reunion
Easter
Pitcairn
Marquesas
Tristan/ Gough
(Sleep, 1990)
3He/4He (R/RA)
40
30
20
10
0
5
10
Flux (km3/y)

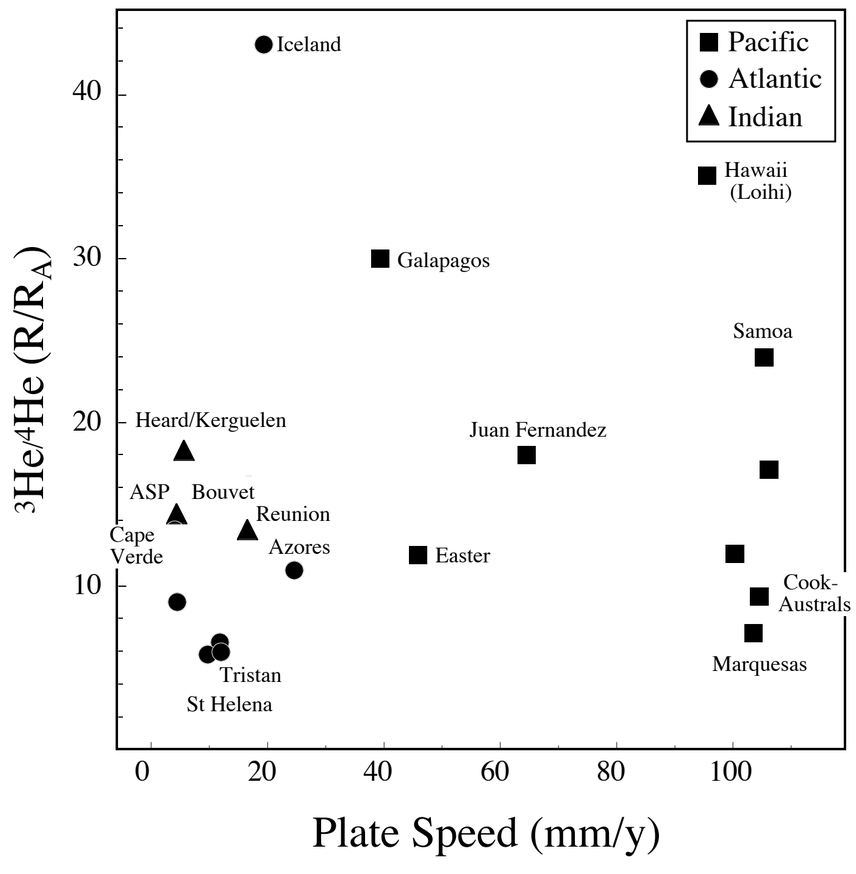
Iceland
Pacific
Atlantic
Indian
Hawaii (Loihi)
Galapagos
Samoa
Heard/Kerguelen
Juan Fernandez
ASP
Bouvet
Reunion
Cape Verde
Azores
Easter
Cook-Australs
Marquesas
Tristan
St Helena
3He/4He (R/RA)
40
30
20
10
0
20
40
60
80
100
Plate Speed (mm/y)

Fig. 5

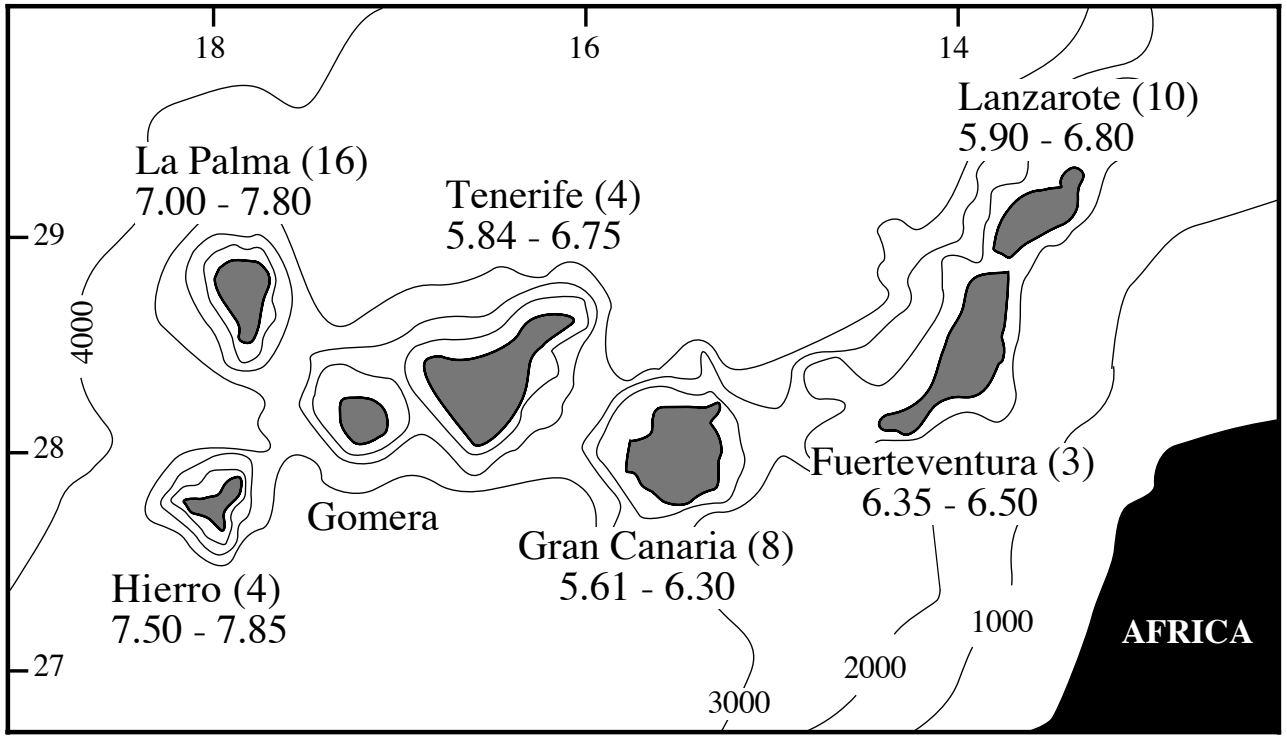
18
16
14
Lanzarote (10)
5.90 - 6.80
La Palma (16)
7.00 - 7.80
Tenerife (4)
5.84 - 6.75
29
4000
28
Fuerteventura (3)
6.35 - 6.50
Gomera
Gran Canaria (8)
5.61 - 6.30
Hierro (4)
7.50 - 7.85
1000
AFRICA
27
2000
3000

Fig. 6

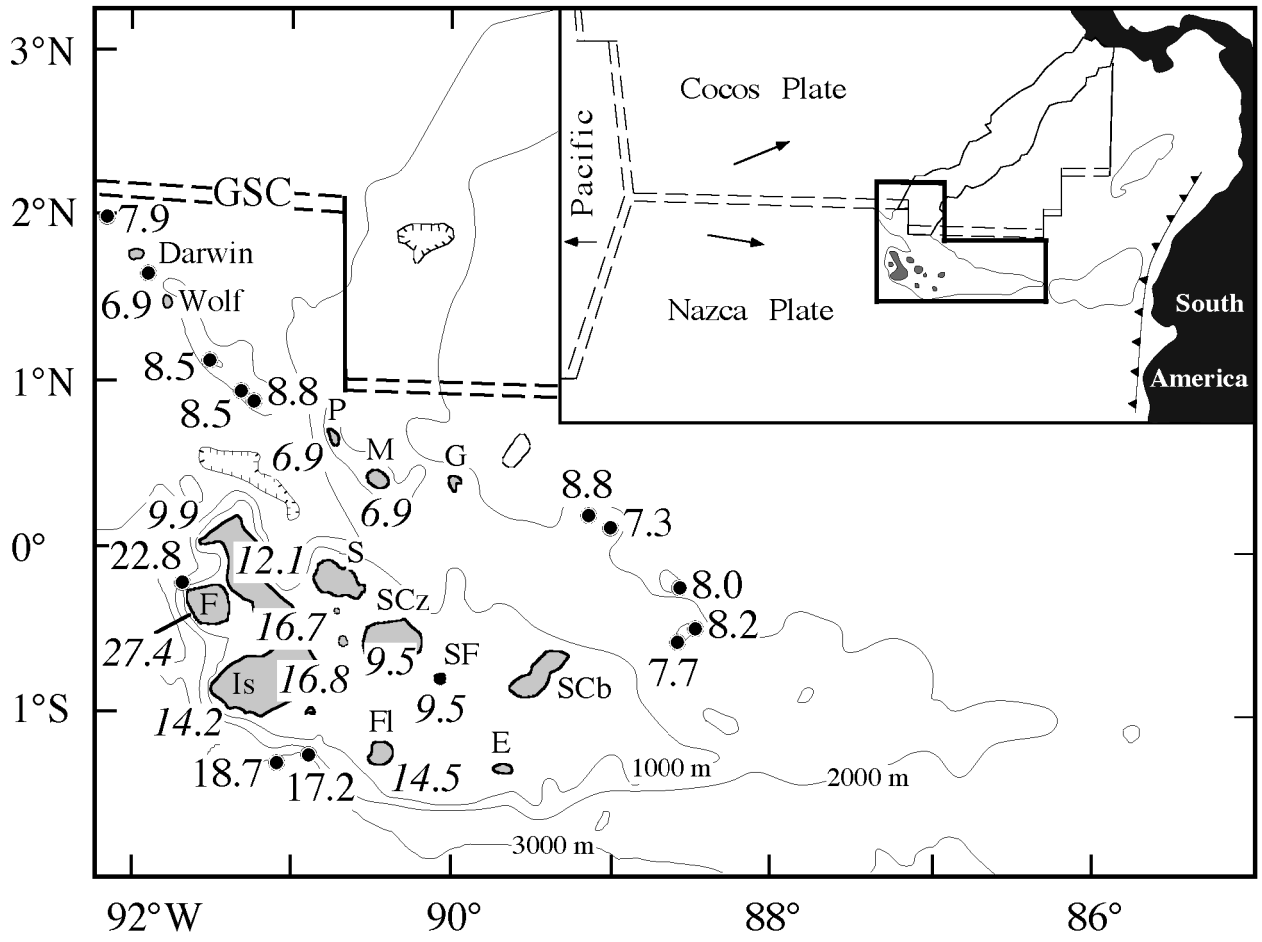
3°N
2°N
1°N
0°
1°S
92°W
90°
88°
86°
GSC
7.9
Darwin
6.9
Wolf
8.5
8.8
8.5
P
M
G
6.9
6.9
9.9
22.8
12.1
S
F
SCz
16.7
27.4
9.5
SF
Is
16.8
SCb
9.5
14.2
Fl
E
18.7
17.2
14.5
8.8
7.3
8.0
8.2
7.7
1000 m
2000 m
3000 m
Cocos Plate
Pacific
Nazca Plate
South
America

Fig. 7

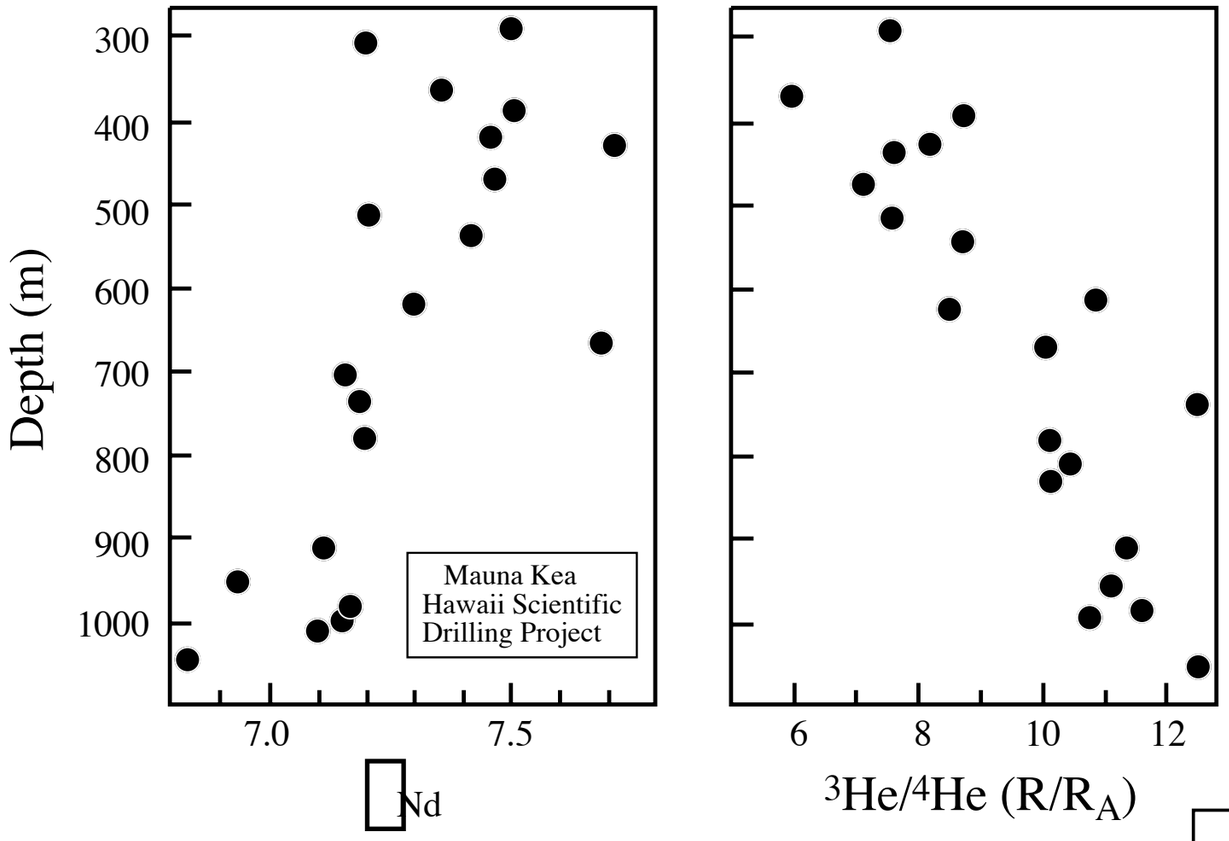

Figure 8

Figure 9

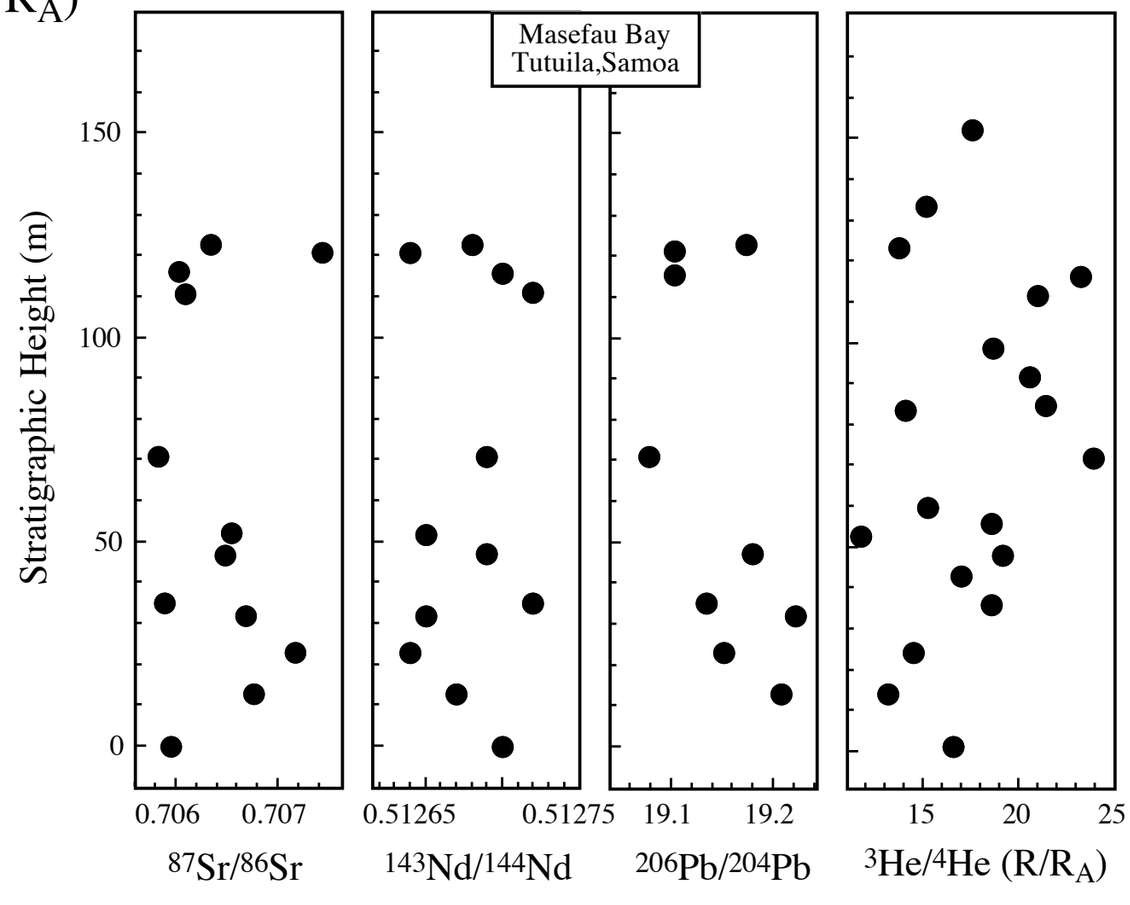

Fig. 10

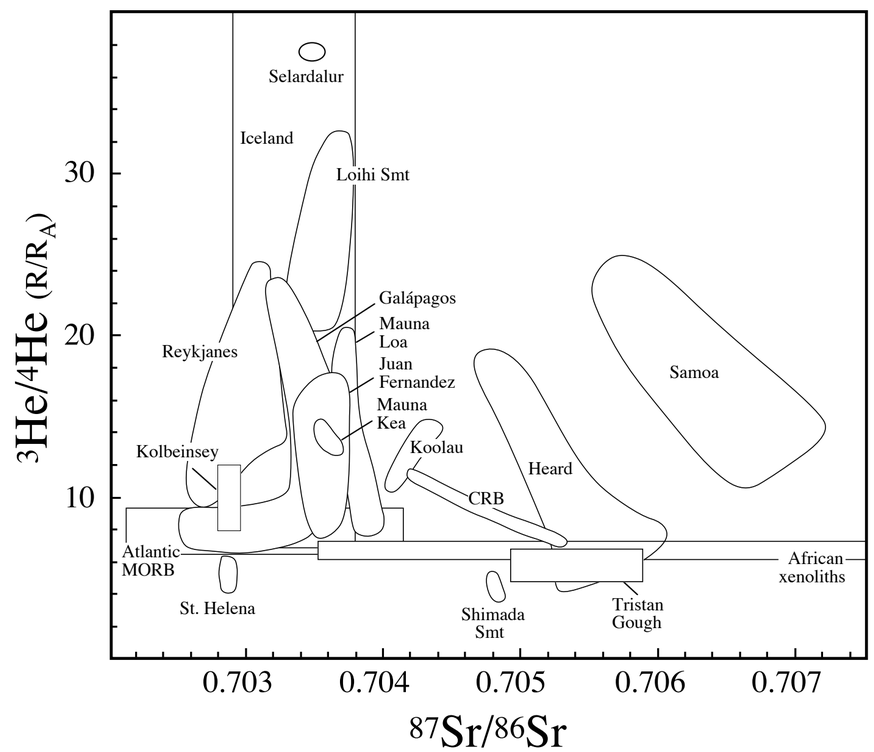
Selardalur
Iceland
Loihi Smt
Galápagos
Mauna
Loa
Juan
Fernandez
Mauna
Kea
Reykjanes
Kolbeinsey
Koolau
Heard
CRB
Samoa
Atlantic
MORB
St. Helena
Shimada
Smt
Tristan
Gough
African
xenoliths
30
20
10
0.703
0.704
0.705
0.706
0.707
3He/4He (R/RA)
87Sr/86Sr

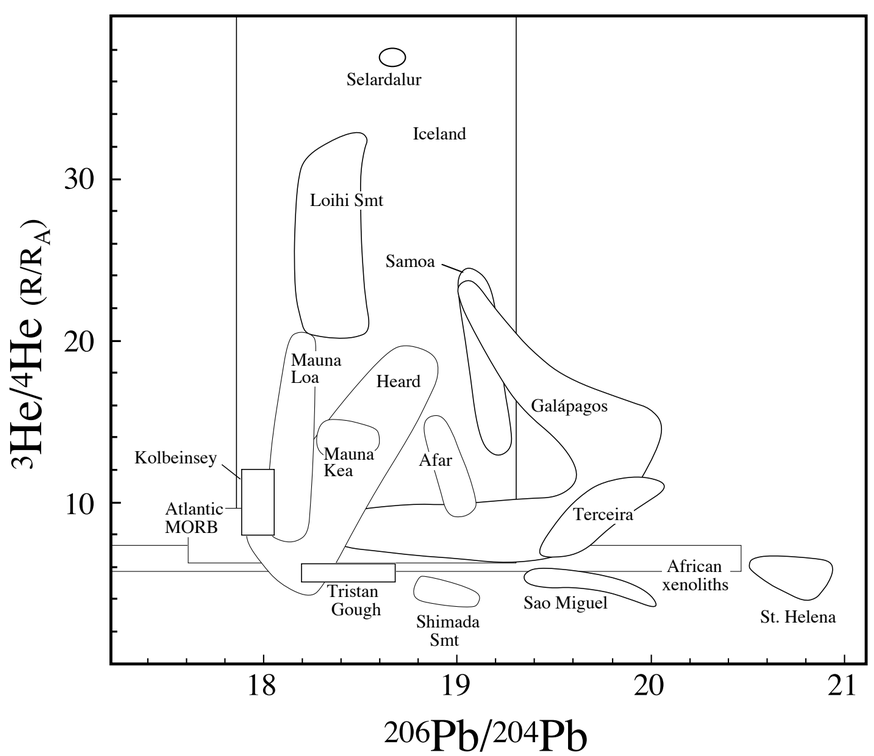
Selardalur
Iceland
Loihi Smt
Samoa
Mauna
Loa
Heard
Galápagos
Kolbeinsey
Mauna
Kea
Afar
Atlantic
MORB
Terceira
African
xenoliths
Tristan
Gough
Sao Miguel
Shimada
Smt
St. Helena
30
20
10
18
19
20
21
3He/4He (R/RA)
206Pb/204Pb

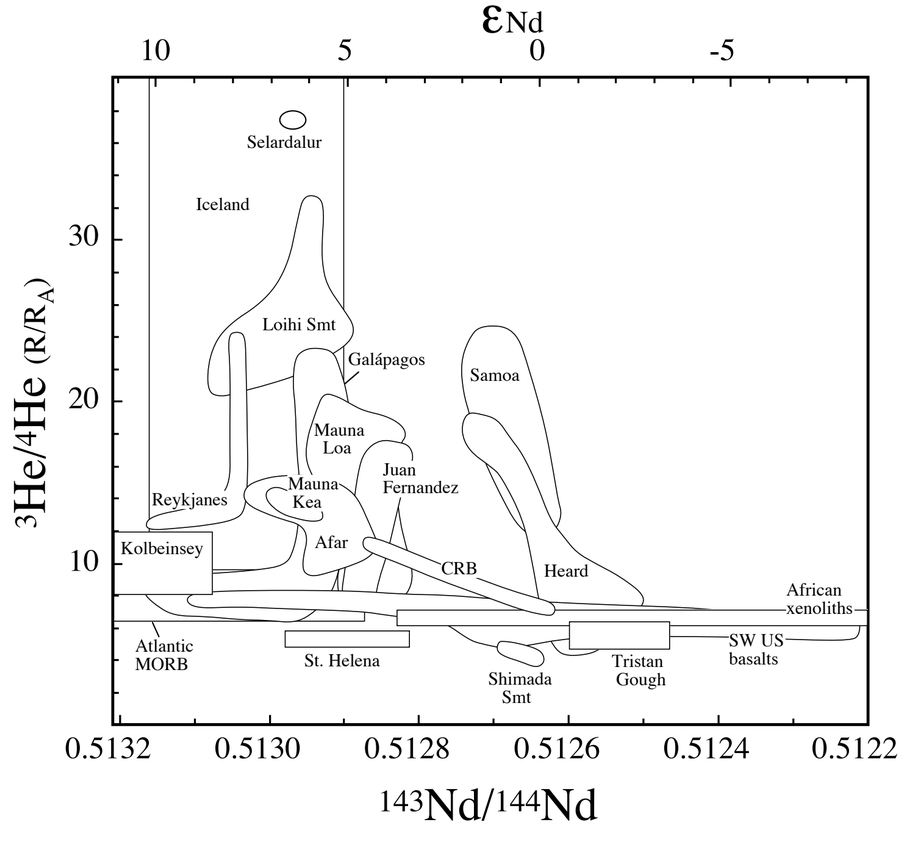
εNd
10
5
0
-5
Selardalur
Iceland
Loihi Smt
Galápagos
Samoa
Mauna
Loa
Juan
Fernandez
Reykjanes
Mauna
Kea
Afar
Kolbeinsey
CRB
Heard
African
xenoliths
Atlantic
MORB
St. Helena
SW US
basalts
Shimada
Smt
Tristan
Gough
30
20
10
0.5132
0.5130
0.5128
0.5126
0.5124
0.5122
3He/4He (R/RA)
143Nd/144Nd

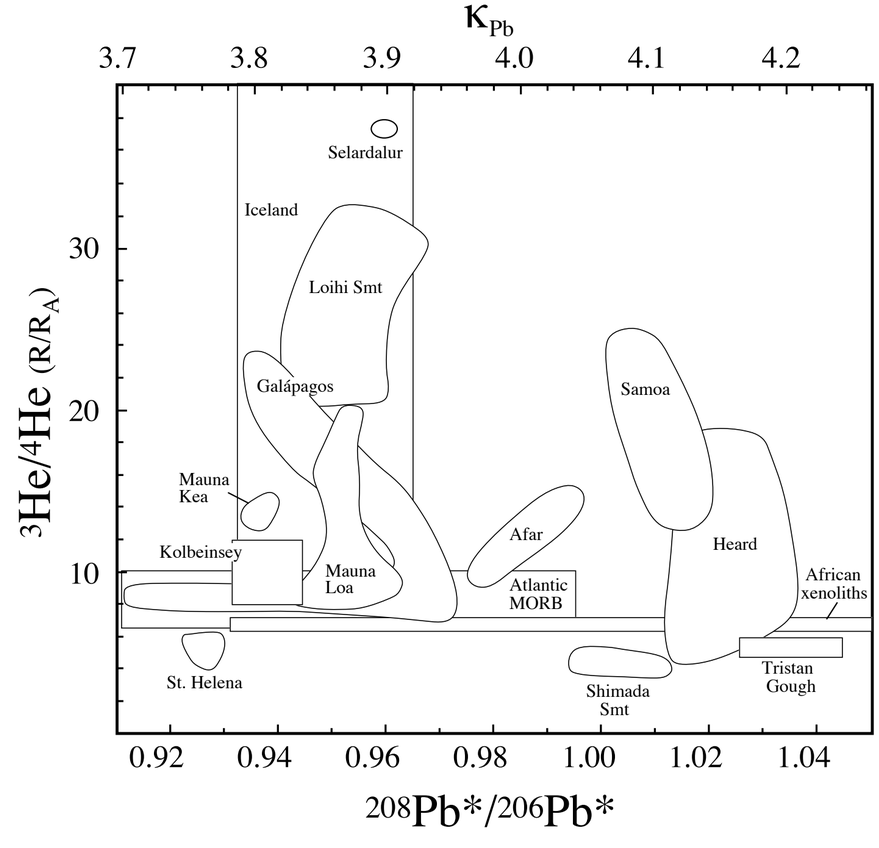
κPb
3.7
3.8
3.9
4.0
4.1
4.2
Selardalur
Iceland
Loihi Smt
Galápagos
Samoa
Mauna
Kea
Afar
Kolbeinsey
Heard
Mauna
Loa
Atlantic
MORB
African
xenoliths
St. Helena
Shimada
Smt
Tristan
Gough
30
20
10
0.92
0.94
0.96
0.98
1.00
1.02
1.04
3He/4He (R/RA)
208Pb*/206Pb*

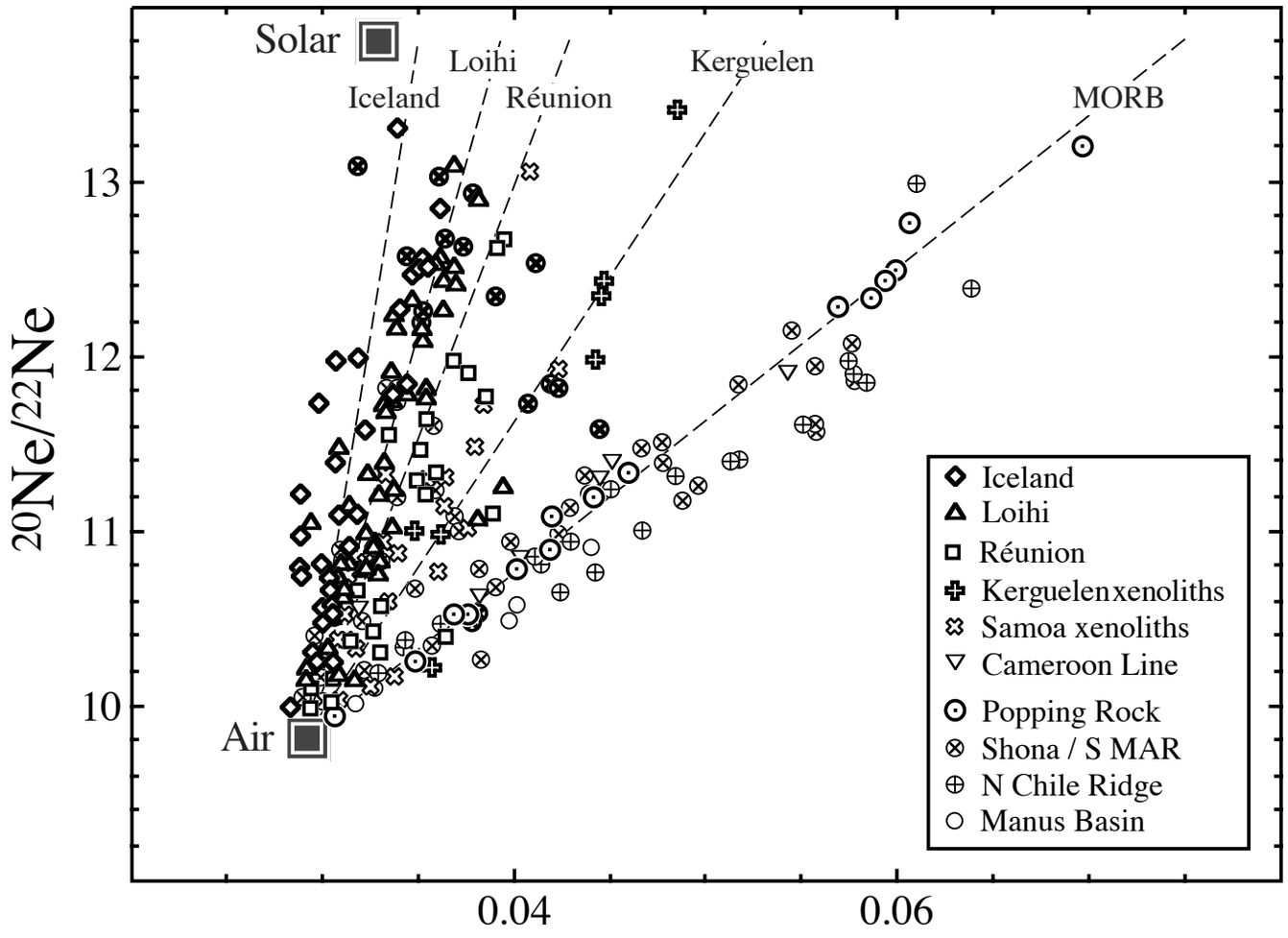

Figure 11

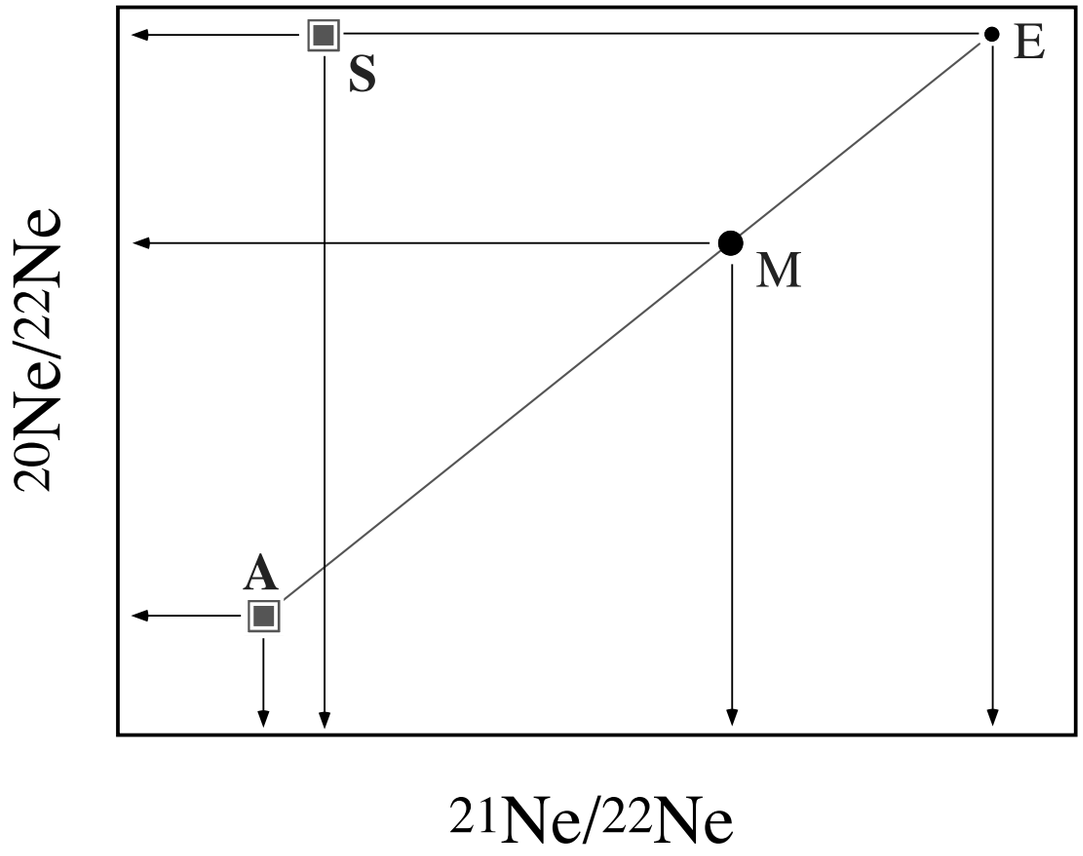

Figure 12

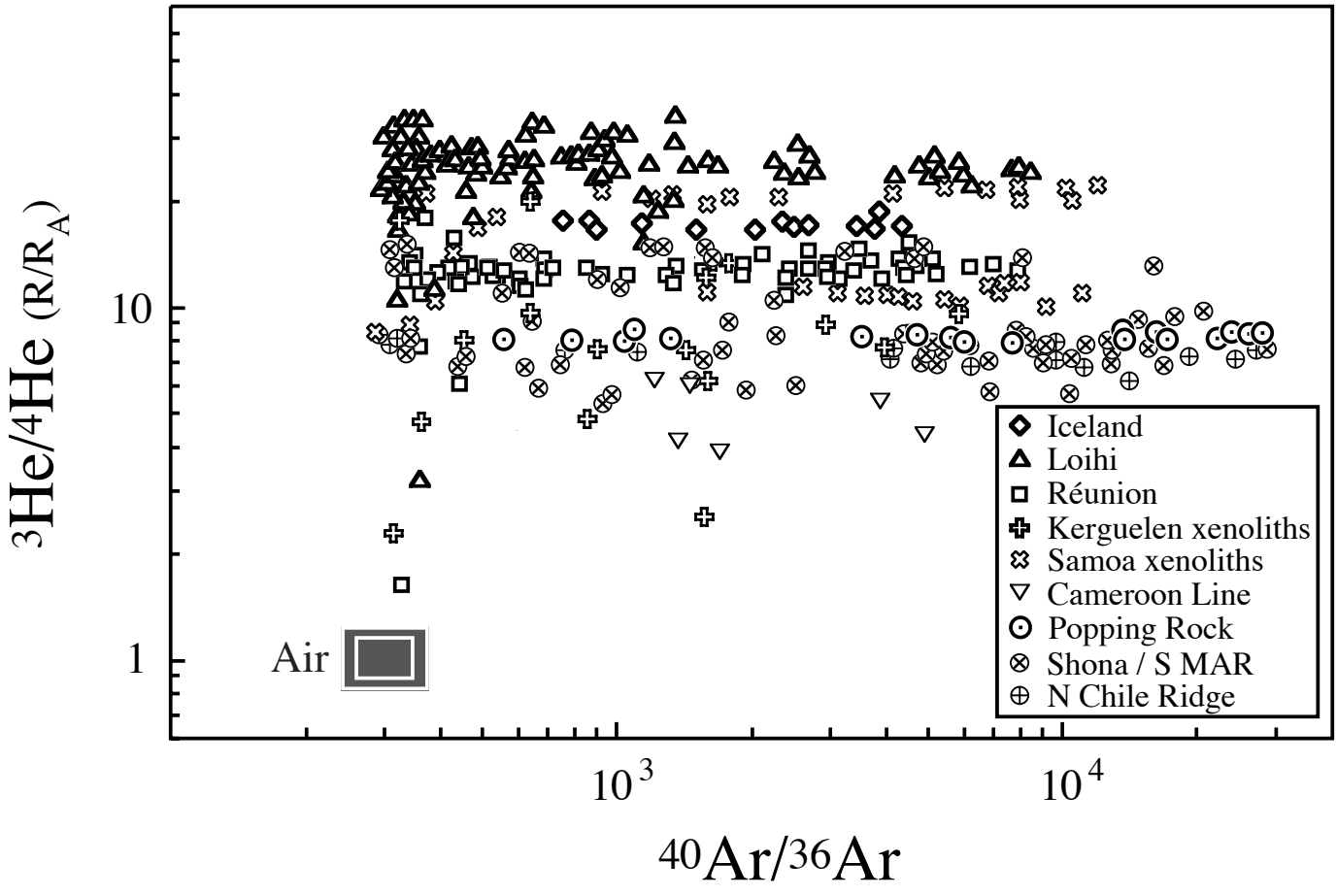
$^3He/^4He$ (R/R_A)
10
1
Air
10^3
10^4
$^{40}Ar/^{36}Ar$
Iceland
Loihi
Réunion
Kerguelen xenoliths
Samoa xenoliths
Cameroon Line
Popping Rock
Shona / S MAR
N Chile Ridge

Fig. 13

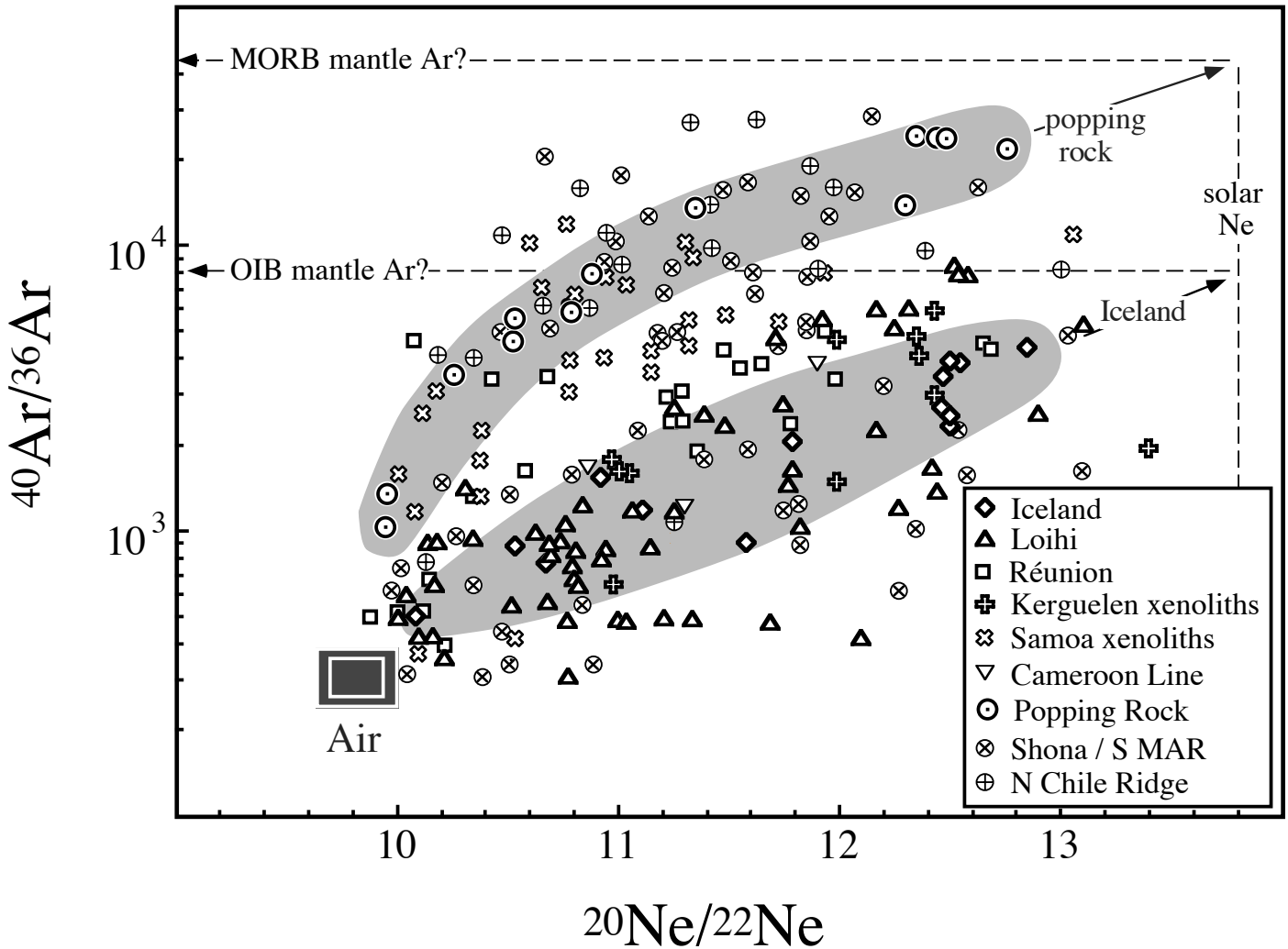
MORB mantle Ar?
OIB mantle Ar?
popping rock
solar Ne
Iceland
Air
Iceland
Loihi
Réunion
Kerguelen xenoliths
Samoa xenoliths
Cameroon Line
Popping Rock
Shona / S MAR
N Chile Ridge
10^4
10^3
10
11
12
13
40Ar/36Ar
20Ne/22Ne

Fig.14

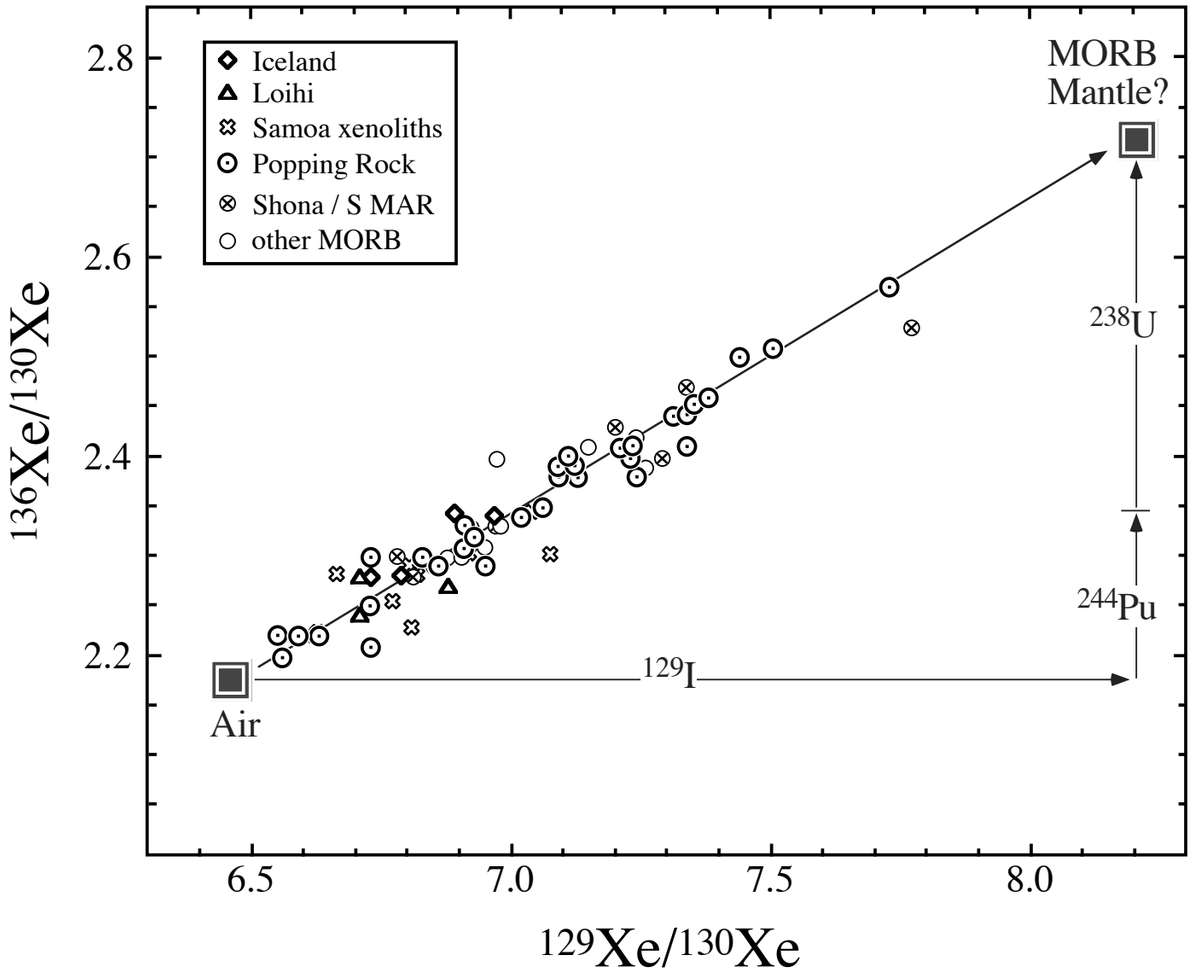
Iceland
Loihi
Samoa xenoliths
Popping Rock
Shona / S MAR
other MORB
MORB
Mantle?
238U
244Pu
129I
Air
2.8
2.6
2.4
2.2
6.5
7.0
7.5
8.0
136Xe/130Xe
129Xe/130Xe

Fig. 15

Fig. 16

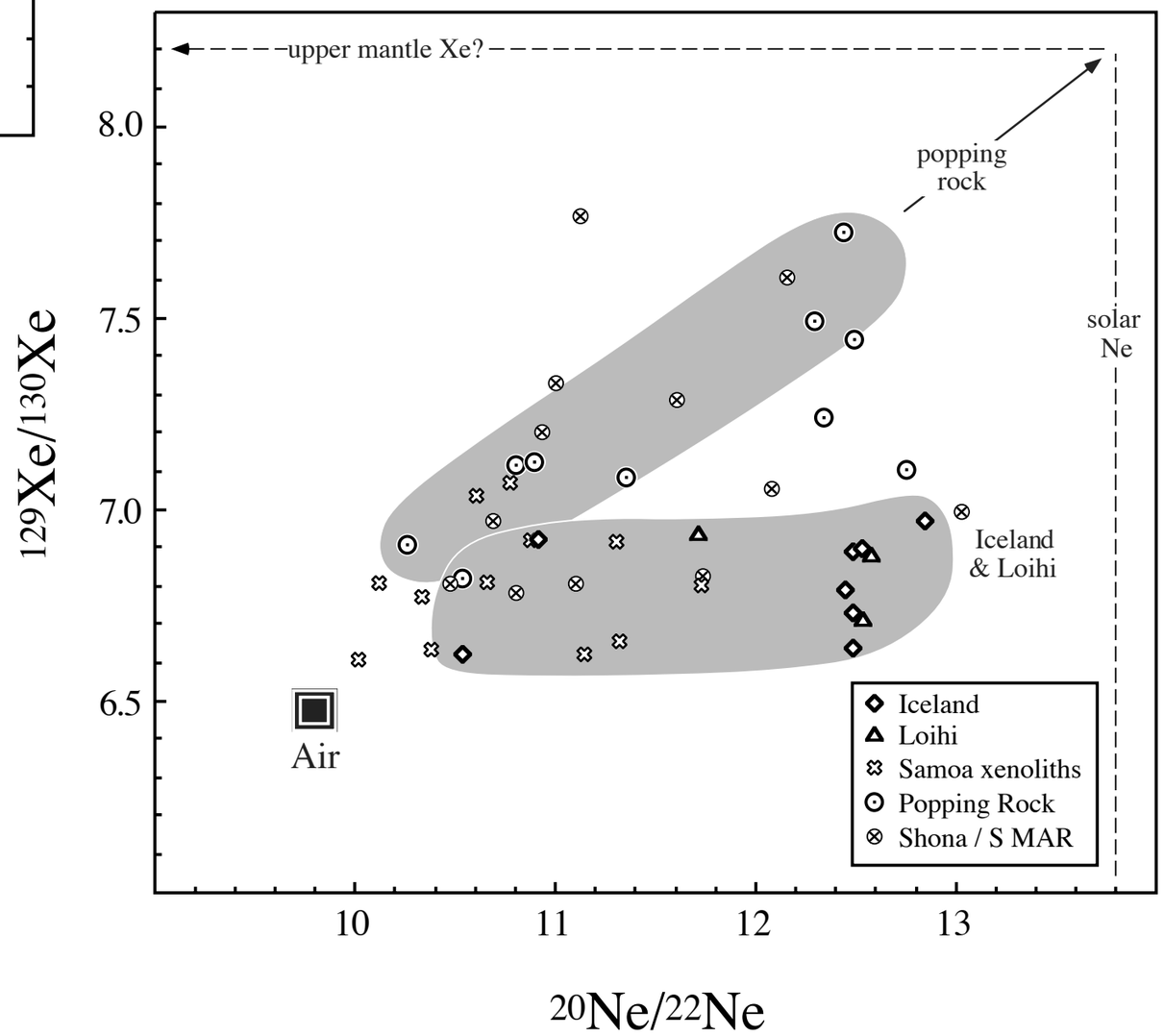
upper mantle Xe?
popping
rock
solar
Ne
Iceland
& Loihi
Air
Iceland
Loihi
Samoa xenoliths
Popping Rock
Shona / S MAR
8.0
7.5
7.0
6.5
10
11
12
13
129Xe/130Xe
20Ne/22Ne

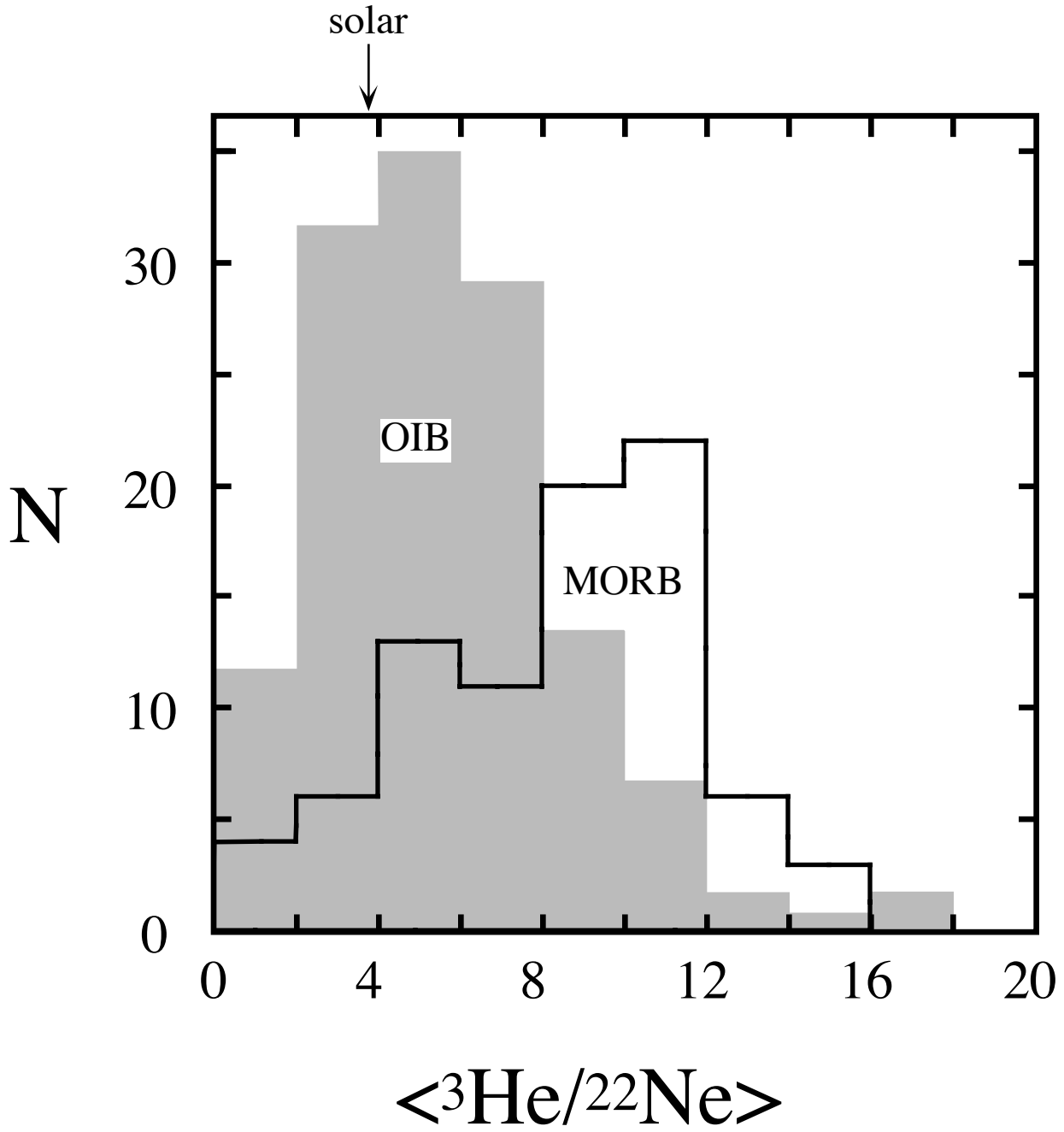

Fig. 17

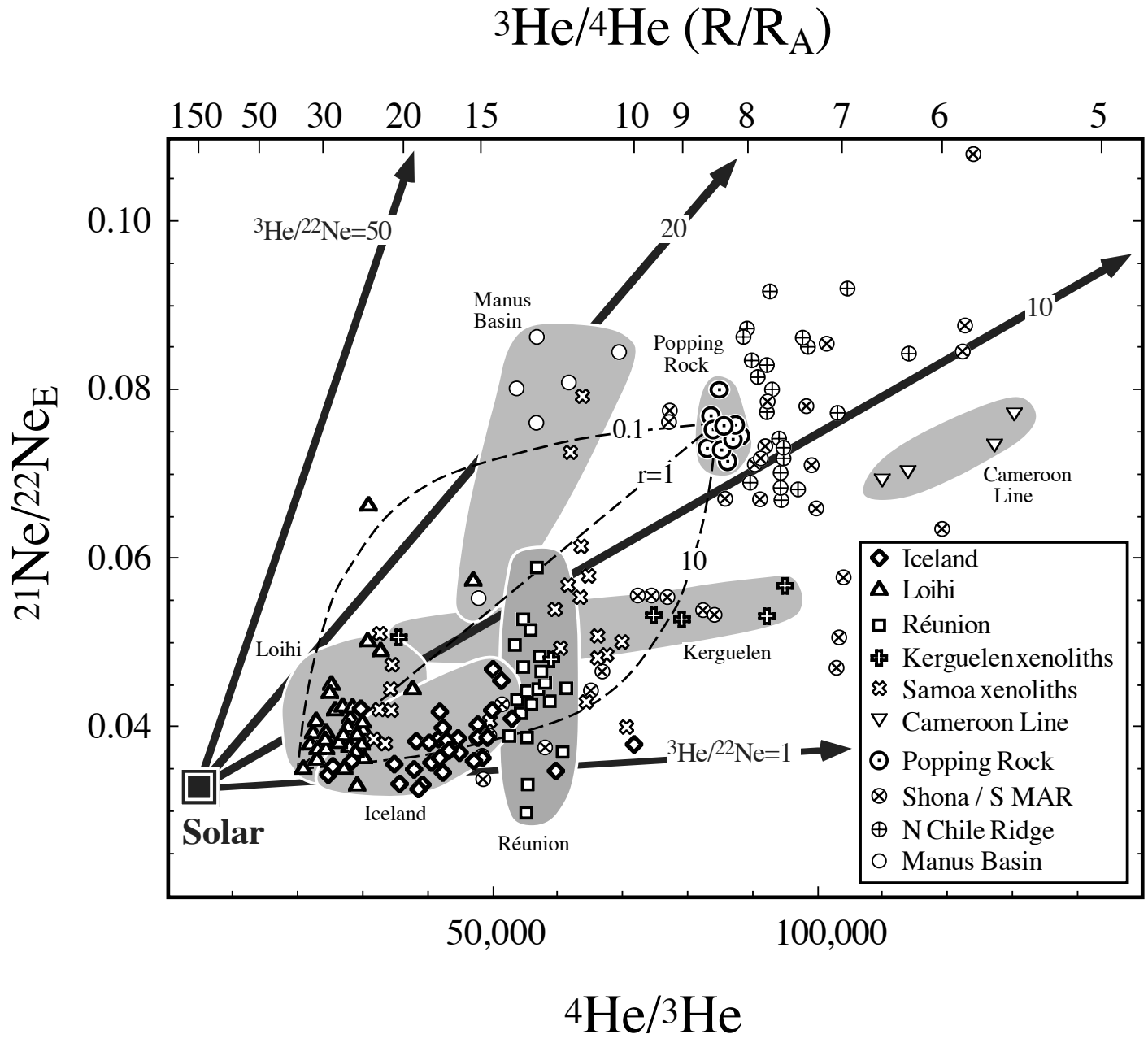
$^3He/^4He$ (R/R_A)
150 50 30 20 15 10 9 8 7 6 5
0.10
0.08
0.06
0.04
$^{21}Ne/^{22}Ne_E$
$^3He/^{22}Ne$=50
20
10
0.1
r=1
10
Manus Basin
Popping Rock
Cameroon Line
Loihi
Kerguelen
Iceland
Réunion
Solar
$^3He/^{22}Ne$=1
Iceland
Loihi
Réunion
Kerguelen xenoliths
Samoa xenoliths
Cameroon Line
Popping Rock
Shona / S MAR
N Chile Ridge
Manus Basin
50,000
100,000
$^4He/^3He$

Fig. 18

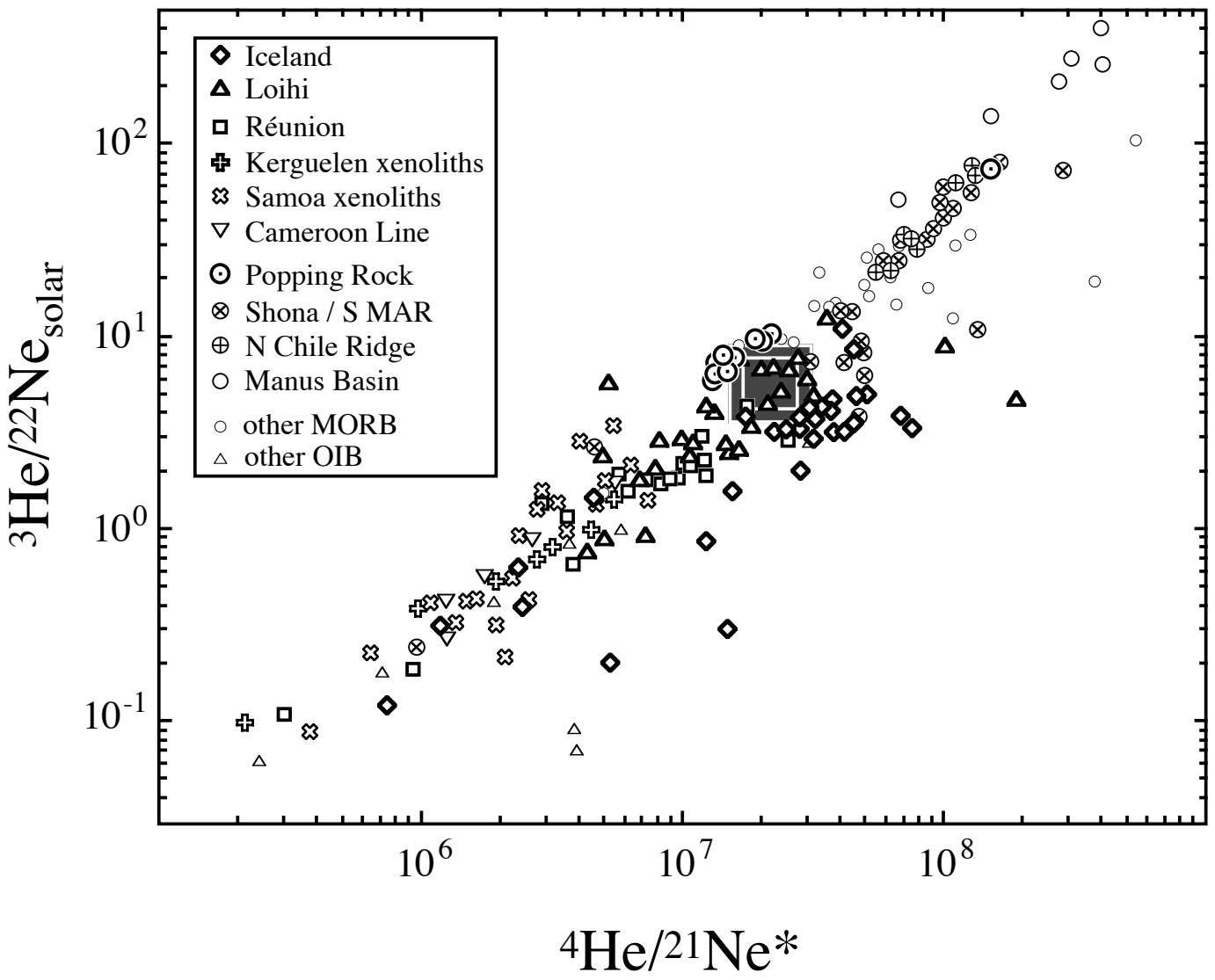
Iceland
Loihi
Réunion
Kerguelen xenoliths
Samoa xenoliths
Cameroon Line
Popping Rock
Shona / S MAR
N Chile Ridge
Manus Basin
other MORB
other OIB
$^3He/^{22}Ne_{solar}$
$^4He/^{21}Ne^*$
10^{-1}
10^0
10^1
10^2
10^6
10^7
10^8

Fig. 19

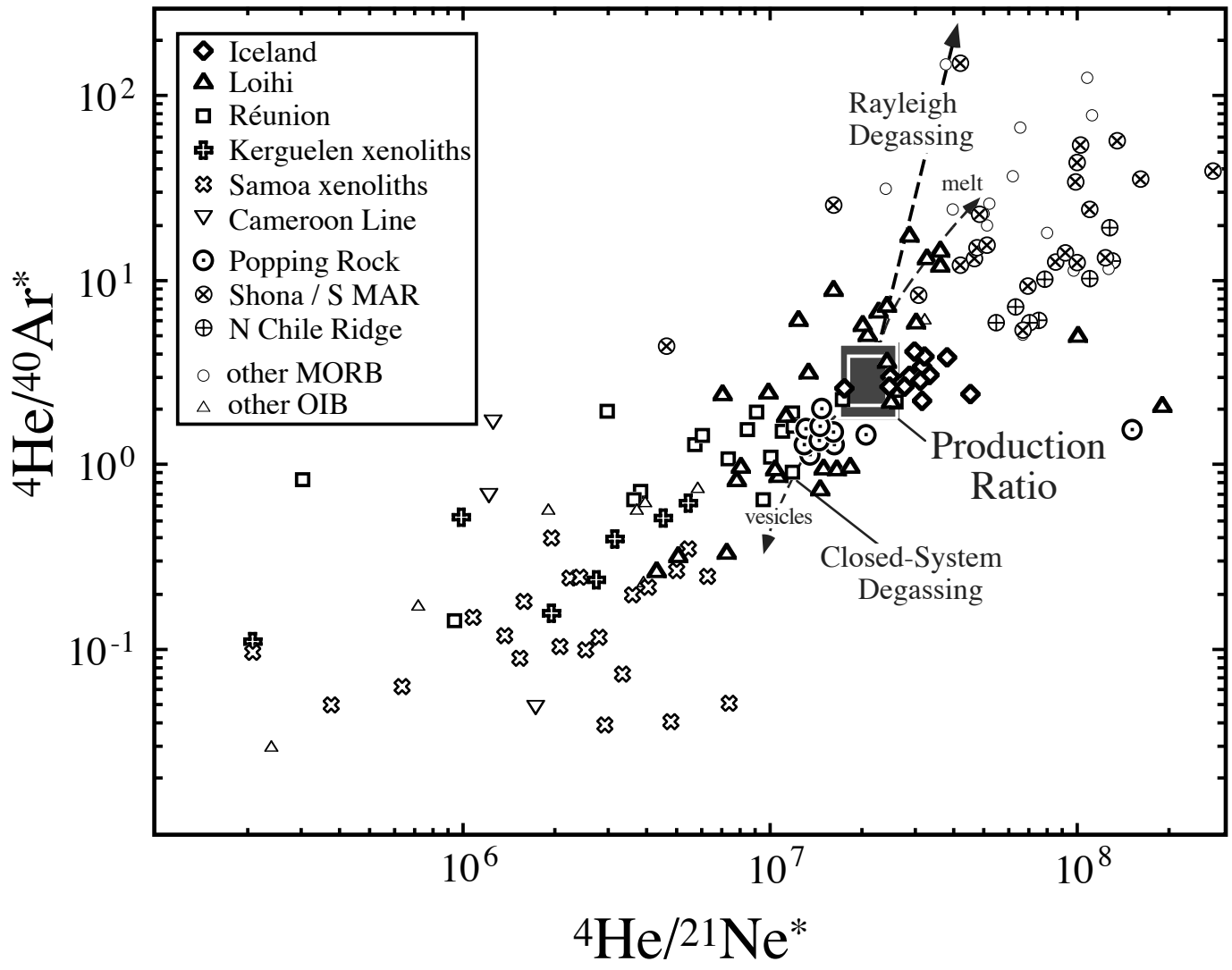
Iceland
Loihi
Réunion
Kerguelen xenoliths
Samoa xenoliths
Cameroon Line
Popping Rock
Shona / S MAR
N Chile Ridge
other MORB
other OIB
Rayleigh Degassing
melt
Production Ratio
vesicles
Closed-System Degassing
10^2
10^1
10^0
10^{-1}
10^6
10^7
10^8
$^4He/^{40}Ar^*$
$^4He/^{21}Ne^*$

Fig. 20

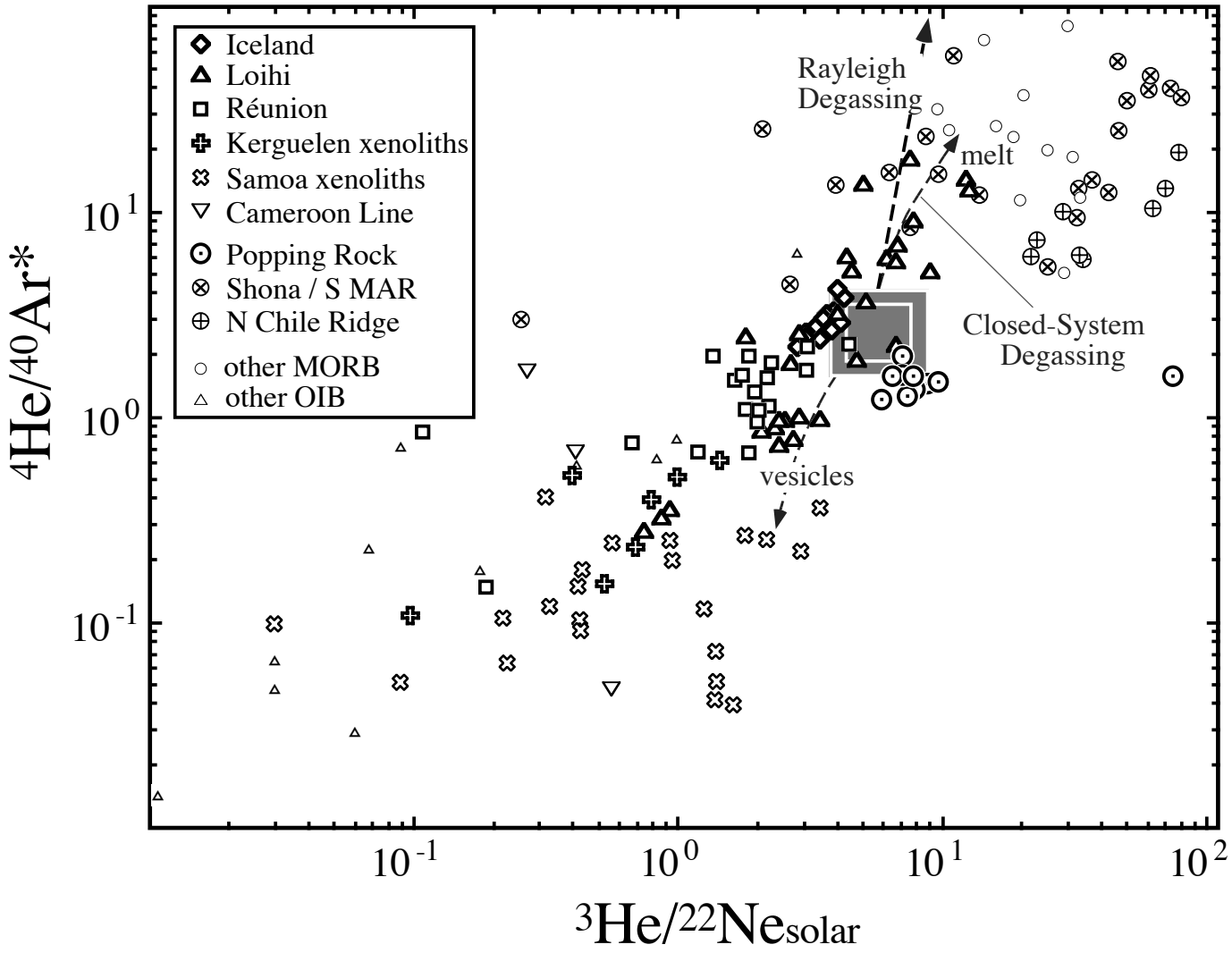
Iceland
Loihi
Réunion
Kerguelen xenoliths
Samoa xenoliths
Cameroon Line
Popping Rock
Shona / S MAR
N Chile Ridge
other MORB
other OIB
Rayleigh
Degassing
melt
Closed-System
Degassing
vesicles
$^4He/^{40}Ar^*$
$^3He/^{22}Ne_{solar}$
10^{-1}
10^0
10^1
10^2

Fig. 21

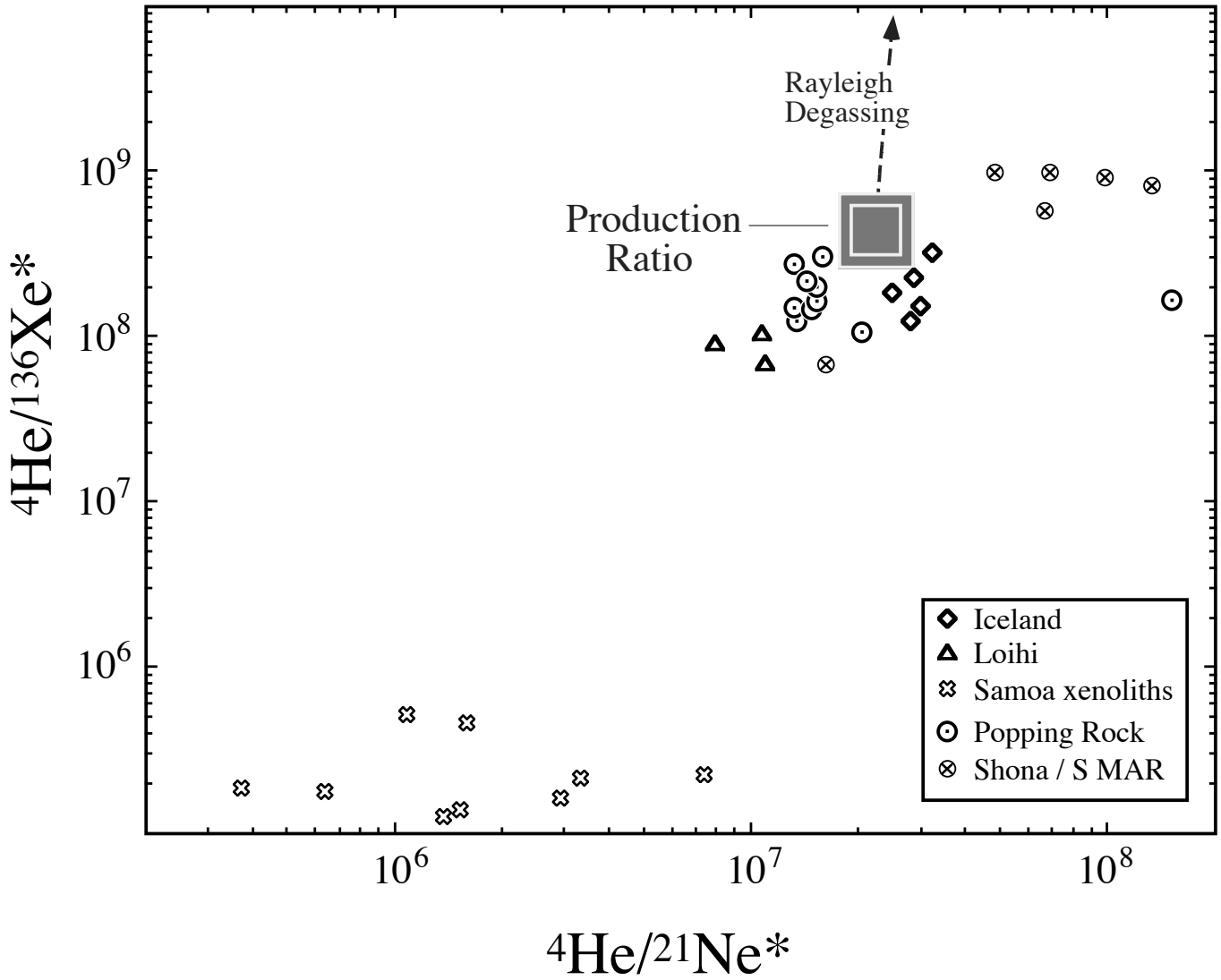
Rayleigh
Degassing
Production
Ratio
Iceland
Loihi
Samoa xenoliths
Popping Rock
Shona / S MAR
10^9
10^8
10^7
10^6
10^6
10^7
10^8
$^4He/^{136}Xe^*$
$^4He/^{21}Ne^*$

Fig. 22

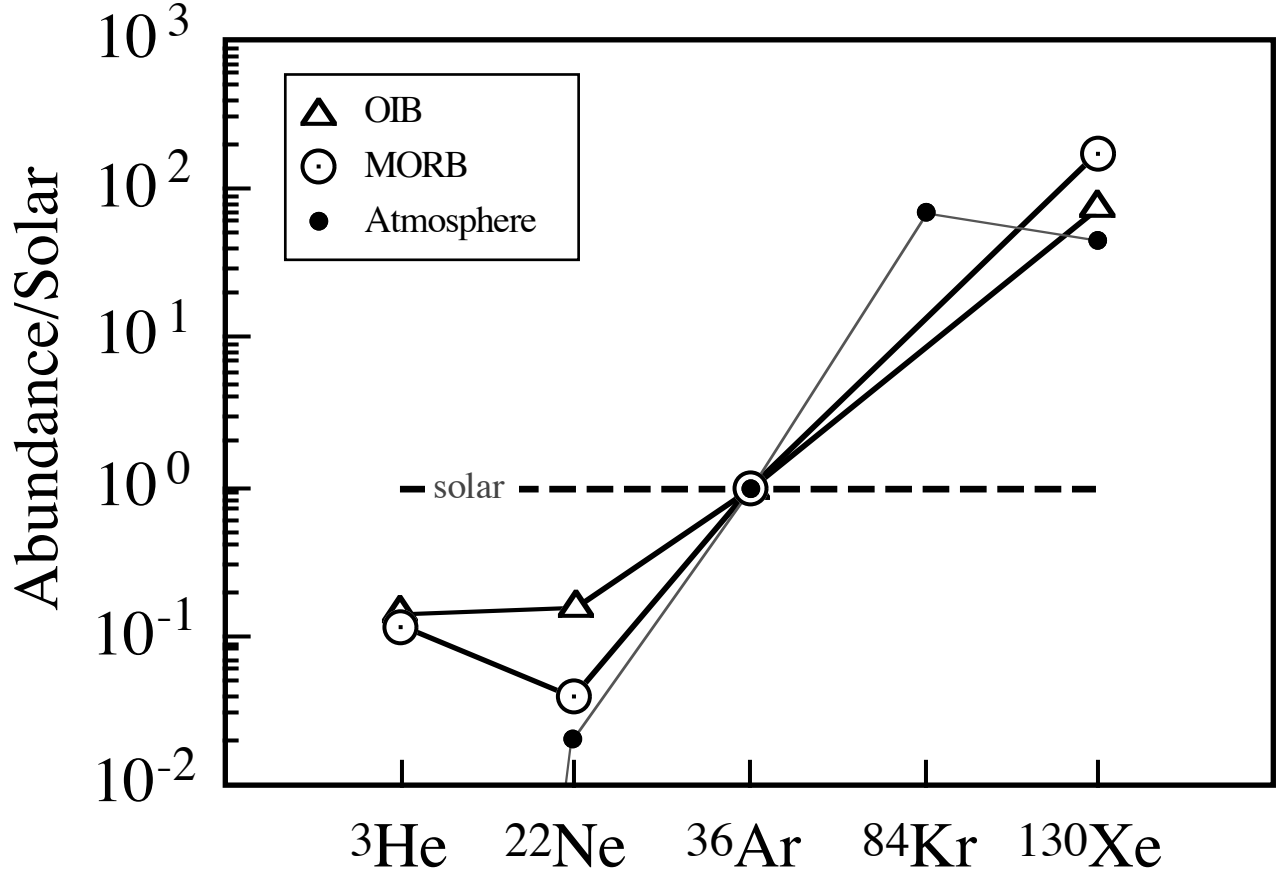

Fig. 23